QUANTITATIVE ANALYSIS

OF

EARTH RESISTIVITY DATA

by

KEEVA VOZOFF

B.Phys., University of Minnesota

(1949)

M.S., Pennsylvania State College

(1951)

SUBMITTED IN PARTIAL FULFILLMENT

OF THE REQUIREMENTS OF THE

DEGREE OF DOCTOR OF

PHILOSOPHY

at the

MASSACHUSETTS INSTITUTE OF TECHNOLOGY

June, 1956

Signature of Author . . . . . .
Department of Geology and Geophysics, May 4, 1956.

Certified by . . . . . .
Thesis Supervisor

Accepted by . . . . . .
Chairman, Departmental Committee on Graduate Students.

QUANTITATIVE ANALYSIS OF EARTH RESISTIVITY DATA

by

Keeva Vozoff

Submitted to the Department of Geology and Geophysics on May 4, 1956, in partial fulfillment of the requirements for the degree of Doctor of Philosophy.

ABSTRACT

The direct numerical solution of resistivity data for the case of horizontal layering is presented as the solution of a set of nonlinear algebraic equations. Two specific methods, Newton and Steepest Descent, were set up for three layer analyses on a digital computer. These were applied to field data, and to data derived theoretically for three and four layer cases.

The case of a thin second layer was found to display a special kind of indeterminacy. It was found that the analyses do not and cannot theoretically be expected to yield the actual values of resistivity and thickness for these thin layers, but rather, a good value for their ratio (conductive layer) or product (resistive layer) can be obtained. The question of ultimate resolubility of this type of information in the presence of measurement error is discussed quantitatively. It was found that, as the resistivity of the third (lowermost) layer increases, it becomes increasingly difficult to detect a thin, resistive second layer. When the second layer is not thin relative to the first, the resistivities and thicknesses are determined with reasonable

accuracy. These solutions do not appear to be unique, but alternate solutions differ sufficiently for the true solution to be easily distinguished.

In addition, the problem of analysis in the case of resistivity variations in three dimensions is discussed. The exact solution is shown to be intractable due to mathematical limitations. By an approximation the equations can be linearized, and a numerical method for solution of the approximate equations is proposed, but not applied.

It is concluded that these numerical methods will not find immediate widespread application due to the time and expense involved in computation. When necessary, however, reasonable solutions can be obtained.

ACKNOWLEDGEMENTS

This thesis was done as part of a project on the broad problems of earth resistivity, in which Theodore R. Madden, Philip G. Hallof, and the author, were working very closely. I am deeply indebted to both of them for many of the ideas appearing here, although they are seldom specifically mentioned. In addition, numerous fruitful discussions were held with Prof. S. M. Simpson of the Department of Geology and Geophysics.

The numerical portion of this work was sponsored by the Morse committee on Machine Methods of Computation and Numerical Analysis. Availability of Digital Computer Laboratory time was made possible by the Office of Naval Research.

The author would also like to thank Mrs. M. L. Anderson for typing the thesis, Mr. J. C. Benlow for preparing the drawings.

TABLE OF CONTENTS

PART ONE

TABLE OF CONTENTS (cont'd)

PART TWO

PART ONE

I INTRODUCTION

The direct interpretation of earth resistivity data is an inverse boundary value problem. As such, few general mathematical tools are available for its solution, as compared with those available for the direct problem. The few inverse problems which have been solved are quite specific. The resistivity problem has been attacked by several authors, however, no practical general solution has been presented.

Langer (1933) derived an analytical method for developing the terms of a series expansion of resistivity, $\rho(z)$, which varies continuously with depth. Attempts at application of the method by Slichter (1933) and Langer proved it to be excessively laborious and the assumption of a continuous resistivity variation in practical examples is questionable.

In most practical examples where it may be assumed that conductivity is a function of depth alone, a rather better assumption would seem to be that of stepwise changes, i.e. a medium composed of several homogeneous horizontal strata, each of fixed resistivity and thickness. In a second paper, Langer (1936) extends his first derivation to the case of continuous variation with a single discontinuity. In application, however, this method is more cumbersome than the first, and thus of even more limited practicality. Pekeris (1940) presented a graphical solution for the case of discrete horizontal layers. This technique works quite well, but is limited in application by the assumption that succeeding layer thicknesses increase with depth (Rogers, 1951).

Stevenson (1934) treats the problem of three-dimensional, continuous resistivity variation. He reduces the exact solution to an approximate linear integral equation, but is unable to solve it. Applying this same approximation to the case of horizontal layers, however, Stevenson derives a series solution which gives a better result on the one example done than does the Langer-Slichter method. The methods are equally laborious, unfortunately.

The present work gives the development and results of a numerical method for solution of the horizontal layering problem, and an approximate numerical method for solution in the case of three-dimensional variation. These methods are useful only with the aid of high speed computers.

II HORIZONTAL STRATIFICATION

MATHEMATICAL FORMULATION OF THE PROBLEM

If we assume that the earth actually is composed of homogeneous, horizontal strata, then any electrical measurements which are made on its surface can be reduced to give the surface potential variation about a point source, $\phi(r)$. It is with this function and functions derivable from it, that we shall deal. It is a well known fact that, for the geometry considered, (surface resistivity normalized to unity)

$$2\pi\phi(r) = \int_0^\infty J_0(\lambda r) k_{12\ldots n}(\lambda)\, d\lambda \qquad (1)$$

(e.g. see Sunde (1949) pp. 40 ff), where n is the number of layers,

$$k_{12\ldots n}(\lambda) = \frac{1-\mu_{12\ldots n}\, e^{-2\lambda d_1}}{1-\mu_{12\ldots n}\, e^{-2\lambda d_1}}$$

$$\mu_{12\ldots n} = \frac{\rho_1 - \rho_2 k_{23\ldots n}(\lambda)}{\rho_1 + \rho_2 k_{23\ldots n}(\lambda)}$$

$$k_{(m-1)m\ldots n}(\lambda) = \frac{1-\mu_{(m-1)m\ldots n}\, e^{-2\lambda d_{m-1}}}{1+\mu_{(m-1)m\ldots n}\, e^{-2\lambda d_{m-1}}} \qquad \ldots (2)$$

$$\mu_{(m-1)m\ldots n} = \frac{\rho_{m-1} - \rho_m k_{(m+1)\ldots n}}{\rho_{m-1} + \rho_m k_{(m+1)\ldots n}}$$

$$k_{(m-1)m}(\lambda) = \frac{1-\mu_{(m-1)m}\, e^{-2\lambda d_{m-1}}}{1+\mu_{(m-1)m}\, e^{-2\lambda d_{m-1}}}$$

$$\mu_{(m-1)m} = \frac{\rho_{m-1} - \rho_m}{\rho_{m-1} + \rho_m}$$

and ρ_i and d_i are the resistivity and thickness, respectively of the i-th layer. As is also well known, equation (1) can be solved immediately for $k_{12\ldots n}(\lambda)$ by an inversion theorem of Hankel. The solution is

$$k_{12\ldots}(\lambda) = \lambda \int_0^\infty r\, \phi(r) J_0(\lambda r)\, dr \qquad (3)$$

and the function $k_{12\ldots n}(\lambda)$ is known as the Slichter kernel. It is seen that a Slichter kernel can be (a) derived from field data by an integration, and (b) calculated algebraically from

equations (2) for any given set of assumptions as to the ρ_i and d_i. The method of analysis presented in this paper starts with the kernel integrated from field data by means of (a), and, by a process of iteration, adjusts the values of the parameters ρ_i and d_i in a calculation of type (b) until the kernel calculated in this fashion fits very closely the integrated kernel. It is then assumed that the final values of the parameters in (b) are the desired solution. There is, at present, no mathematical justification for this last assumption, i.e., whereas a perfect fit undoubtedly indicates one solution to the problem, there is no reason to believe there are not other solutions. In fact, experience indicates that more than one solution does exist; however, the physical requirements (positive and real ρ_i and d_i) reduce the number of allowable solutions.

The following is a mathematical description of the problem. Beginning with the potential function as measured in the field, and using equation (3), a kernel is calculated for m values of λ

$$k(\lambda_j) = \lambda_j \int_0^\infty r\,\phi(r) J_0(\lambda_j r)\,dr \qquad (4)$$

Next, values of $k_{12\cdots n}(\lambda_j)$ are calculated from equations (2) using the same λ_j, assuming n layers $(m \geq n)$, and guessing at the values of ρ_i and d_i (by comparison of the apparent resistivity or kernel $k(\lambda_j)$ with available curves of these functions). There results the set of equations to be satisfied:

$$K = \sum_{j=1}^{m} \left[k_{12\cdots n}(\lambda_j) - k(\lambda_j) \right]^2 = 0 \qquad m = 2n-3 \qquad (5a)$$

or

$$= \sum_{j=1}^{m} \left[k_{12\cdots n}(\lambda_j) - k(\lambda_j) \right]^2 = \text{minimum} \qquad m > 2n-3 \qquad (5b)$$

For a slight simplification of notation, the unknowns ρ_i and d_i are designated by the more general ξ_α. Since there are $(n-1)$ unknown thicknesses and $(n-2)$* unknown resistivities,

$$\alpha = 1, 2, - - - - , 2n - 3$$

Further, in order to denote the number of iterations having taken place, the first estimates of the ξ_α are $\xi_\alpha^{(0)}$, etc. The problem is to minimize the function $K\left(\xi_\alpha^{(i)}\right)$ and, by definition,

$$K(\xi_\alpha) = \text{minimum} \qquad m > 2n-3 \qquad (6)$$

The problem is similar to that of approximating the roots of a set of nonlinear transcendental equations.

METHODS OF SOLUTION

Several general methods are described in the literature. Two of these have been tried in the numerical work - Functional Iteration[1] (Newton's Method) and Steepest Descent[2] - and the latter was found to be somewhat more effective in the difficult case of thin intermediate layers.

Newton's Method

In this approach it is assumed that the kernel is an analytic function of its variables. As such, it can be expanded in a Taylor Series in these variables, and its partial derivatives relative to each can be evaluated for any set of assumed values. The relative sizes of these derivatives determine the

* The resistivities ρ_1 and ρ_n are assumed known inasmuch as they are the asymptotes of the apparent resistivity curves at very small r and very large r, respectively.

1. see von Sanden, 1923; Householder, 1955.
2. see Householder, 1955.

relative changes to be made in each, and the values of an "error", ϵ , determines the magnitude of the change. The series expansion of the kernel takes the form:

$$k_{12\ldots m}(\lambda_j, \xi_\alpha + d\xi_\alpha) = k_{12\ldots m}(\lambda_j, \xi_\alpha) + \sum_{\alpha=1}^{2n-3} \left[\frac{\partial k}{\partial \xi_\alpha} d\xi_\alpha + \frac{\partial^2 k}{\partial \xi_\alpha^2} (d\xi_\alpha)^2 \right] \tag{7}$$

(neglecting cross terms and higher derivatives).

The Newton first approximation is:

$$k_{12\ldots m}(\lambda_j, \xi_\alpha + \Delta\xi_\alpha) \approx k_{12\ldots m}(\lambda_j, \xi_\alpha) + \sum_{\alpha=1}^{2n-3} \frac{\partial k}{\partial \xi_\alpha} \Delta\xi_\alpha \tag{8}$$

and is obviously exact only for linear functions. For a function as complex as is the Slichter kernel the approximation is generally useful only when $\Delta\xi_\alpha$ is small.

The normal iterative technique of Newton is applicable for m = 2n - 3, and can be formulated:

$$\Delta k^{(i)}_{12\ldots m}(\lambda_j) = \epsilon_j^{(i)} \tag{9}$$

where

$$\epsilon_j^{(i)} = k(\lambda_j) - k^{(i)}_{12\ldots m}(\lambda_j) \tag{9a}$$

and

$$\Delta k^{(i)}_{12\ldots m}(\lambda_j) = \sum_{\alpha=1}^{2n-3} \frac{\partial k}{\partial \xi_\alpha} \Delta^{(i)} \xi_\alpha \tag{9b}$$

for every value $\lambda = \lambda_j$. Since there are a like number of equations and unknowns (2n-3), the ϵ_j can be reduced, in theory, to zero. (More than one iteration is required because of the assumption involved in equation (8)). When the ϵ_j are zero, the condition of equation (5a) is satisfied.

For the purpose of reducing the effect of errors in individual data points, the following least-square modification

was used. Minimize the function:

$$\sum^{m} \left[\epsilon_j^{(i)} - \Delta k_{12\ldots n}^{(i)}(\lambda_j)\right]^2 \qquad m > 2n-3 \tag{10}$$

with respect to the $\Delta\xi_\alpha$, viz:

$$\begin{aligned} 0 &= \frac{\partial}{\partial \Delta\xi_\alpha} \sum_{j=1}^{m} \left[\epsilon_j^{(i)} - \Delta k_{12\ldots n}^{(i)}(\lambda_j)\right]^2 \qquad \alpha = 1, 2, \ldots 2n-3 \\ &= \sum_{j=1}^{m} \frac{\partial}{\partial \Delta\xi_\alpha} \left[\epsilon_j^{(i)} - \Delta k_{12\ldots n}^{(i)}(\lambda_j)\right]^2 \\ &= \sum_{j=1}^{m} \left[\epsilon_j^{(i)} - \Delta k_{12\ldots n}^{(i)}(\lambda_j)\right] \frac{\partial \Delta k_{12\ldots n}^{(i)}(\lambda_j)}{\partial \Delta\xi_\alpha} \\ &= \sum_{j=1}^{m} \left[\epsilon_j^{(i)} - \Delta k_{12\ldots n}^{(i)}(\lambda_j)\right] \frac{\partial k_{12\ldots n}^{(i)}(\lambda_j)}{\partial \xi_\alpha} \end{aligned} \tag{11}$$

By virtue of (9b) this becomes:

$$\begin{aligned} &\sum_{j=1}^{m} \frac{\partial k_{12\ldots n}^{(i)}(\lambda_j)}{\partial \xi_\alpha} \sum_{\beta=1}^{2n-3} \frac{\partial k_{12\ldots n}^{(i)}(\lambda_j)}{\partial \xi_\beta} \Delta\xi_\beta = \sum_{j=1}^{m} \epsilon_j^{(i)} \frac{\partial k_{12\ldots n}^{(i)}(\lambda_j)}{\partial \xi_\alpha} \\ &\sum_{\beta=1}^{2n-3} \Delta\xi_\beta \sum_{j=1}^{m} \frac{\partial k_{12\ldots n}^{(i)}(\lambda_j)}{\partial \xi_\alpha} \frac{\partial k_{12\ldots n}(\lambda_j)}{\partial \xi_\beta} = \sum_{j=1}^{m} \epsilon_j^{(i)} \frac{\partial k_{12\ldots n}(\lambda_j)}{\partial \xi_\alpha} \end{aligned} \tag{12}$$

for $\alpha = 1, 2, \ldots, 2n-3$. These equations can be summarized in matrix notation, as follows:

$$\left[\Pi_{\alpha\beta}\right]\left\{\Delta\xi_\beta\right\} = \left\{\Lambda_\alpha\right\} \tag{13}$$

$$\Pi_{\alpha\beta} = \sum_{j=1}^{m} \frac{\partial k_{12\ldots n}^{(i)}(\lambda_j)}{\partial \xi_\alpha} \frac{\partial k_{12\ldots n}^{(i)}(\lambda_j)}{\partial \xi_\beta}$$

$$\Lambda_\alpha = \sum_{j=1}^{m} \epsilon_j^{(i)} \frac{\partial k_{12\ldots n}(\lambda_j)}{\partial \xi_\beta}$$

The solution vector is obtained in a straightforward manner by any of the standard methods of linear algebraic equations. Then

$$\xi_\alpha^{(i+1)} = \xi_\alpha^{(i)} + \Delta\xi_\alpha^{(i)}$$

$$k_{12\ldots n}^{(i+1)}(\lambda_j) = k_{12\ldots n}^{(i)}(\lambda_j, \xi^{(i+1)})$$

and the entire process is repeated until the $\epsilon_j^{(i)}$ no longer diminish in size at each iteration, or until the minimum significant error (data roundoff) in K is reached.

Here, it is seen that a solution to this formulation also satisfies equation (6), but the solution is obtained in a rather roundabout fashion.

Steepest Descent

The usual procedure is to minimize the function by changing one parameter at a time so as to make as great a reduction as possible, and then to proceed with another parameter, repeating the process until no further improvement can be made. The parameter chosen to be changed at each iteration is that which contributes the largest component to the gradient of the function K, and the amount by which it is to be changed is estimated by an approximation of the Newton type $\left(K/\frac{\partial K}{\partial \xi}\right)$, or by trial and error. The method as applied in this work was modified in several ways, as dictated by the computing facility and the particular problem.

Rather than search for the best parameter to change each time, it was thought more advisable to change all parameters simultaneously. Thus

$$K\left(\xi_\alpha^{(i+1)}\right) = K\left(\xi_\alpha^{(i)} - MK_\alpha^{(i)}\right) \tag{14}$$

where M is chosen to minimize $K\left(\xi_\alpha^{(i+1)}\right)$ each time, and $K_\alpha{}^{(i)}$ is the contribution of a change in $\xi_\alpha^{(i)}$ to the gradient of $K\left(\xi_\alpha^{(i)}\right)$. In practice it was found expedient to modify $K^{(i)}$

from its true value

$$K_\alpha^{(i)} = \frac{\partial K(\xi_\alpha^{(i)})}{\partial \xi_\alpha^{(i)}} \left[\sum_\beta \left(\frac{\partial K(\xi_\beta^{(i)})}{\partial \xi_\beta^{(i)}} \right)^2 \right]^{-\frac{1}{2}}$$

to

$$K_\alpha^{(i)} = \xi_\alpha \frac{\partial K(\xi_\alpha^{(i)})}{\partial \xi_\alpha^{(i)}} \left[\sum_\beta \left(\xi_\beta \frac{\partial K(\xi_\beta^{(i)})}{\partial \xi_\beta^{(i)}} \right)^2 \right]^{-\frac{1}{2}} \qquad (15$$

in order to compensate for the tendency of the method to ignore parameters of very large numerical values until the very end of the iteration. The change was helpful in some cases, but it is not certain that it was helpful in all. This tendency to ignore some parameters could be very troublesome in a problem of this nature, where all parameters are not dimensionally equivalent.

The method of calculation of M (equation 14) was developed in an empirical fashion, and could probably be improved upon with great advantage in reducing computing time. A first estimate was obtained by approximating the ratio of first to second derivatives of K along the path, s, of grad K,

$$M = \frac{K_s}{K_{ss}} \quad \frac{\sum_i \frac{\partial K}{\partial \xi_\alpha} \Big/ \frac{d\xi_\alpha}{ds}}{\sum_i \frac{\partial^2 K}{\partial \xi_\alpha^2} \Big/ \left(\frac{d\xi_\alpha}{ds}\right)^2} \qquad (16)$$

Trial values of K were then calculated using multiples $c_1 M'$ and $c_2 M'$ and equation (14), c_1 and c_2 being near unity and unequal. The trial values of K obtained, plus the value $K(\xi_\alpha^{(i)})$ itself (corresponding to M' multiplied by $c_3 = 0$) were used to interpolate for a new value of M. Two kinds of interpolation were used, depending on proximity of K to a minimum. Letting the first two trial values of K be Θ_1 and Θ_2 ,

corresponding to c_1 and c_2, when

$$|\theta_1-\theta_2| < K(\xi_\alpha^{(i)})$$

a linear interpolation to $\theta=0$ was used. When

$$|\theta_1-\theta_2'| \geq K(\xi_\alpha^{(i)})$$

however, a second order interpolation to θ = minimum was used. That is, at the beginning of the calculations, when $K(\xi_\alpha^{(i)})$ is large, it was assumed

$$\theta_1 = c_1\alpha + \beta$$
$$\theta_2 = c_2\alpha + \beta$$

Solving for $\theta = 0$

$$c = \frac{\theta_2-\theta_1}{c_1-c_2}$$

As the iterations proceeded, $K(\xi_\alpha^{(i)})$ decreased, until a point was reached at which

$$|\theta_1-\theta_2| \geq K(\xi_\alpha^{(i)})$$

and thence the second order interpolation was employed. Assuming

$$\theta_1 = c_1^2\alpha + c_1\beta + \gamma$$
$$\theta_2 = c_2^2\alpha + c_2\beta + \gamma$$
$$\theta_3 = K(\xi_\alpha^{(i)}) = \gamma \qquad (c_3=0)$$

and solving for θ = minimum

$$c = -\frac{c_1^2(\theta_2-\theta_3) + c_2^2(\theta_3-\theta_1)}{\theta_1 c_1 - \theta_2 c_2 + \theta_3(c_1-c_2)}$$

In the numerical analyses, c has generally been between $\frac{1}{2}$ and 3/2, indicating that the estimate M' is not too far wrong.

The iteration then proceeded, using

$$M = cM'$$

in equation (14).

Because of the very great flexibility of the procedure, M' could probably be estimated sufficiently well by replacing equation (16) with

$$M' = \frac{K}{K_s}$$

at a considerable saving in computing time. Alternatively, the interpolations might be eliminated by a better estimate of M' in the third order iteration.

The procedure followed here, effectively an interpolation within an interpolation, might be critized as highly inefficient, inasmuch as three times as many values of K are calculated as are actually used in a normal iteration. However, it was found that the procedure justified itself by a convergence of K at four to five times the rate without these inner interpolations.

RESULTS AND DISCUSSION

Programs which would perform the analyses were written for the M I T Whirlwind computer. These programs were designed for the three-layer case (n=3), with the object of studying the accuracy required of a kernel for a definite solution, and for observing the behavior of the method under the non-ideal circumstances (excess layers, random errors, lateral resistivity

variations, etc.) which exist in field data.

In the majority of cases, 10 values of $\lambda_j (m=10)$, were used. All kernels were normalized to $\rho_1 = 1$, and the theoretical kernels to $d_1 = 1$. The input data were:

(a) the number and values of λ_j

(b) values of ρ_1 and ρ_3

(c) estimates of ρ_1 , d_1, and d_2

(d) the kernel values $k(\lambda_j)$

and the output consisted of the values computed for ρ_2, d_1, and d_2. Operation was entirely automatic, calculation ceasing only when the value of K reached a preset value, or began to oscillate in random fashion. Before beginning, an algebraic simplification was made by dealing with

$$f(\lambda) = 1/[1 + k(\lambda)] - \tfrac{1}{2} \qquad \text{(data)}$$

and

$$f_{123}(\lambda) = 1/[1 + k_{123}(\lambda)] - \tfrac{1}{2} = \tfrac{1}{2}\mu_{123}\, e^{-2\lambda d} \qquad \text{(function)}$$

rather than with $k(\lambda)$ and $k_{123}(\lambda)$.

Several hundreds of kernels were calculated on the Whirlwind, using expressions (2). Others, including apparent resistivity data from the field, were made available through the kindness of Mr. E. E. Maillot, of Douglas, Arizona. It was believed that the thin second layer situation would be the most critical test of the method, and 25 three-layer cases of this kind were analyzed, in addition to two four-layer cases and five field cases. The majority were first done with a Newton technique developed earlier (Vozoff, 1955a). The Steepest Descent ap-

proach was used to attempt to overcome the difficulties encountered with the Newton method and proved to be better able to handle the thin-layer case.

All theoretical kernels were calculated to an accuracy of seven decimal places, and rounded off to the desired accuracy, usually three places, for analysis. The result of this, of course, was the introduction of a random error ϵ of .5 maximum in the last place. Since the values of $k_3(\lambda)$ ranged between zero and 10, the individual errors in $f_3(\lambda)$ were between ϵ and $\epsilon/11$. However, the individual percentage errors in $f_3(\lambda)$ were in general much higher than in $k_3(\lambda)$, especially at large λ where $k_3(\lambda)$ went to unity asymptotically.

Results obtained with both techniques applied to theoretical three-layer kernels are presented in Table 1, and Figures 2 - 31 . Analyses of four-layer kernels by the Newton Method are presented in Table 2 and Figures 32 - 35 , and analyses of field data by both methods are given in Table 3 and Figures 36 - 41 . Slichter kernels for the cases analyzed are shown in Figures 2,4,7,12,16,20,25,29,32,38.

With regard to the three-layer analyses, Steepest Descent was applied in cases where the Newton Method had difficulty, as mentioned earlier. Two additional very difficult cases were done with Steepest Descent only (26 and 27).

The nature of the results was found to rest upon several factors, some of which are not yet fully understood. Success of solution can be measured by two criteria, the closeness of fit, K, and the quantity $\rho_2 d_2$ or d_2/ρ_2, as appropriate.

a) The ratio d_2/d_1 appears to be the single most important factor, as might be expected. The larger this ratio, the better the solution. No obvious correlation would be found with any of the other parameters.

b) Improvement of data accuracy will usually result in a better solution (compare Cases 9a and 9b, 13a and 13b, 14a and 14b, 17a and 17b and 19a and 19b). Case 26, an extremely difficult one, shows little improvement with more accurate data.

c) Different initial estimates of parameter values sometimes led to slightly different solutions in the Newton Method. This behaviour was not observed in Steepest Descent analyses.

Experience with the Newton Method in the present application has shown that, in initial iterations, the magnitude of changes are often over-estimated. In addition, the direction of change for some (never all) of the parameters may be in the wrong direction during a large portion of the iterations. As $K(\xi_\alpha)$ becomes smaller, predictions assume their expected behaviour. The iterations normally continue in this fashion until some small value of $K(\xi_\alpha)$ is reached at which time they begin to oscillate in apparently random manner. Due to the unusual nature of the function being minimized, the oscillations may be unstable if $K(\xi_\alpha)$ is sufficiently large. Two possible causes of the overshoot are:

a) negative second partial derivatives of $k_{12}...(\lambda_j)$ with respect to the ξ_α*.

b) non-zero minimum error.

In most cases, the solution could be made to converge only by reducing the magnitude of changes made in the parameters at each iteration to a small fraction of that calculated. The fraction was then systematically increased to unity near the solution.

It appears that, in view of the factors discussed, the Newton Method is more sensitive to data inaccuracy than is Steepest Descent as used here and therefore the latter is to be preferred in any practical work.

Figure 1 shows the progress and final results of one Steepest Descent solution (Case 27). In the first row are true values of ρ_2, d_2, d_1, ρ_1 and ρ_3. The numbers to the right of the vertical slashes representing the exponent of ten. In the second row are the first estimates of ρ_2, d_2 and d_1 and $K(\xi_\alpha)$ due to error of estimation. The third and fourth lines are θ_1 and θ_2 (see section on Method), and the fifth line is c. On the sixth line are the results of the first iteration. The second layer resistivity, ρ_2, has gone from 5×10^{-2} to 2.1295×10^{-1}, d_2 from 1×10^{-1} to -6.2728×10^{-2}, d_3 from 1.4×10^{0} to 1.3568×10^{0}; and $K(\xi_\alpha)$ from 7.307×10^{-2} to 1.034×10^{-4}. The θ_1 and θ_2 of the second

* see Hildebrand, 1949, p. 364.

iteration appear on lines 7 and 8, etc. The space between lines 8 and 9, 12 and 13, etc. which does not occur between lines 4 and 5 indicates that the program has switched from the linear interpolation to the second order interpolation.

Comparison of lines 1, 2 and 6 shows that, although $K(\xi_\alpha)$ has been reduced considerably, the changes in ρ_2 and d_2 have overshot the mark, and the solution is forced to backstep, $K^{(2)}(\xi_\alpha)$ being considerably larger than $K^{(1)}(\xi_\alpha)$. In the second iteration, this overshoot is compensated by a large increase in d_1. Succeeding iterations then recover slowly from the shock of the first estimates. The entire process required about 4.5 minutes on the Whirlwind Computer.

A comparison of the results of the two methods applied to field cases B and C, shows that the solutions are very similar. In all cases, however, $d_2 > d_1$ so that the agreement is not unexpected.

Examination of the curves of resistivities, integrated potentials, and Slichter kernels, Figures 36 - 38 shows several interesting factors regarding their behavior. With the possible exception of case B, none of the resistivity curves display the form expected of a three-layer case. The curves are ragged, especially at small r. In the process of integration to $r\phi(r)$ many of the "irregularities" have disappeared, and after the second integration to $k(\lambda)$ the curves have become quite smooth. However, much of this detail may have appeared in $k(\lambda)$ for $\lambda > 1$. At this highest value of the kernels differ considerably from their asymptotic value

($k(\lambda)\rightarrow 1$ as $\lambda\rightarrow\infty$), and therefore a great deal of shallow detail must have been eliminated.

Regarding individual cases, Case A did not satisfy the initial assumptions in two respects:

a) the $r\phi(r)$ did not reach a constant value at large r, and smoothing was necessary with attendant uncertainty in ρ_3.

b) lateral variation and possible anisotropy existed as shown by later field measurements.

Drilling showed a weak conductor at a depth of 6.2. Note that the solution is nearly degenerate.

Case B drilling encountered a conductor at a depth of 5.0. Case C would appear to be of at least four layers, from the apparent resistivity curves. Likewise, Case E appears to be at least four layers. Note that its solution is degenerate giving an equivalent two-layer solution of

$$\rho_1 = 1.0 \qquad \rho_2 = 0.147$$
$$d_1 = 0.53$$

Case D, which had the smoothest apparent resistivity variation, also had the smallest minimum error of solution, 3.1×10^{-7}. This value is probably considerably smaller than the data errors, and, as such, is deceptive.

No drill data are available on cases C, D, or E.

It would seem that, in the present work on field data, the kernels should have been integrated to a larger value of λ in order to allow definition of shallower structure. For this same purpose, further analysis programs should assume more

layers: at least four, and probably five.

One interesting result noted in all of the work with theoretical kernels is that, in these thin layered cases, a fixed relationship was found to hold between the resistivity and thickness of the second layer in successive iterations. That is, if

$$d_2 \ll 1 \qquad (\rho_1 = d_1 = 1)$$

then

$$d_2 \rho_2 = c_1 \qquad \rho_2 \gg 1$$

and

$$d_2 / \rho_2 = c_2 \qquad \rho_2 \ll 1$$

where c_1 or c_2 is approximately equal to the value obtained using the exact values of d_2 and ρ_2. This was so even if the individual values of resistivity and thickness were far from their true values. That this should be so, and is a kind of indeterminacy can be shown as follows. The approximate expression for $f_{123}(\lambda)$ in the case $d_2 \ll 1$, is

$$f_{123}(\lambda) \approx \frac{t_1}{2} \frac{\rho_1 - \rho_3 - (\rho_1 + \rho_2)(\rho_2 - \rho_3)\lambda d_2 / \rho_2}{\rho_1 + \rho_3 - (\rho_1 - \rho_2)(\rho_2 - \rho_3)\lambda d_2 / \rho_2}$$

where $t_1 = e^{-2\lambda d_1}$, and assuming

$$e^{-2\lambda d_2} \approx 1 - 2\lambda d_2$$

Thus, if

$$\rho_2 \to \infty$$

in a manner such that

$$\rho_2 d_2 = c_1$$

then

$$f_{123}(\lambda) \to \frac{t_1}{2} \frac{\rho_1 - \rho_3 - c_1 \lambda}{\rho_1 + \rho_3 + c_1 \lambda}$$

If

$$\rho_2 \longrightarrow 0$$

in a manner such that

$$d_2/\rho_2 = c_2$$

$$f_{123}(\lambda) \longrightarrow \frac{t_1}{2} \frac{\rho_1 - \rho_3 + \rho_1\rho_3 c_2 \lambda}{\rho_1 + \rho_3 + \rho_1\rho_3 c_2 \lambda}$$

The limiting value of $f_{123}(\lambda)$ in both cases is independent, to a first approximation, of ρ_2 or d_2 individually.

Ultimate Resolving Power of Resistivity Data

Given a thin conductor, whose depth, thickness, and resistivity are known approximately, it would be highly desirable to be able to predict whether its presence can be verified and its location established by field measurements, neglecting analysis difficulties. Assuming for simplicity that the problem is to distinguish a two-layer kernel (ρ_1, d_1, ρ_3) from a three-layer kernel ($\rho_1, d_1, \rho_2, d_2, \rho_3$) in which $d_2 << d_1$, and

$$\rho_2 d_2 = c_1$$

or

$$d_2/\rho_2 = c_2$$

as appropriate, a functional inequality would be required relating c to the data errors and layer parameters. That is

$$F_1(c) > F_2(d_1, \rho_1, \rho_3, \Delta_R)$$

in order for the center layer to be detectable, where Δ_R is the largest relative error in any data point. If it can

be assumed that the condition

$$\sum_{i=1}^{m}\left[\Delta f_3(\lambda_i)\right]^2 > \sum_{i=1}^{m}\left[\epsilon_f(\lambda_i)\right]^2$$

is necessary for the analysis to be able to differentiate between the two nearly identical cases, it can be shown that

$$c_1^2\sum_i\left[\frac{t_i\lambda_i}{\rho_1+\rho_3+c_1\lambda_i}\right]^2 > \frac{\Delta^2 k}{16\rho_1^2}\sum_i\left[\rho_1+\rho_3-(\rho_1-\rho_3)t_1\right]^2 \qquad \rho_2\to\infty$$

and

$$c_2^2\sum_i\left[\frac{t_i\lambda_i}{\rho_1+\rho_3+c_i\lambda_i}\right]^2 > \frac{\Delta^2 k}{16\rho_3^2}\sum_i\left[\rho_1+\rho_3-(\rho_1-\rho_3)t_1\right]^2 \qquad \rho_2\to 0$$

are <u>sufficient</u> conditions for resolution. In these inequalities the $\Delta f_3(\lambda_i)$ are the differences between the exact values of the functions $f_3(\lambda_i)$ and $f_2(\lambda_i)$, and the $\epsilon_f(\lambda_i)$ are the absolute errors of the function $f_3(\lambda_i)$ resulting from errors in the original measurements. Several examples were calculated for $d_1=\rho_1=1$, and for various values of ρ_3, to examine the importance of the value of this latter parameter. Using the same values of λ as were used in the analyses (1.0, .6, .4, .2, .1, .06, .04, .02, .01, .006, m=10), and Δ_k=.01 (relative error of measurements), the following minimum values of c_1 and c_2 were obtained:

ρ_3	c_1	c_2
10^{-3}	10^{-2}	Impossible
10^{-2}	10^{-2}	170
10^{-1}	1.4×10^{-2}	1.5
1	9.6×10^{-2}	9.6×10^{-2}
10	5.5	4.6×10^{-2}
10^2	3.3×10^{3}	4.1×10^{-2}
10^3	Impossible	4.1×10^{-2}

It is seen that, with data accurate to one percent, a conductive center layer cannot be distinguished if $\rho_3 < 10^{-3}$, and a resistive center layer cannot be distinguished if $\rho_3 > 10^3$. An increase of data accuracy to .1 percent would extend this range of ρ_3 by a factor of 10, roughly.

III GENERAL RESISTIVITY VARIATION IN THREE DIMENSIONS

The general approach used in solving the horizontal layering problem cannot be extended to cover general multi-dimensional variation. This is so because the differential equation relating potential and conductivity is no longer separable, as will be seen below. What is sought, then, is some other method of relating subsurface conductivity to surface potential variations.

Assuming a continuous, inhomogeneous, isotropic resistivity function,

$$\sigma = \sigma(P) \qquad 0 < \sigma < \infty$$

the differential equation for potential at a point P due to a source at point Q, is

$$\nabla^2 \phi(P,Q) = -\nabla S(P) \cdot \nabla \phi(P,Q) - \frac{\delta(P,Q)}{\sigma(Q)} \equiv \rho(P,Q) \quad (17)$$

$$S(P) = \log \sigma(P)$$

$P = P(p_1, p_2, p_3)$ observer coordinates

$Q = Q(q_1, q_2, q_3)$ source coordinates

If the expression is considered a kind of Poisson equation, $\rho(P,Q)$ represents the "sources". Equation (17) arises directly

from conservation of current. The usual boundary conditions must be imposed on all solutions.

For the purposes of the discussion which follows, it is necessary that the differential equation be transformed into the corresponding integral equation. This is done by treating equation (17) as if it were a Poisson equation, and performing the obvious integration:

$$4\pi\phi(P,Q) = \int_R G(P,R)\rho(R,Q)dR \tag{18}$$
$$= \int_R G(P,R)\frac{\delta(R,Q)}{\sigma(Q)}dR + \int_R G(P,R)\nabla S(R)\cdot\nabla\phi(R,Q)dR$$

over all space. In the geophysical problem measurements are made on the surface $p_3=0$ of a half-space, and

$$\sigma = \sigma(P) \quad p_3 > 0$$

$$\sigma = 0 \quad p_3 < 0$$

The boundary conditions are satisfied if we take

$$G(P,Q) = 1/r_{PQ}$$

$$\sigma(p_1,p_2,p_3) = \sigma(p_1,p_2,-p_3)$$

$$r_{PQ} = \left[(p_1-q_1)^2 + (p_2-q_2)^2 + (p_3-q_3)^2\right]^{\frac{1}{2}}$$

Rewriting equation (18) and substituting the Green's function.

$$4\pi\phi(P,Q) = \frac{1}{r_{PQ}\sigma(Q)} + \int_R \frac{\nabla S(R)\cdot\nabla\phi(R,Q)}{r_{RP}}\,dR \tag{19}$$

and we desire a solution for σ in terms of ϕ. Equation (19) is an integro-differential equation for σ which is

(a) nonlinear

(b) inhomogeneous

and (c) singular in kernel and limits

in three dimensions. As such, no exact solution could be devised, and it can be safely said that none exists. Mathematical work is being carried on at the present time on problems (a) and (c).

The most formidable of the individual difficulties, probably, is the nonlinearity. Since a linear approximation can be devised rather readily, an effort was made to see if this approximation could be solved, and under what conditions it was valid. The simplification consists of setting

$$\phi(R,Q) \approx 1/r_{RQ}\ \sigma(Q)$$

in the right side of equation (19). Thus

$$4\pi\phi(P,Q) \approx \frac{1}{\sigma(Q)r_{PQ}} + \frac{1}{\sigma(Q)}\int_R \frac{VS(R)\cdot V(1/r_{RQ})dR}{r_{RP}}$$

$$\approx \frac{1}{\sigma(Q)r_{PQ}} + \frac{1}{\sigma(Q)}\int_R \frac{VS(R)\cdot r_{RQ}dR}{r_{RP}\ r_{RQ}^3} \qquad (20)$$

This is equivalent to substituting the entire expression for ϕ (right side of equation (19)) for ϕ under the integral, and retaining the first term only. The substitution is a standard method of solving integral equations.

The problem was carried to this point by Stevenson (1934) who was unable to solve it. Several methods of solution, including expansions in Fourier integrals and in orthogonal functions, were attempted in connection with present work, with no results of practical value.

A practicable numerical solution was devised, however, from rather different considerations. Assuming (a) that all resistivity changes occur within a limited volume, T, and (b) that the actual resistivity distribution of this volume can be approximated by an array of rectangular blocks, each homogeneous and isotropic, equation (20) can be written

$$\sigma(Q)4\pi\phi(P,Q) - \frac{1}{r_{PQ}} \approx \int_T \frac{\nabla S(R)\cdot r_{RQ}}{r_{RP}\, r_{RQ}^3} dR \equiv \theta(P,Q) \qquad (21)$$

Contributions to the integral will arise only at the faces of blocks. At such an interface the integrand will become

$$\frac{\nabla S(R)\cdot r_{RQ}}{r_{RP}\, r_{RQ}^3} = \frac{\Delta S_\alpha \hat{n}_\alpha \cdot r_{RQ}}{r_{RP}\, r_{RQ}^3} \qquad (22)$$

and the integral will be

$$\theta(P,Q) = \sum_\alpha \Delta S_\alpha \hat{n}_\alpha \cdot \int_\alpha \frac{r_{RQ}}{r_{RP} r_{RQ}^3} dR \qquad (23)$$

where

$\hat{n}_\alpha$ is the unit vector normal to the interface
α is an index for the particular interface, $\alpha = 1, 2, - - -, \beta$

The integrals are now in two dimensions rather than three. Equation (23) can be rewritten

$$\theta(P,Q) = \sum_\alpha C_\alpha(P,Q)\Delta S_\alpha \qquad (24)$$

$$C_\alpha(P,Q) = \int_\alpha \frac{\hat{n}_\alpha \cdot r_{RQ}}{r_{RP} r_{RQ}^3} dR$$

which is a linear equation in the ΔS_α. If the blocks are cubes

of unit dimension, and the volume of variation is assumed to be of dimensions lxmxn, there are l(mxn) + (m+1) (lxn) + (n+1) (lxm) = $\wp$ interfaces, and lxmxn = γ unknown conductivities. Thus equation (24) can be written as a linear equation in γ unknowns

$$\theta(P,Q) = \sum D_{ijk}(P,Q)\, S_{ijk}$$

$$D_{ijk}(P,Q) = 2\left\{\hat{i}\cdot\left[\iint_{\alpha_1} I(P,Q,R) - \iint_{\alpha_2} I(P,Q,R)\right] + \hat{j}\cdot\left[\iint_{\alpha_3} I(P,Q,R) - \iint_{\alpha_4} I(P,Q,R)\right] + \hat{k}\cdot\left[\iint_{\alpha_5} I(P,Q,R) - \iint_{\alpha_6} I(P,Q,R)\right]\right\}$$

$$I(P,Q,R) = \frac{r_{RQ}\, dA}{r^3_{RQ}\, r_{RP}}$$

where α_1 is the surface bounding cubes (i-1), j, k and (i,j,k), α_2 bounds cubes (i,j,k) and (i+1), j, k , α_3 bounds i, (j-1), k and (i,j,k), etc. The factor of 2 arises from the symmetry about the plane p_3=0.

Values of the coefficients d_{ijk} are now being integrated on the M.I.T. Whirlwind Computer by Hallof and Ness (1955). It remains to be seen just how effectively the method will handle the problem.

IV CONCLUSIONS

The methods described can be applied in a straightforward manner, with the aid of a high-speed computer. The solutions

obtained, at least in the horizontal layering analysis, are probably as good as can be obtained by any means, depending chiefly on the quality of the data. From the standpoint of the geophysicist in the field, however, neither is very satisfactory, as they require time-consuming, expensive processing of the data. The improvement of the solution, over that obtainable by matching curves, is questionable with the data accuracy ordinarily obtained. Only in situations where it is considered sufficiently important to improve the accuracy of measurements will these techniques be of real advantage.

TABLE 1

THREE-LAYER ANALYSES OF THREE-LAYER KERNELS

Case	TRUE VALUES ρ_1 / d_1	ρ_2 / d_2	ρ_3	$\rho_2 d_2$ / d_2/ρ_2	SOLUTION ρ_1 / d_1	ρ_2 / d_2	ρ_3 / K	$\rho_2 d_2$ / d_2/ρ_2	A**
1*	1 1	1 1	1		1. 1.06	1.00 2.05	1 10^{-14}		8
2	1 1	.1 10	10	100	1 1.00	.100 9.98	10 7×10^{-8}	100.	4
3	1 1	.1 1	1	10	1 .997	.105 1.05	1 5×10^{-7}	10.0	5
4	1 1	.1 1	10	10	1 1.00	.0994 .994	10 4×10^{-7}	10.0	5
5	1 1	.05 .5	5	10	1 1.12	2.5×10^{-4} 3.2×10^{-3}	5 6×10^{-3}	12.6	3
5***	1. 1.	.05 .5	5.	10.	1. .962	.101 1.01	5. $6.\times10^{-6}$	10.	3
6	1 1	10 .5	.2			no solution			3
6***	1. 1.	10. .5	.2	5.0	1. .923	4.26 1.20	.2 $5.\times10^{-7}$	5.11	3
7	1 1	.05 .5	.2	10	1 1.002	.0480 .485	.2 2×10^{-7}	10.1	3
8	1 1	10 .5	5	5	1 1.004	11.3 .424	5 9×10^{-8}	4.9	3
9a	1 1	.05 .1	5	2	1 .973	.203 .412	5 8×10^{-8}	2.03	3

TABLE 1

THREE-LAYER ANALYSES OF THREE-LAYER KERNELS

Case	TRUE VALUES ρ_1 / d_1	ρ_2 / d_2	ρ_3	$\rho_2 d_2$ / d_2/ρ_2	SOLUTION ρ_1 / d_1	ρ_2 / d_2	ρ_3 / K	$\rho_2 d_2$ / d_2/ρ_2	A**
9b	1 1	.05 .1	5	2	1 .996	.0888 .178	5 5×10^{-11}	2.00	5
10	1 1	10 .1	.1	1	1 .645	20.9 .0468	.1 3×10^{-3}	.978	3
10a***	1. 1.	10. .1	.1	1.	1. .742	1.42 .893	.1 1.7×10^{-7}	1.27	3
10b***	1 1	10 .1	.1	1	1 .987	19.3 .0524	.1 7×10^{-7}	1.01	3
10c***	1. 1.	10. .1	.1	1.	1. 1.22	19.6 .0443	.1 $9.\times10^{-5}$		3
11	1 1	10 .1	.2	1	no solution				3
11***	1. 1.	10. .1	.2	1.	1. .988	19.5 .0516	.2 $6.\times10^{-7}$	1.01	3
12	1 1	.5 .1	10	.2	1 .688	.992 .504	10 10^{-6}	.508	3
13a	1 1	.1 .1	1	1	1 .903	.436 .535	1 8×10^{-8}	1.23	3
13b	1 1	.1 .1	1	1	1 1.000	.0994 .0994	1 6×10^{-14}	1.00	8
14a	1 1	10 .1	1	1	1 .992	5.98 .171	1 10^{-10}	1.02	5
14b	1 1	10 .1	1	1	1 .996	6.92 .146	1 7×10^{-8}	1.01	3

TABLE 1

THREE-LAYER ANALYSES OF THREE-LAYER KERNELS

Case	TRUE VALUES ρ_1 / d_1	ρ_2 / d_2	ρ_3	$\rho_2 d_2$ / d_2/ρ_2	SOLUTION ρ_1 / d_1	ρ_2 / d_2	ρ_3 / K	$\rho_2 d_2$ / d_2/ρ_2	A**
16	1 1	.75 .1	.1	.133	1 .651	1.87 .155	.1 10^{-3}	.083	3
17a	1 1	.05 .1	.2	2	1 .976	.171 1.12	.2 3×10^{-6}	6.6	3
17b	1 1	.05 .1	.2	2	.1 .997	.075 .158	.2 4×10^{-11}	2.11	5
18*	1 1	10 .1	5	1	1 .917	5.00 -7.18	5 10^{-4}	-36.	3
19a	1 1	1.5 .1	1	.15	1 1.39	.708 .0840	1 10^{-4}		3
19b	1 1	1.5 .1	1	.15	1 .996	1.46 .108	1 5×10^{-12}	.157	5
20	1 1	.1 .01	10	.1	1 3.51	.012 4.08×10^{-4}	10 8×10^{-3}	.033	3
21	1 1	100 .01	1	1	1 .904	2.20 .543	1 10^{-5}	1.20	3
22	1 1	2 .01	10	.02	1 .976	31.4 -.003	10 6×10^{-5}	-.094	3
26a***	1 1	.05 .01	5	.2	1 1.87	.514 -.33	5 3×10^{-6}		4
26b***	1 1	.05 .01	5	.2	1 1.87	.517 -.34	5 2.6×10^{-6}		6
27***	1 1	.1 .01	5	.1	1 .930	.120 .0198	5 9×10^{-8}	.165	6

TABLE 2 THREE-LAYER NEWTON ANALYSIS OF FOUR-LAYER KERNELS

Case	TRUE VALUES ρ_1 / d_1	ρ_2 / d_2	ρ_3 / d_3	ρ_4	SOLUTION ρ_1 / d_1	ρ_2 / d_2	ρ_3 / K	A
23	1 / 1	100 / 1	1 / 4	.01	1 / .977	49.2 / 2.12	.01 / 4×10^{-5}	3
24	1 / 1	.01 / 1	1 / 4	100	1 / .987	.0252 / 2.65	100 / 1.3×10^{-5}	3
25	1 / 1	10 / 4	1 / 1	.1	1 / 1.05	10.7 / 3.63	.1 / 10^{-3}	3

TABLE 3 THREE-LAYER ANALYSIS OF FIELD KERNELS

Case	FIRST ESTIMATE ρ_1 / d_1	ρ_2 / d_2	ρ_3 / K	SOLUTION ρ_1 / d_1	ρ_2 / d_2	ρ_3 / K
A	1. / .15	2.0 / 7.0	1.48 / 8.5×10^{-2}	1 / .145	1.53 / 271.3	1.48 / 2.4×10^{-4}
B	1 / .2	.6 / 4	.2 / 1.7×10^{-3}	1 / .152	.641 / 2.68	.2 / 1.2×10^{-5}
B***	1 / .15	.6 / 3	.2 / $3.\times10^{-4}$	1 / .174	.629 / 2.72	.2 / 1.3×10^{-5}
C	1 / .5	.4 / 4	.21 / 3.7×10^{-2}	1 / .271	.252 / 5.72	.21 / 1.7×10^{-4}
C***	1 / .3	.25 / 6	.2101 / 3.3×10^{-4}	1 / .272	.251 / 5.97	.2101 / 1.7×10^{-4}
D	1 / .1	.75 / 2	.175 / 1.2×10^{-2}	1 / .243	.708 / .882	.175 / 3.1×10^{-7}
E	1 / .2	.2 / 5	.147 / 1.2×10^{-2}	1 / -1.70	1.00 / +2.23	.147 / 2.1×10^{-5}

* Degenerate Solution

*** Steepest Descent Solution

	ρ_2		d_2	d_3	$-\frac{S_1}{K(\bar{\epsilon}_\infty)}$	ρ_2	ρ_3	
1	+1.0000| -01		+9.9999| -03	+9.9994| -01		+9.9994| -01	+5.0000| +00	TRUE VALUES
2	+5.0000| -02		+1.0000| -01	+1.3999| +00	+7.307|-02			FIRST ESTIMATES
3	+7.6| -05	θ_1						
4	+2.7| -03	θ_2						
5	+1.264| +00	ϕ						
6	+2.1295| -01		-6.2728| -02	+1.3568| +00	+1.034| -04	FIRST ITERATION	
7	+9.5| -05	θ_1						
8	+9.8| -05	θ_2						
9	+3.863| +02	ϕ						
10	+6.8679| -01		-5.3563| -01	+3.5125| +00	+3.744| -02	SECOND ITERATION	
11	+5.6| +08	θ_1						
12	+7.3| +05	θ_2						
13	+3.744| -01	ϕ						
14	+4.5066| -02		+9.3221| -02	+7.1077| -01	+7.118| -02	THIRD ITERATION	
	+1.4| -02							
	+2.7| -04							
	+8.577| -01							
	+1.1629| -01		+2.2125| -02	+7.1380| -01	+1.746| -03		
	+2.5| -03							
	+1.6| -04							
	+5.080| -01							
	+1.0480| -01		+3.3590| -02	+7.5295| -01	+5.108| -06		
	+5.7| -06							
	+4.8| -06							
	+4.797| -01							
	+1.0461| -01		+3.3781| -02	+7.5345| -01	+4.669| -06		
	+4.6| -06							
	+4.6| -06							
	-1.287| +01							
	+1.0409| -01		+3.4273| -02	+7.4767| -01	+5.218| -06		
	+5.2| -06							
	+5.1| -06							
	+5.564| -01							
	+1.0420| -01		+3.4169| -02	+7.4757| -01	+5.095| -06		
	+5.0| -06							
	+5.0| -06							
	+3.529| +00							
	+1.0430| -01		+3.4083| -02	+7.5039| -01	+4.984| -06		
	+5.0| -06							
	+4.9| -06							
	+5.648| -01							
	+1.0439| -01		+3.3985| -02	+7.5031| -01	+4.892| -06		
	+4.8| -06							
	+4.8| -06							
	+4.175| +00							
	+1.0440| -01		+3.3900| -02	+7.5364| -01	+4.825| -06		
	+4.8| -06							
	+4.8| -06							
	+5.446| -01							
	+1.0462| -01		+3.3774| -02	+7.5349| -01	+4.666| -06		
	+4.6| -06							
	+4.6| -06							
	+7.717| +00							
	+1.0489| -01		+3.3567| -02	+7.5887| -01	+4.521| -06		
	+4.6| -06							
	+4.3| -06							
	+5.362| -01							
	+1.0429| -01		+3.3425| -02	+7.5868| -01	+4.315| -06		
	+4.2| -06							
	+4.2| -06							
	+3.047| +02							
	+1.1408| -01		+2.5169| -02	+9.5075| -01	+2.513| -04		
	+9.5| -04							
	+1.5| -04							
	+4.227| -01							
	+1.1950| -01		+1.9761| -02	+9.2963| -01	+9.275| -08		
	+9.5| -08							
	+9.2| -08							
	+4.319| -01							
	+1.1949| -01		+1.9770| -02	+9.2969| -01	+9.167| -08		
	+9.1| -08							
	+9.1| -08							
	+1.195| +00							
	+1.1949| -01		+1.9767| -02	+9.2 72| -01	+9.158| -08		
	+9.1| -08							
	+9.1| -08							
	+6.253| -01							
	+1.1949| -01		+1.9766| -02	+9.2973| -01	+9.149| -08		
	+9.1| -08							
	+9.1| -08							
	+4.978| -01							
	+1.1949| -01		+1.9765| -02	+9.2975| -01	+9.156| -08		
	+9.1| -08							
	+9.1| -08							
	+7.17| -01							
	+1.1950| -01		+1.976 3| -02	+9.2977| -01	+9.140| -08		
	+9.1| -08							
	+9.1| -08							
	+4.13| -01							
	+1.1950| -01		+1.9762| -02	+9.2978| -01	+9.146| -08		
	+9.1| -08							
	+9.1| -08							
	+1.875| +00							

STEEPEST DESCENT
ITERATION PROCESS

Figure 1

Case 2

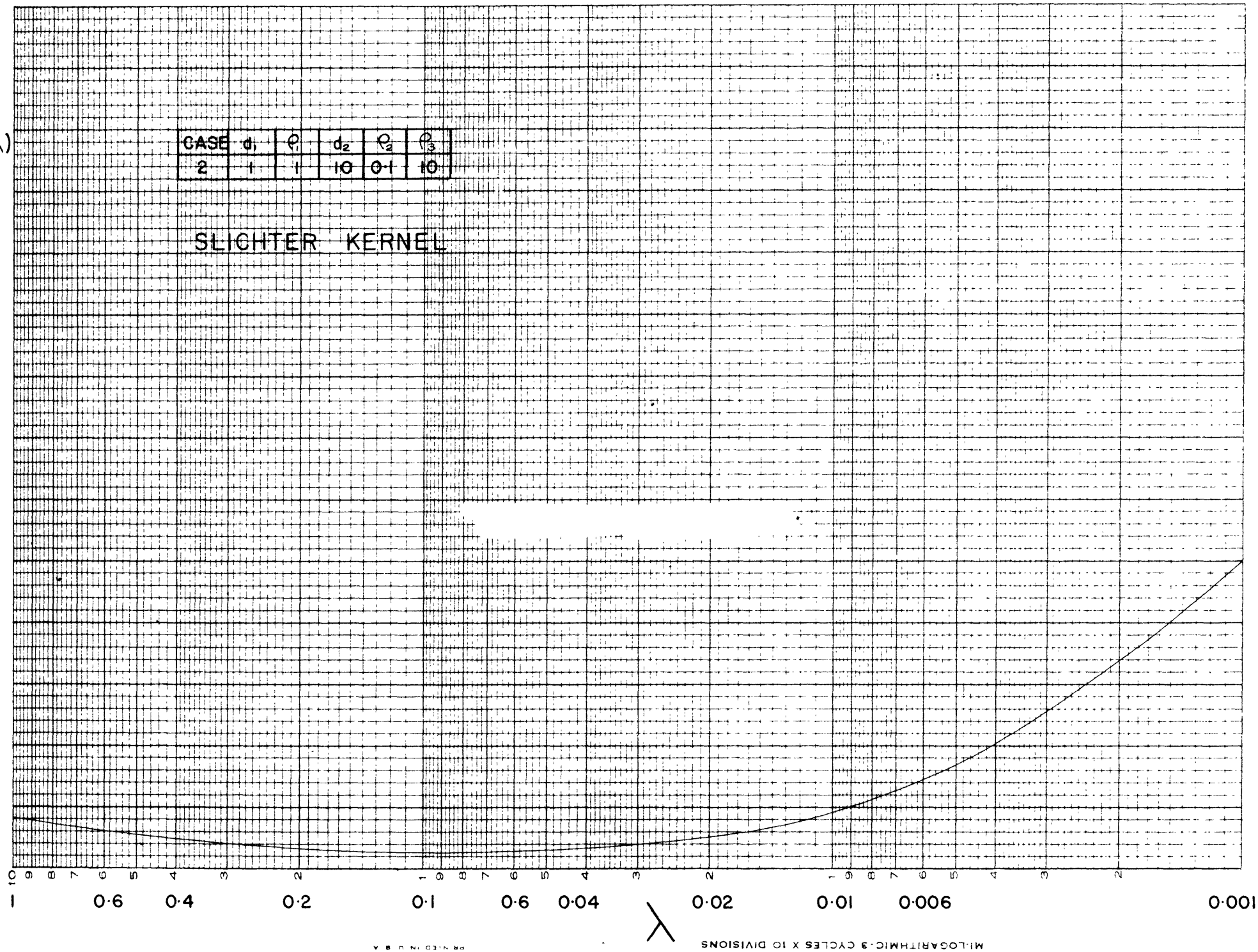

Fig. 2.

Case 2

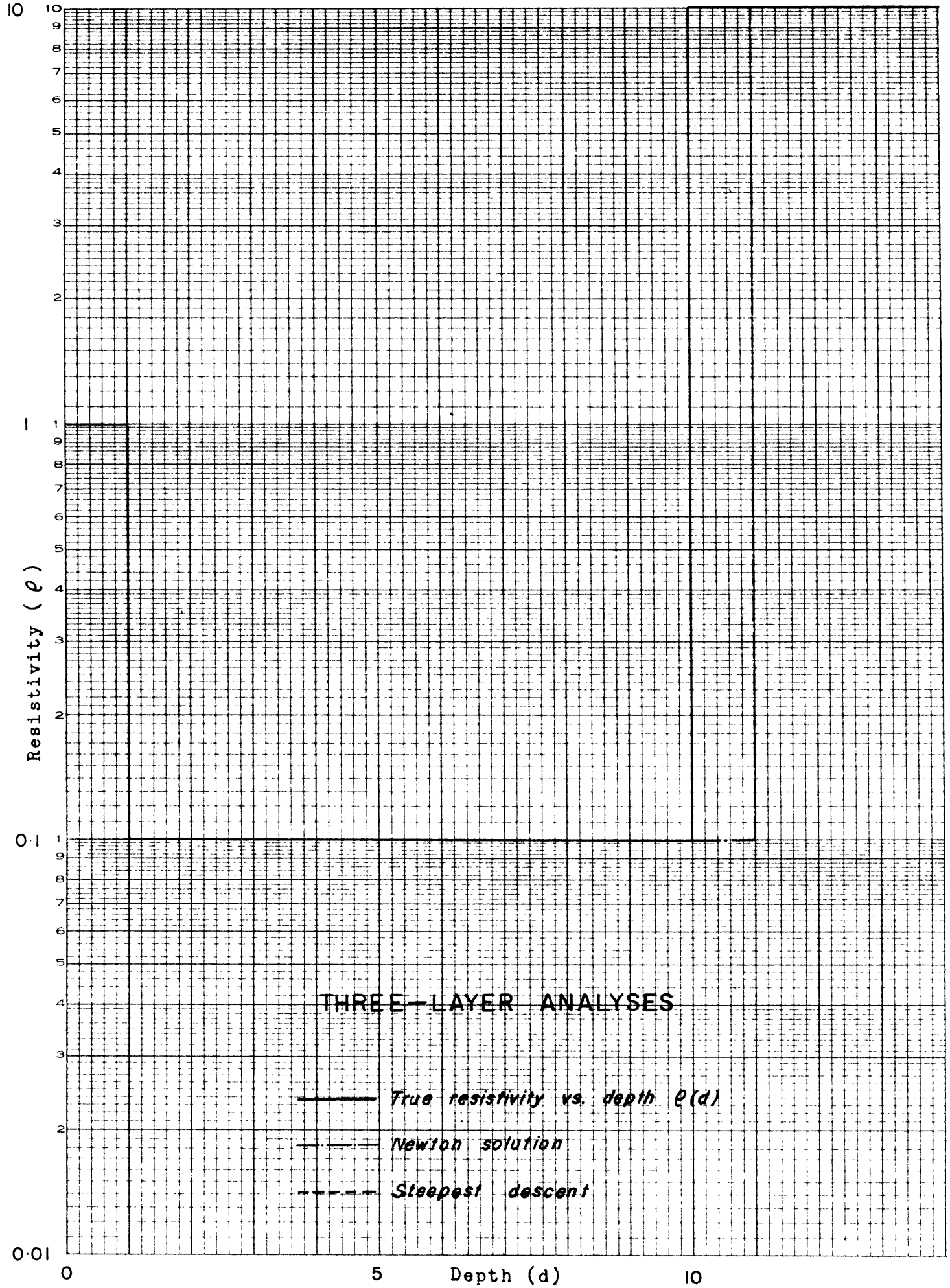
10
1
0·1
0·01
Resistivity (ρ)
0
5
10
Depth (d)
THREE-LAYER ANALYSES
True resistivity vs. depth ρ(d)
Newton solution
Steepest descent

Fig. 3

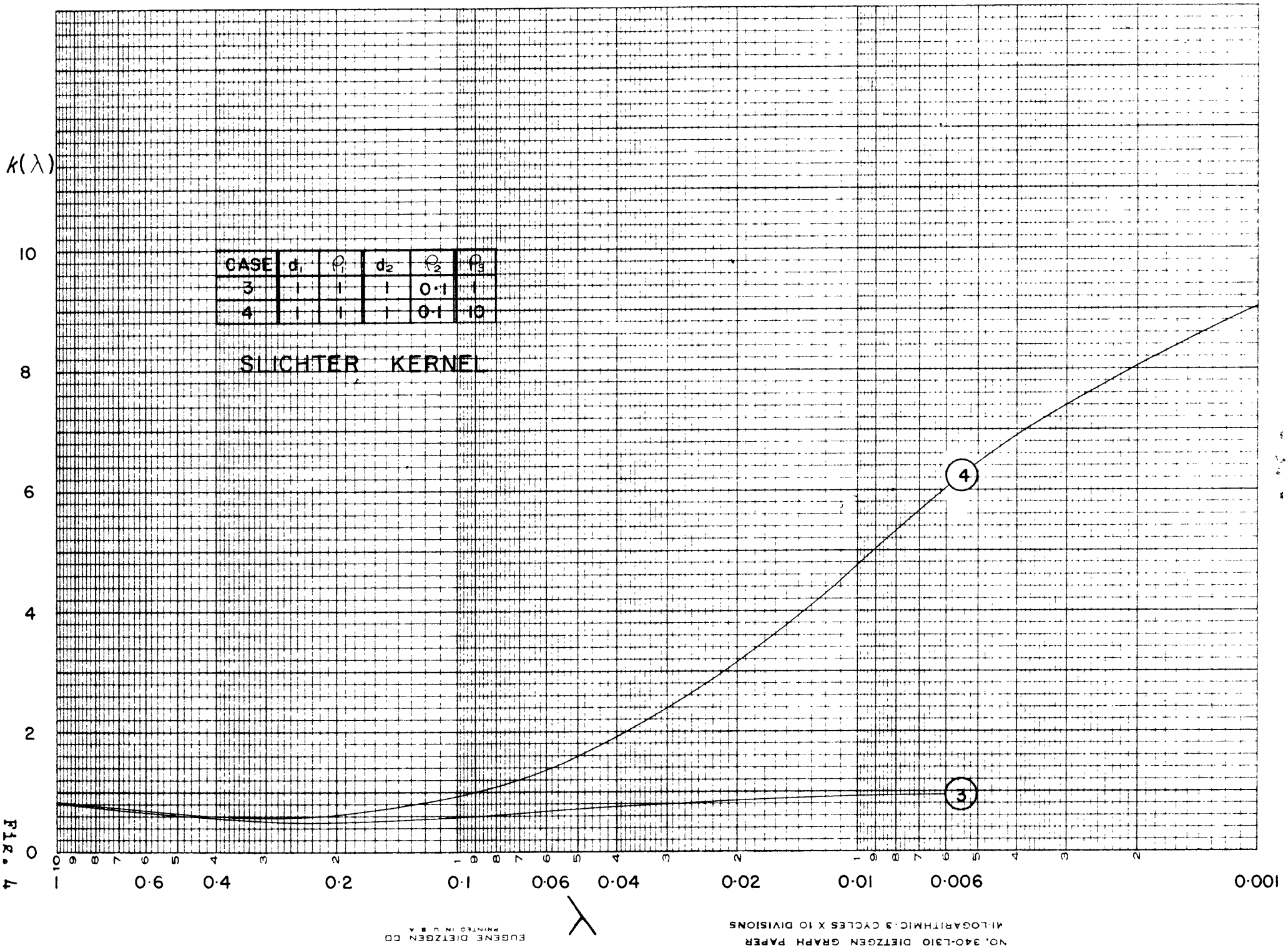

Fig. 4

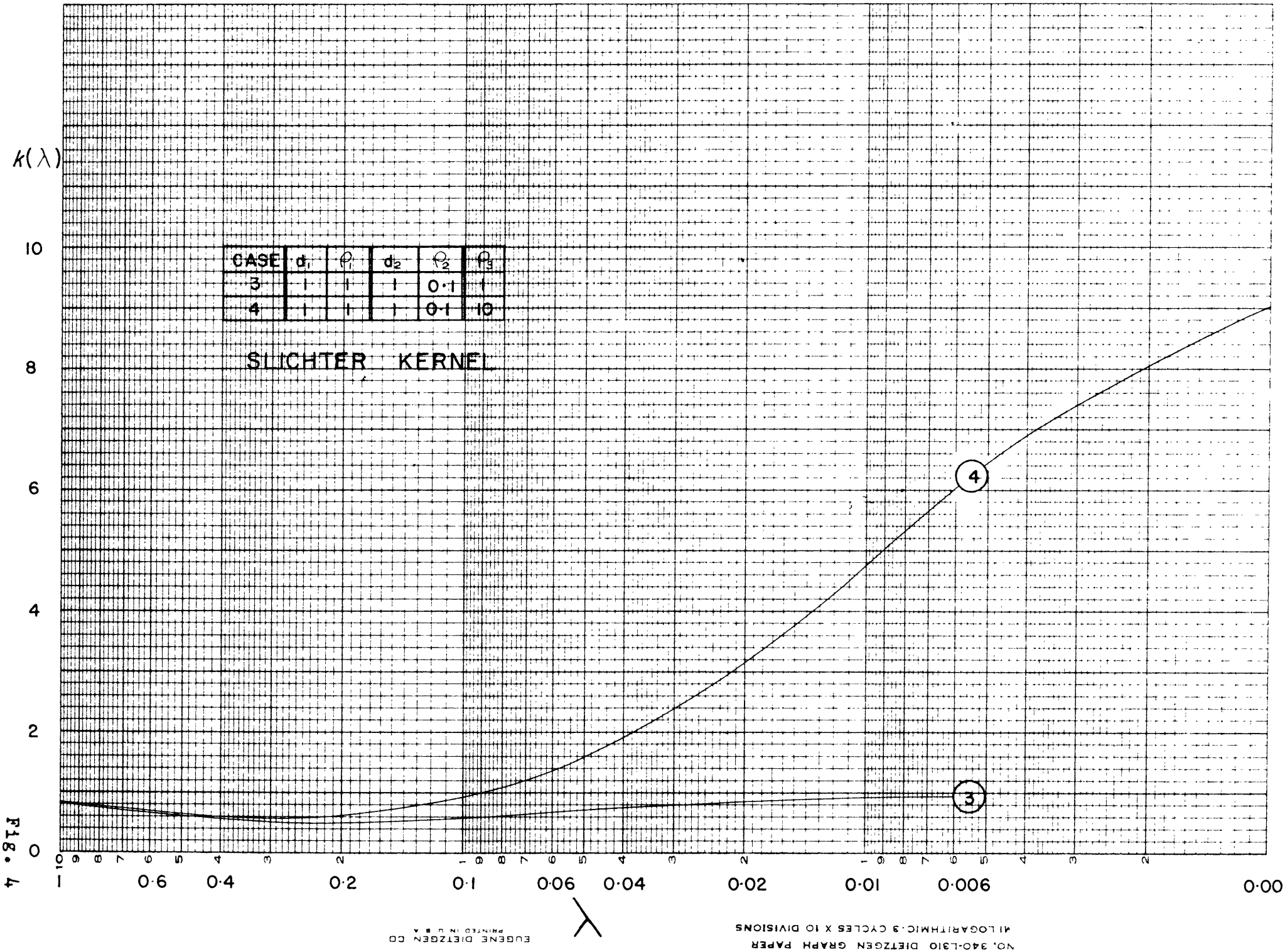

Fig. 4

Case 3

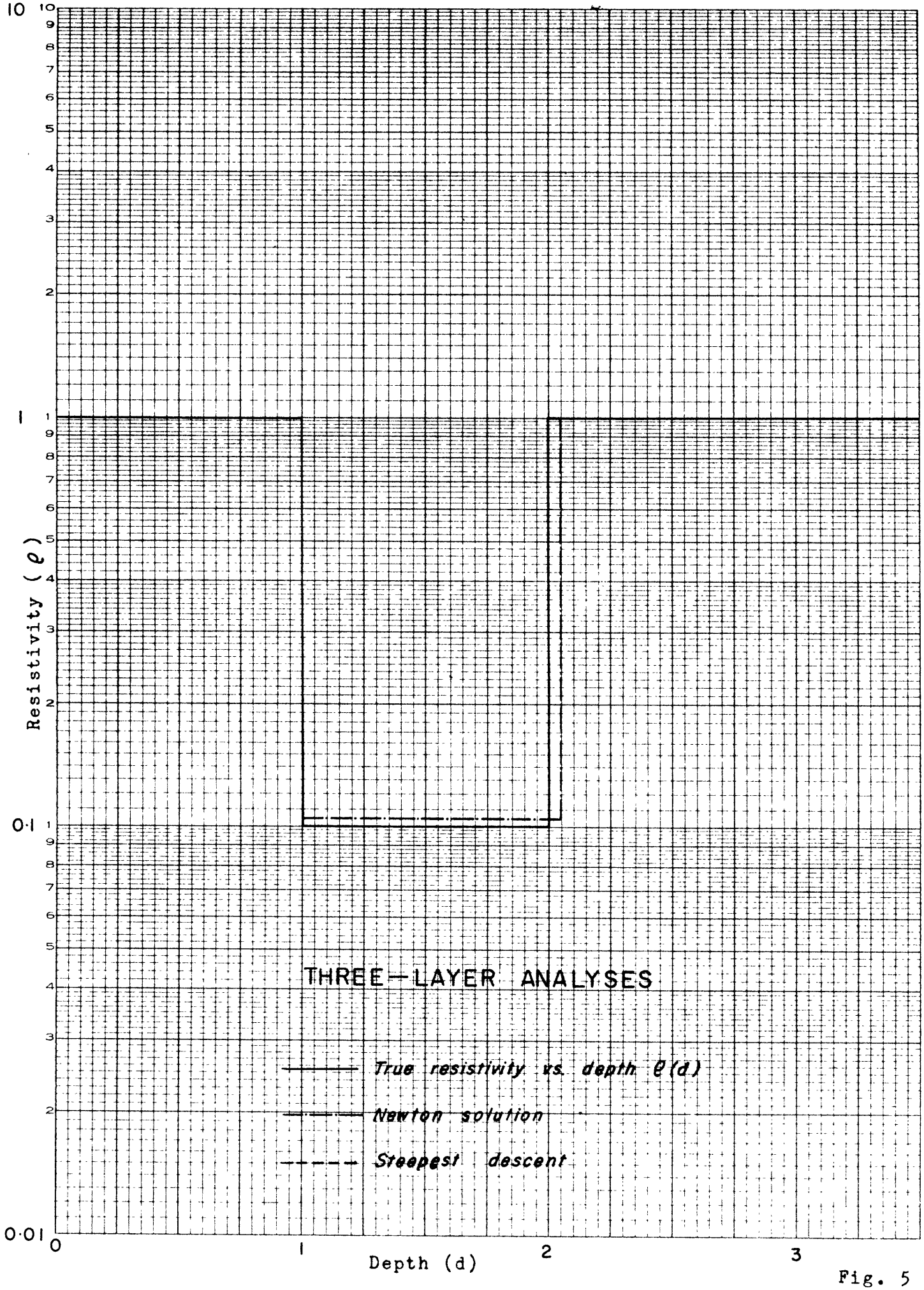
Resistivity (ρ)
Depth (d)
THREE—LAYER ANALYSES
True resistivity vs. depth ρ(d)
Newton solution
Steepest descent
EUGENE DIETZGEN CO.
4 LOGARITHMIC 3 CYCLES X 10 DIVISIONS

Fig. 5

Case 4

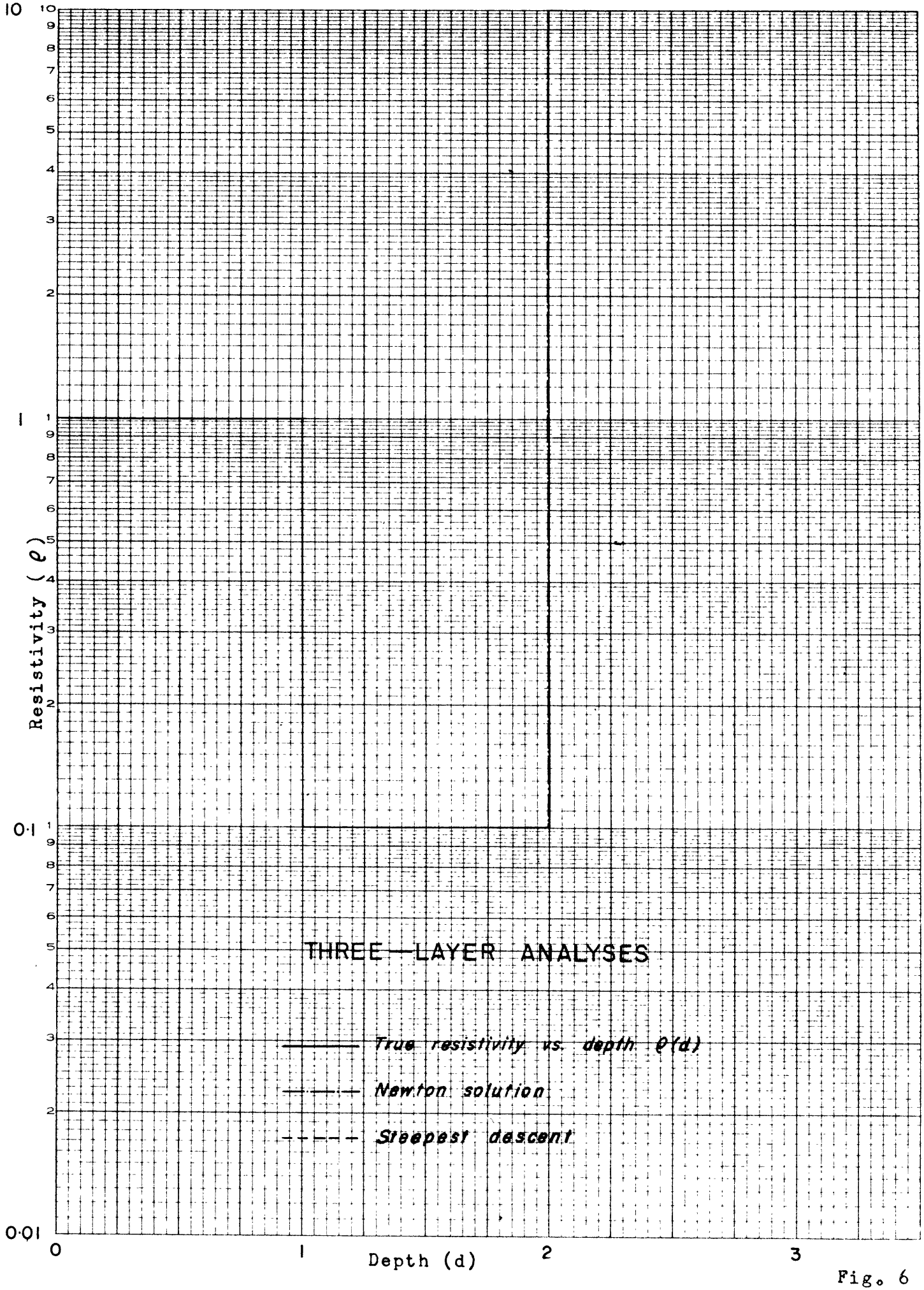

Fig. 6

Cases 5 6 7 8

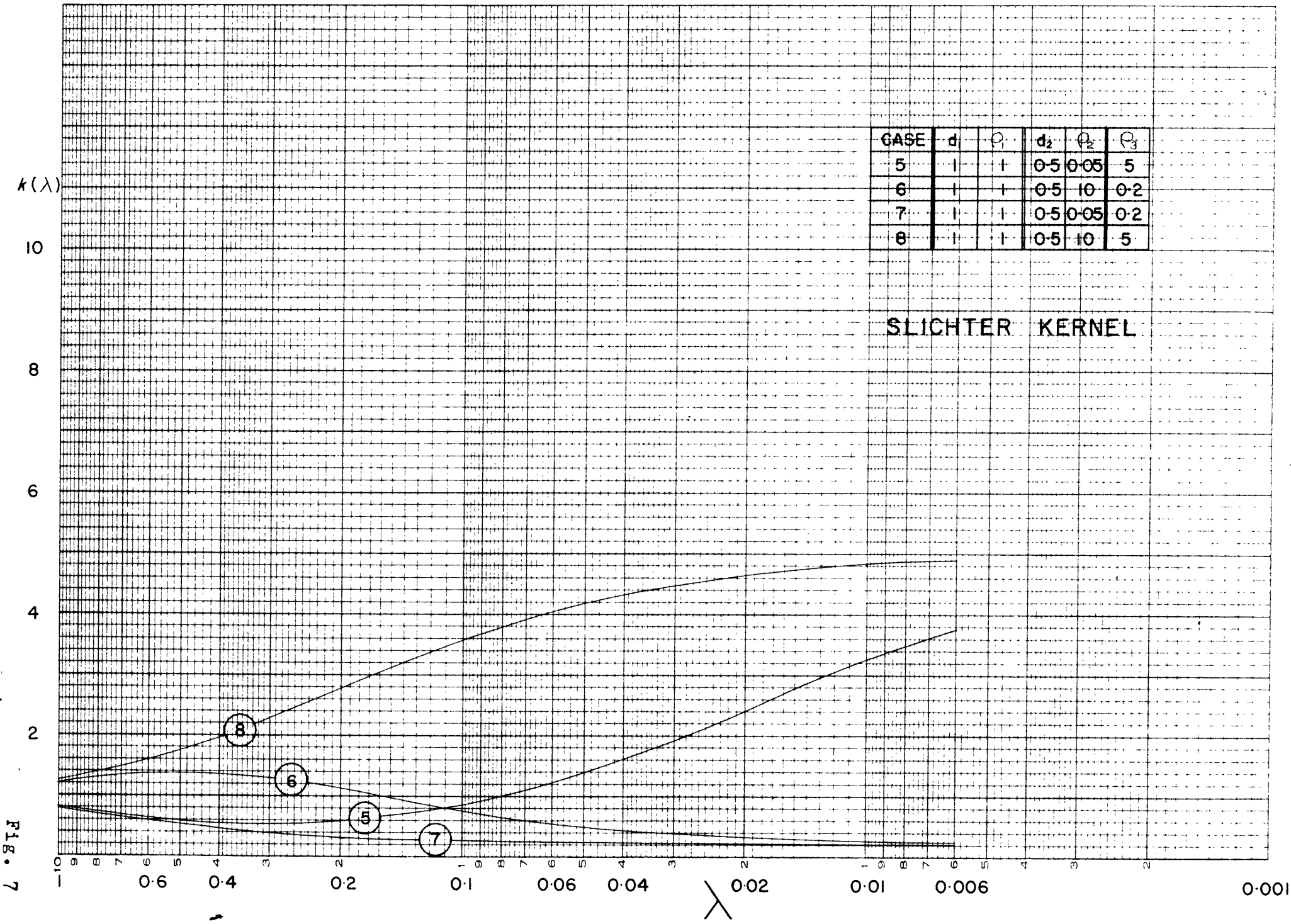

CASE	d_1	ρ_1	d_2	ρ_2	ρ_3
5	1	1	0·5	0·05	5
6	1	1	0·5	10	0·2
7	1	1	0·5	0·05	0·2
8	1	1	0·5	10	5

SLICHTER KERNEL

Fig. 7

Case 5

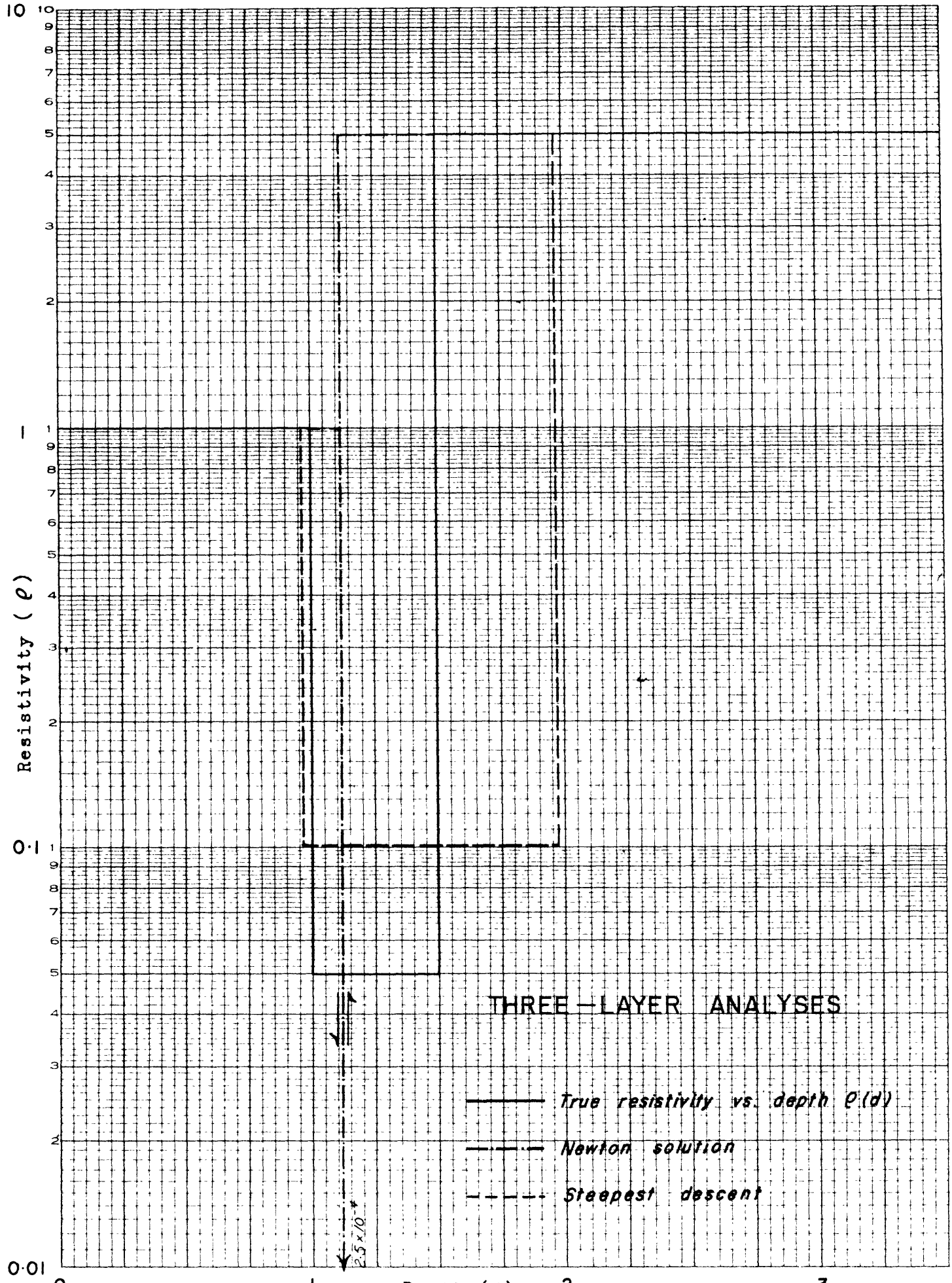

Fig. 8

Case 6

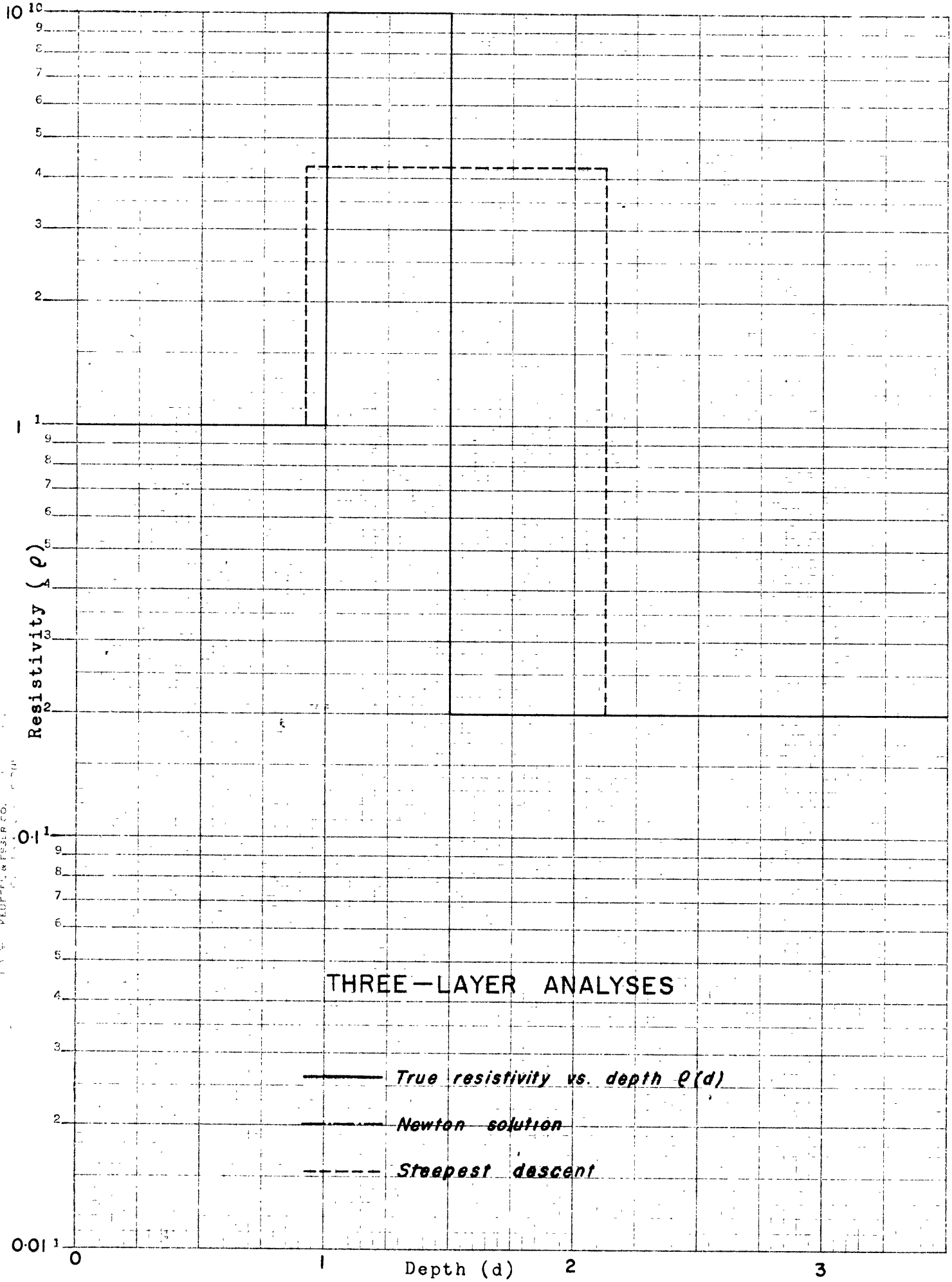

Fig. 9

Case 7

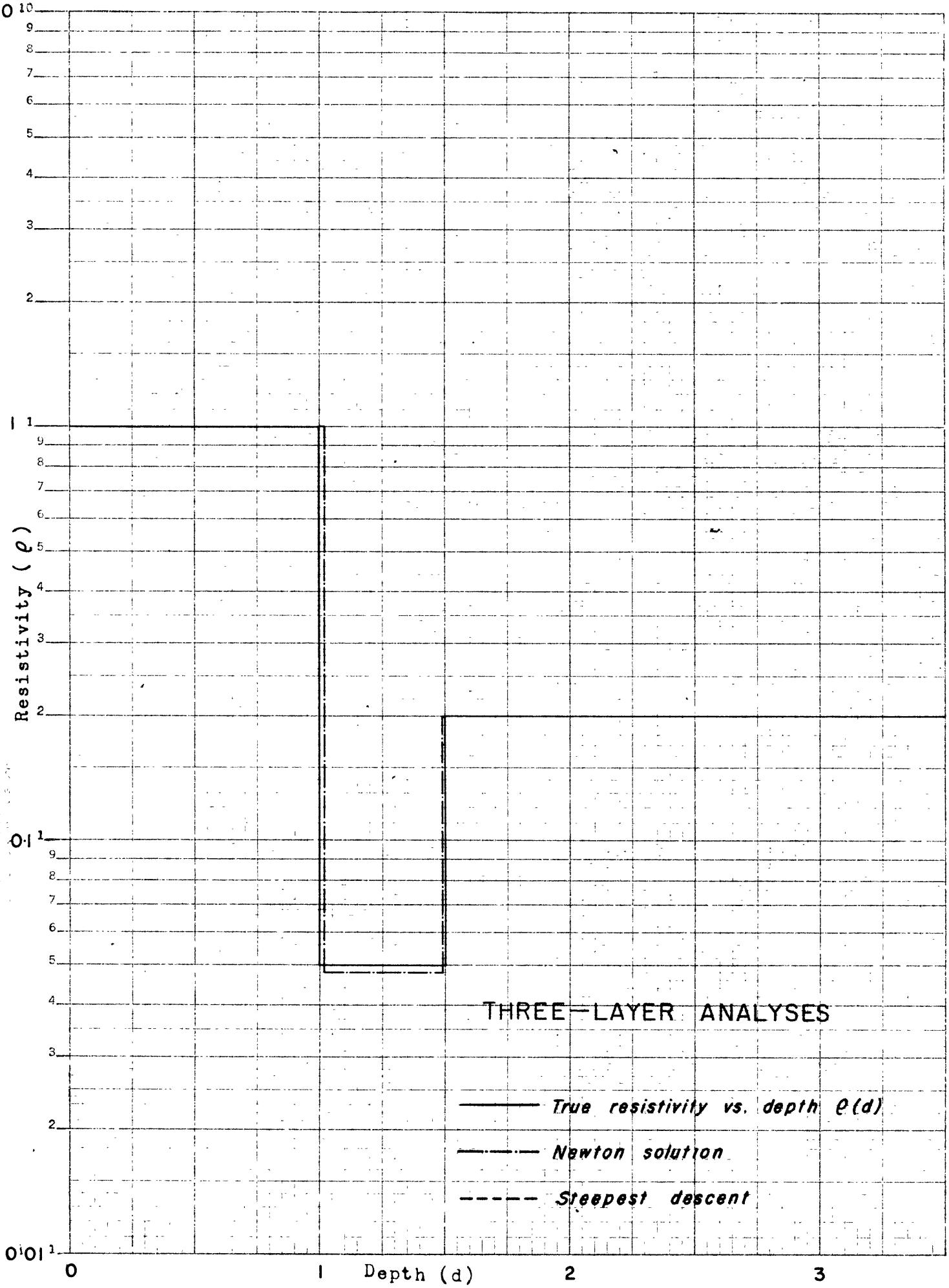
Resistivity (ρ)
Depth (d)
0
1
2
3
10
1
0.1
0.01
THREE—LAYER ANALYSES
True resistivity vs. depth ρ(d)
Newton solution
Steepest descent

Fig. 10

Case 8

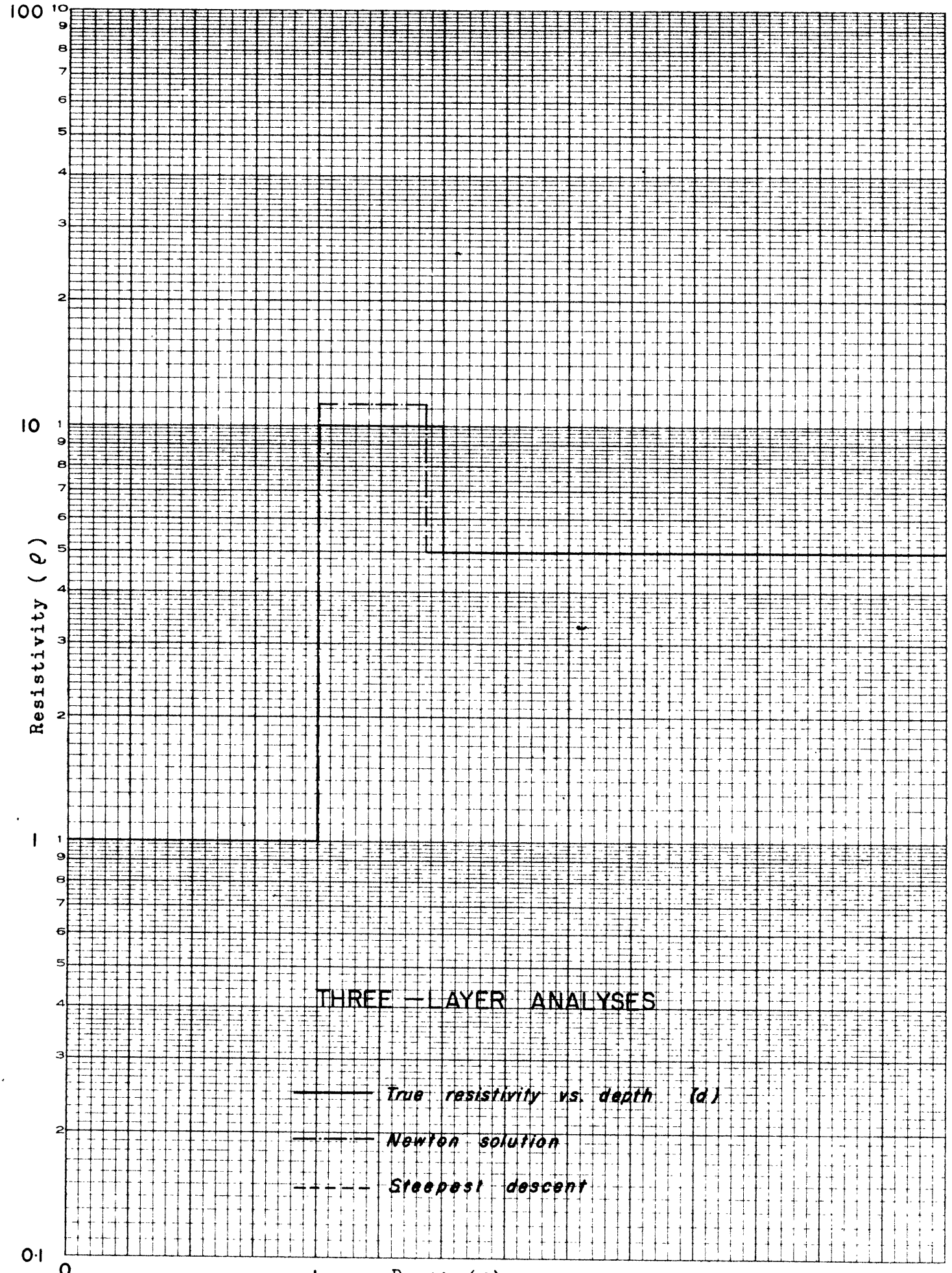

EUGENE DIETZGEN CO
PRINTED IN U.S.A.

41 LOGARITHMIC. 3 CYCLES X 10 DIVISIONS

Fig. 11

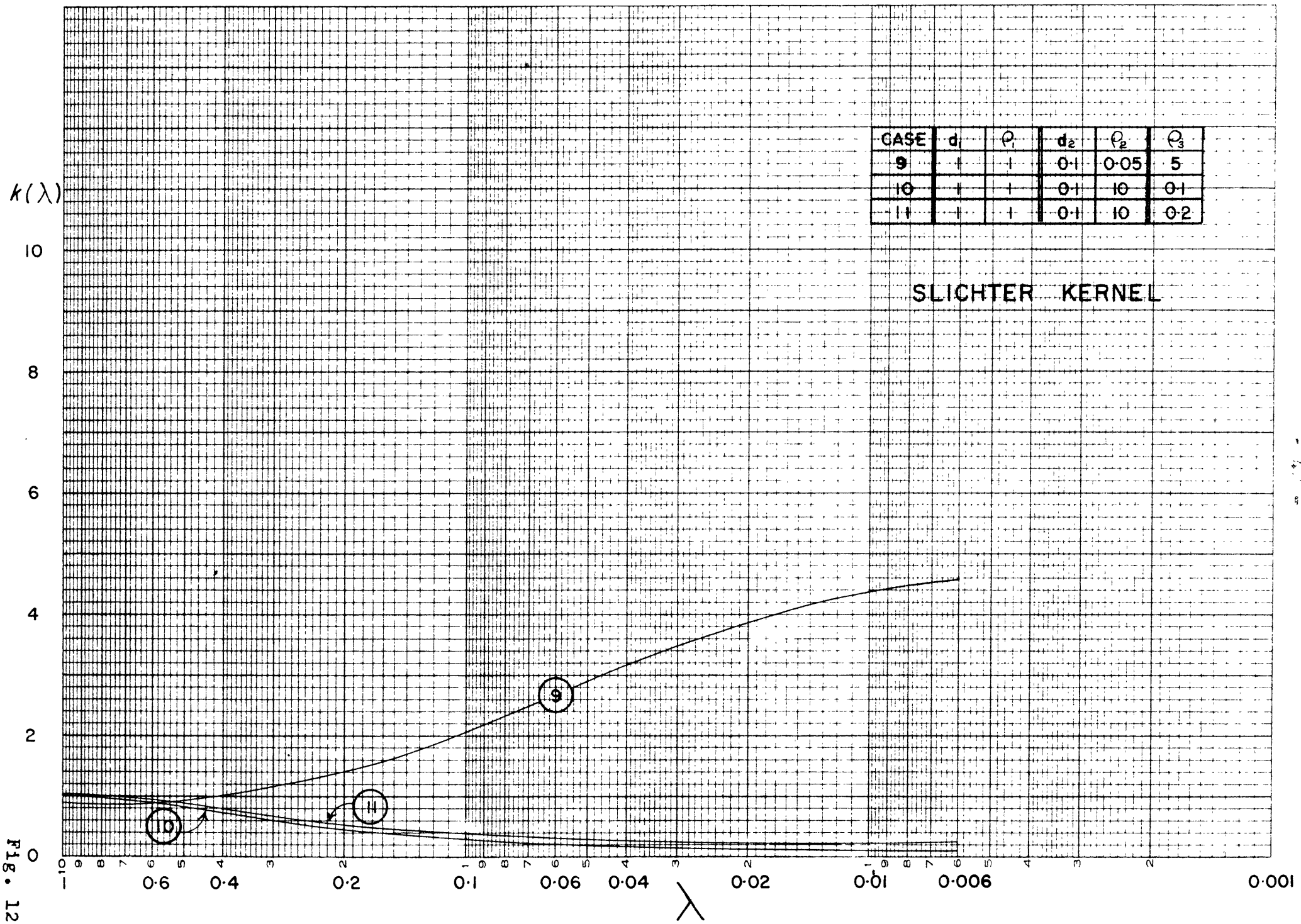

Fig. 12

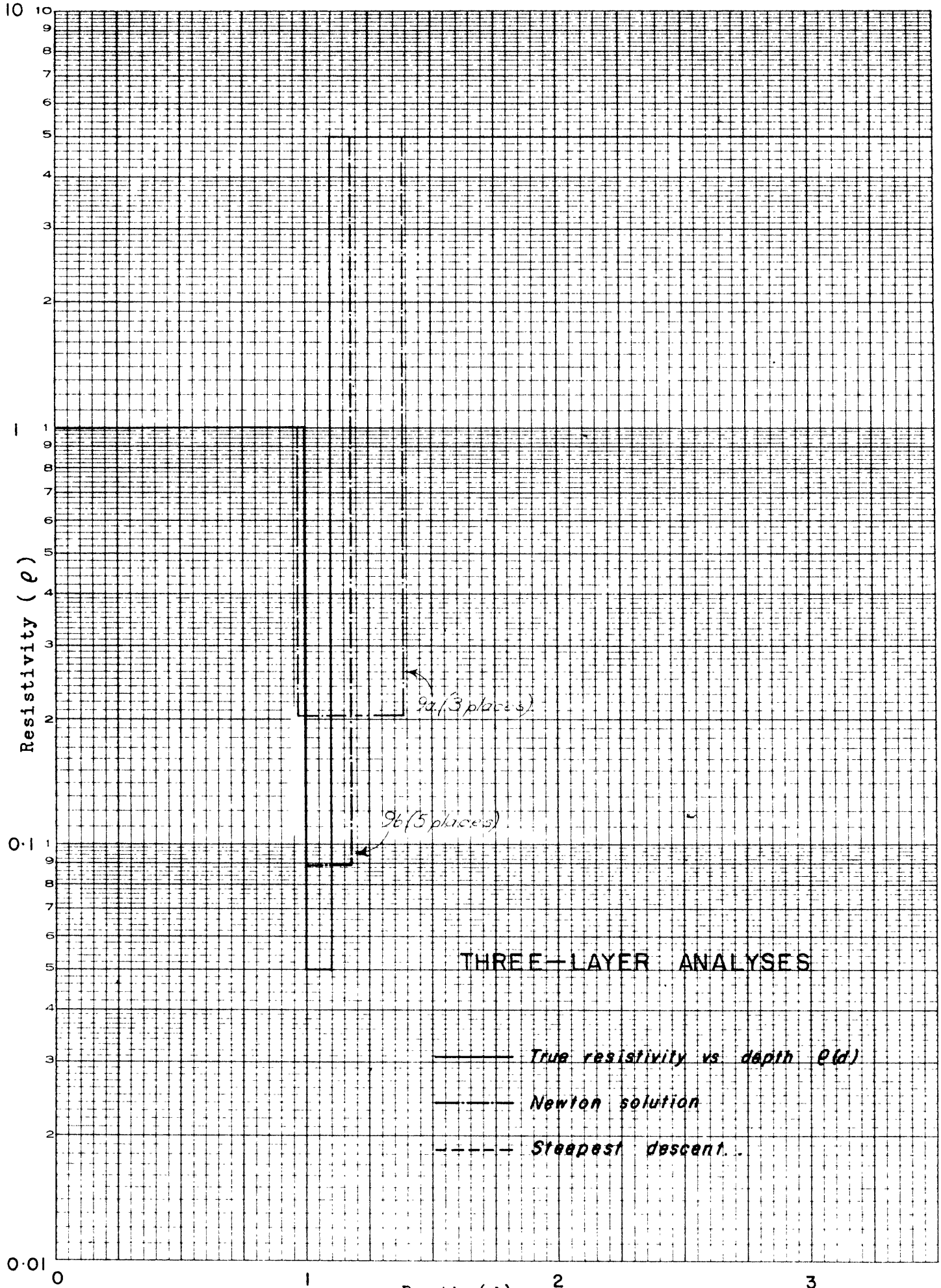

Fig. 13

Cases 10 10a 10b 10c

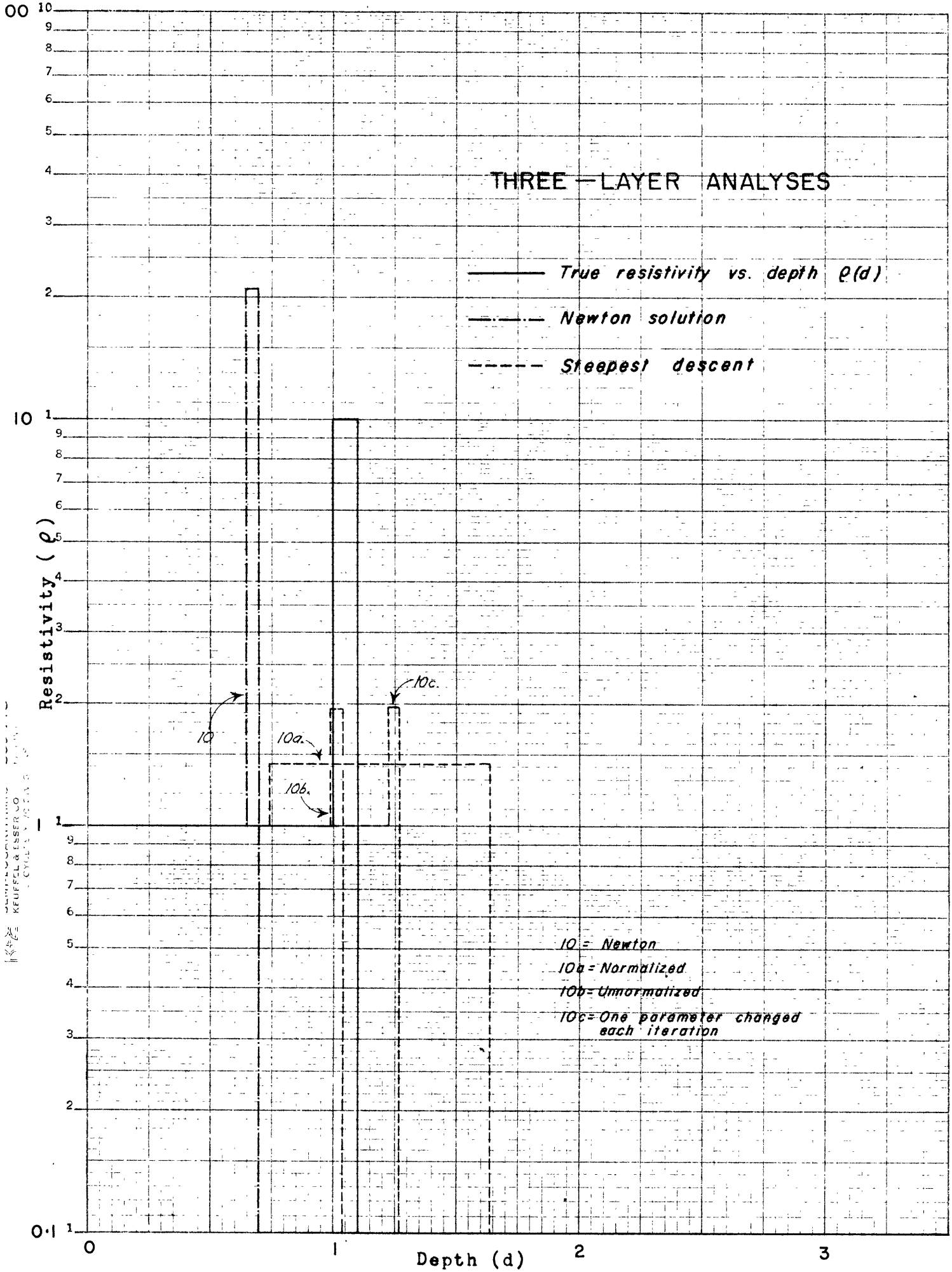

Fig. 14

Case 11

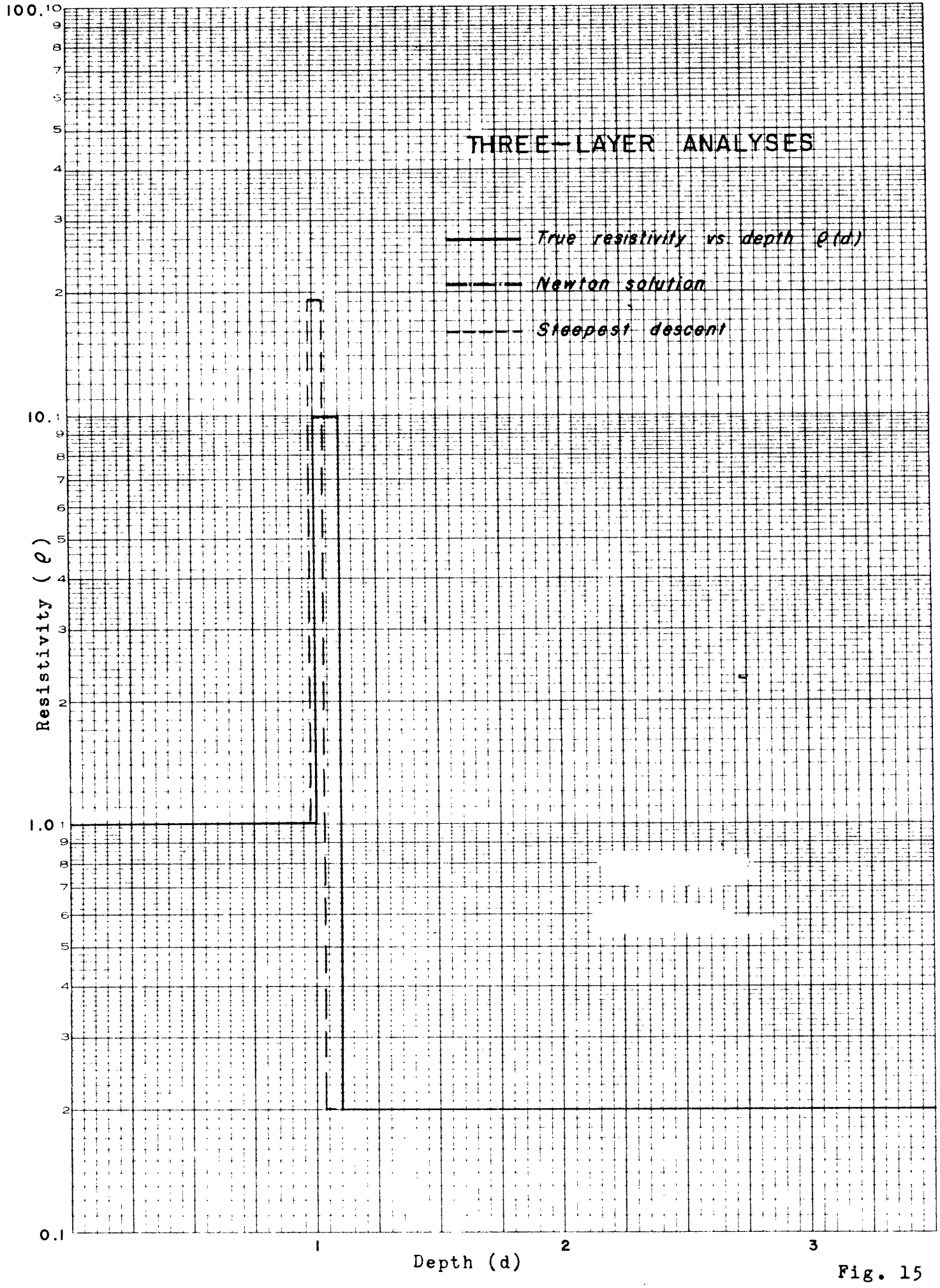

Fig. 15

Cases 12 13 14

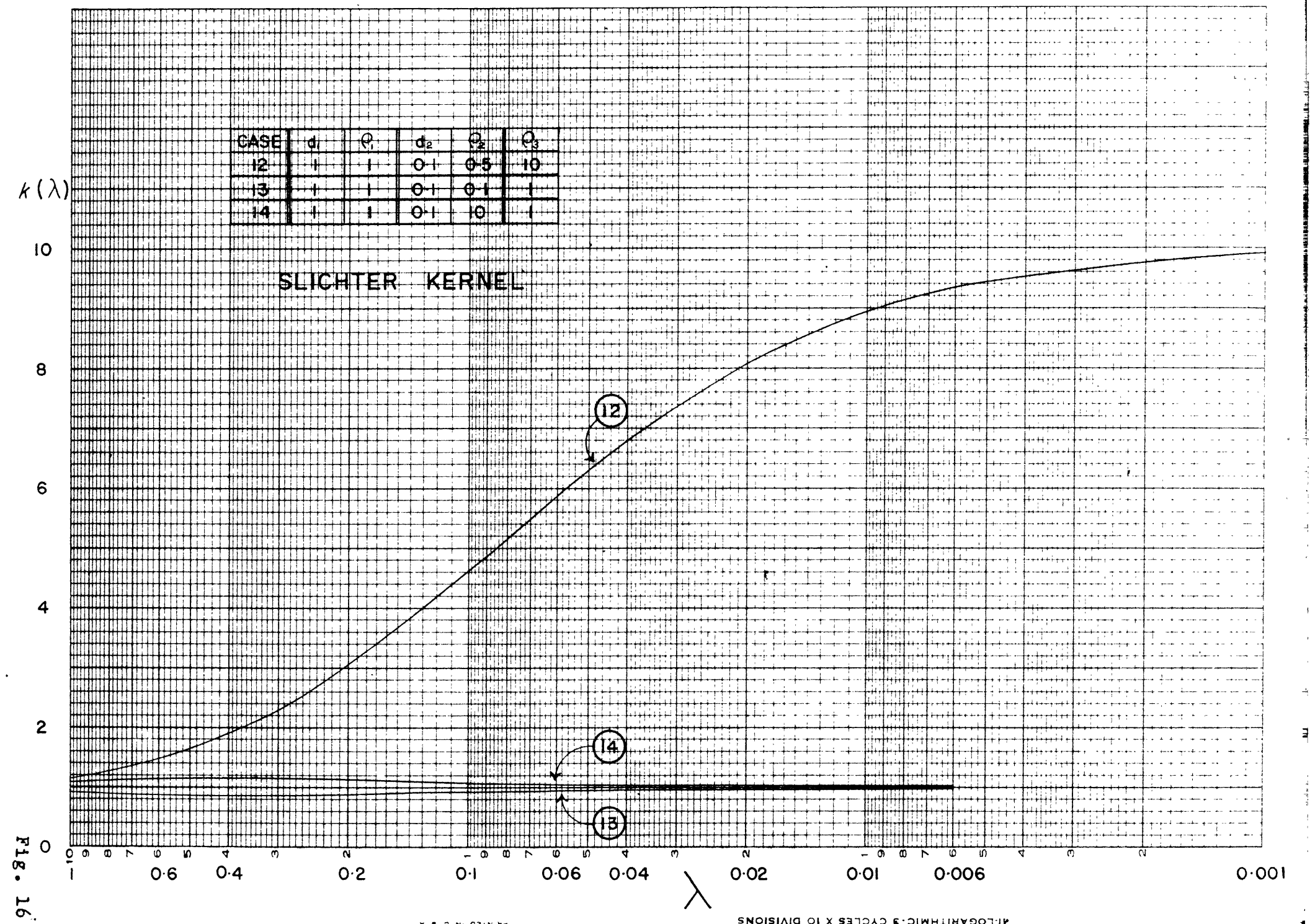

Fig. 16.

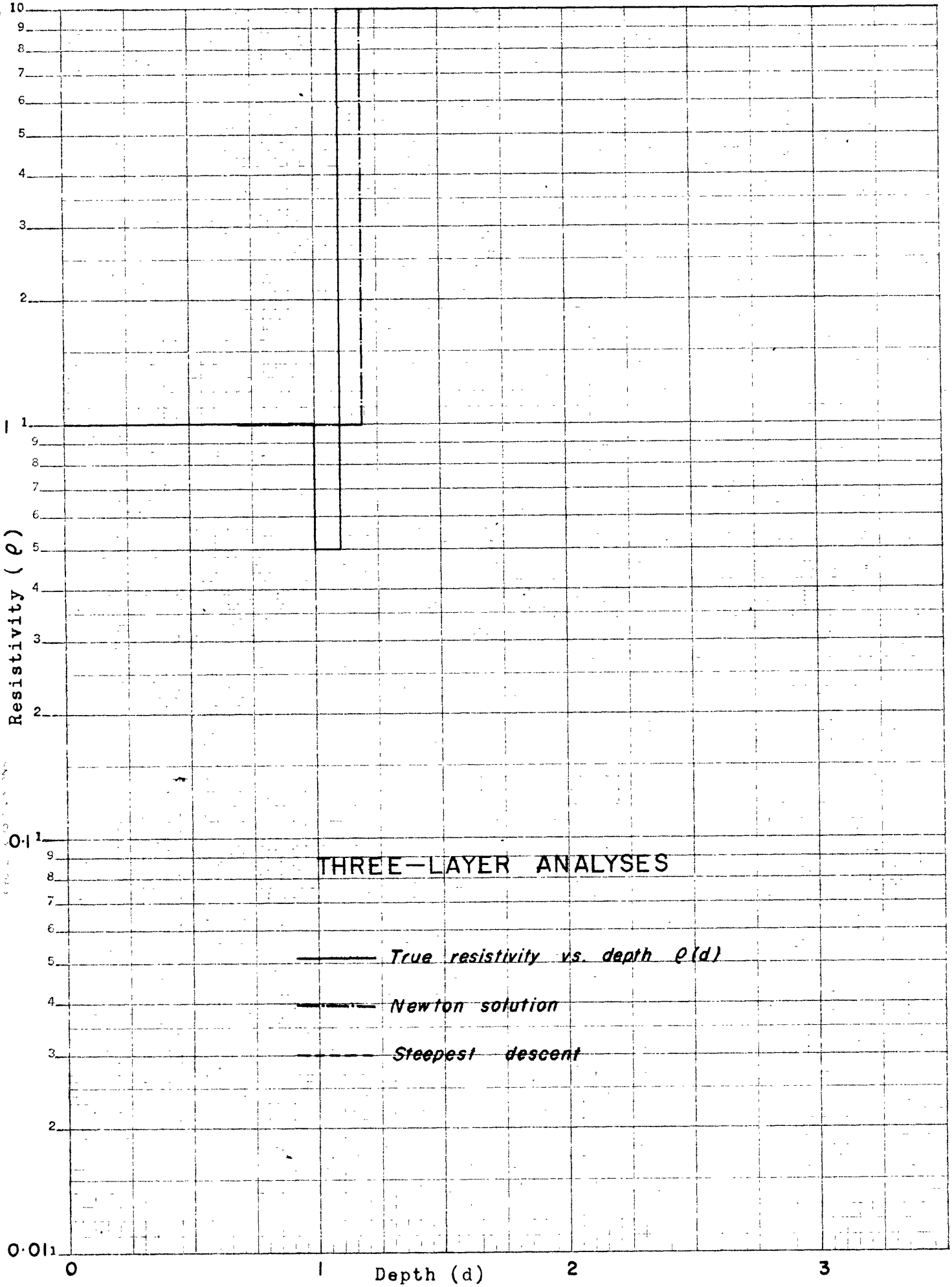
Resistivity (ρ)
10
1
0·1
0·01
0
1
2
3
Depth (d)
THREE—LAYER ANALYSES
True resistivity vs. depth ρ(d)
Newton solution
Steepest descent

Fig. 17

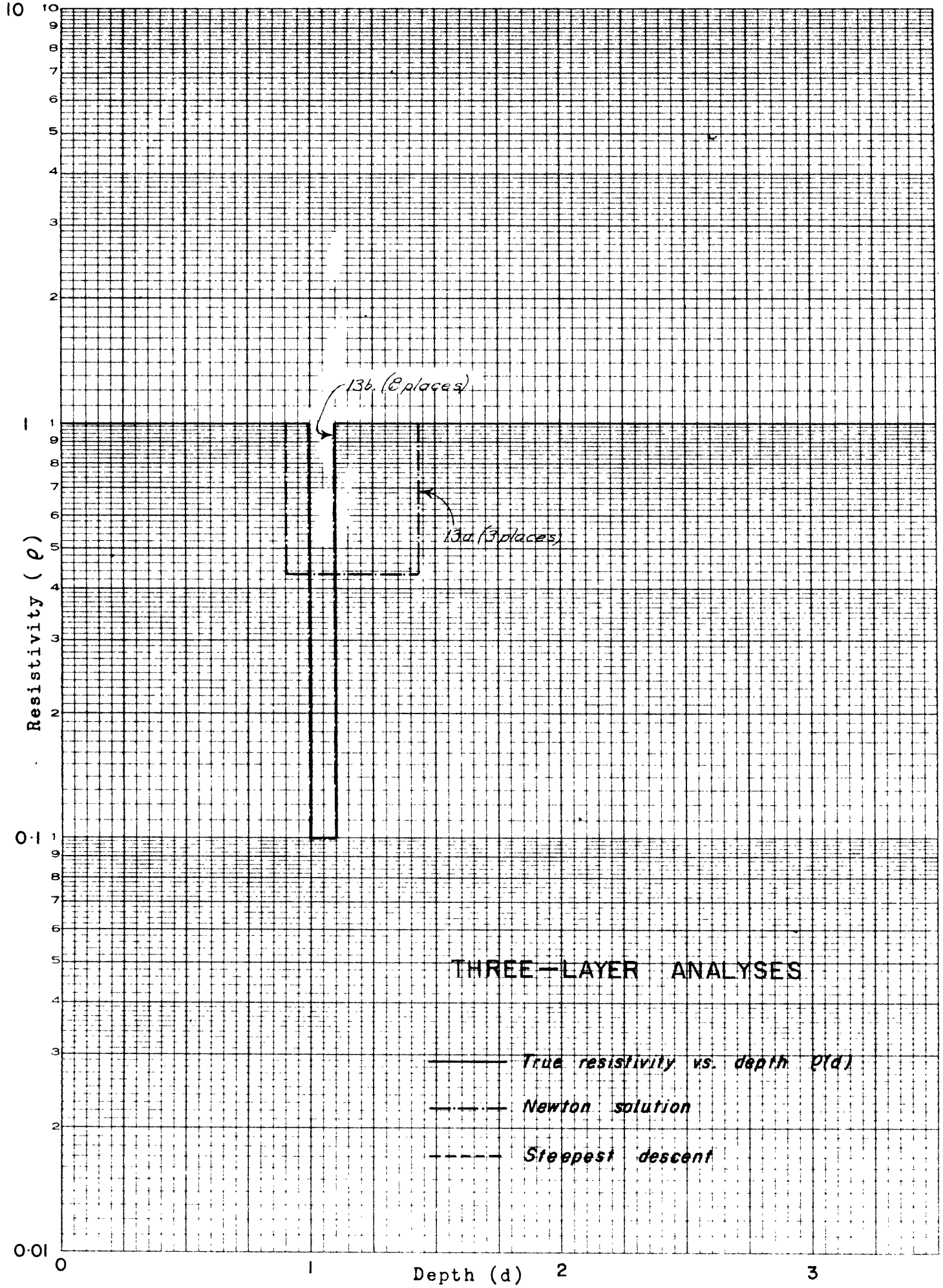

Fig. 18

Cases 14a 14b

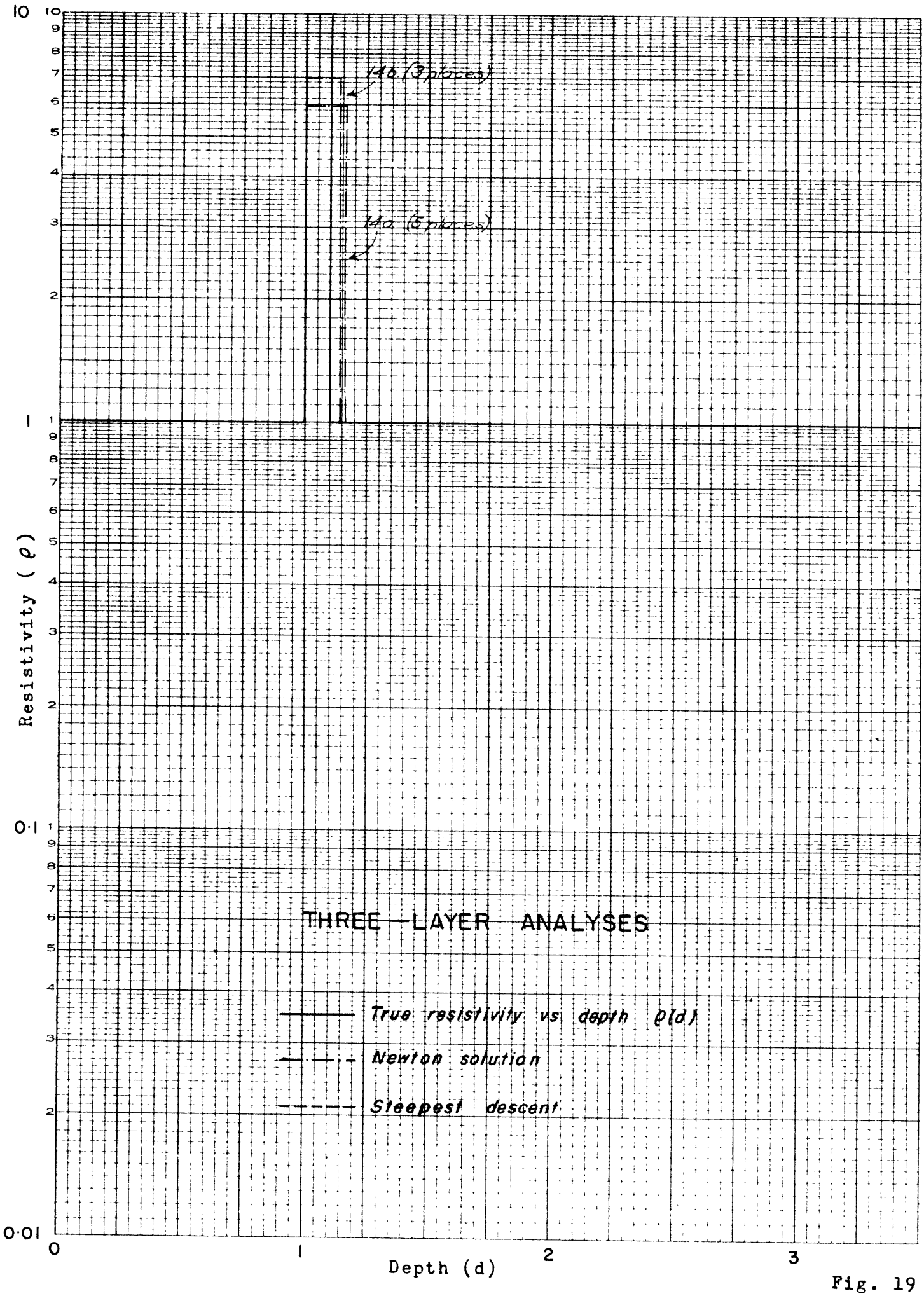

Fig. 19

Cases 16 17 18 19

CASE	d_1	ϱ_1	d_2	ϱ_2	ϱ_3
16	1	1	0·1	0·75	0·1
17	1	1	0·1	0·05	0·2
18	1	1	0·1	10	5
19	1	1	0·1	1·5	1

SLICHTER KERNEL

$k(\lambda)$

10
8
6
4
2
0

1 0·6 0·4 0·2 0·1 0·06 0·04 0·02 0·01 0·006 0·001

λ

19 18 17 16

NO. 340-L310 DIETZGEN GRAPH PAPER
MI-LOGARITHMIC-3 CYCLES X 10 DIVISIONS

EUGENE DIETZGEN CO.
PRINTED IN U.S.A.

Fig. 20

25

Case 16

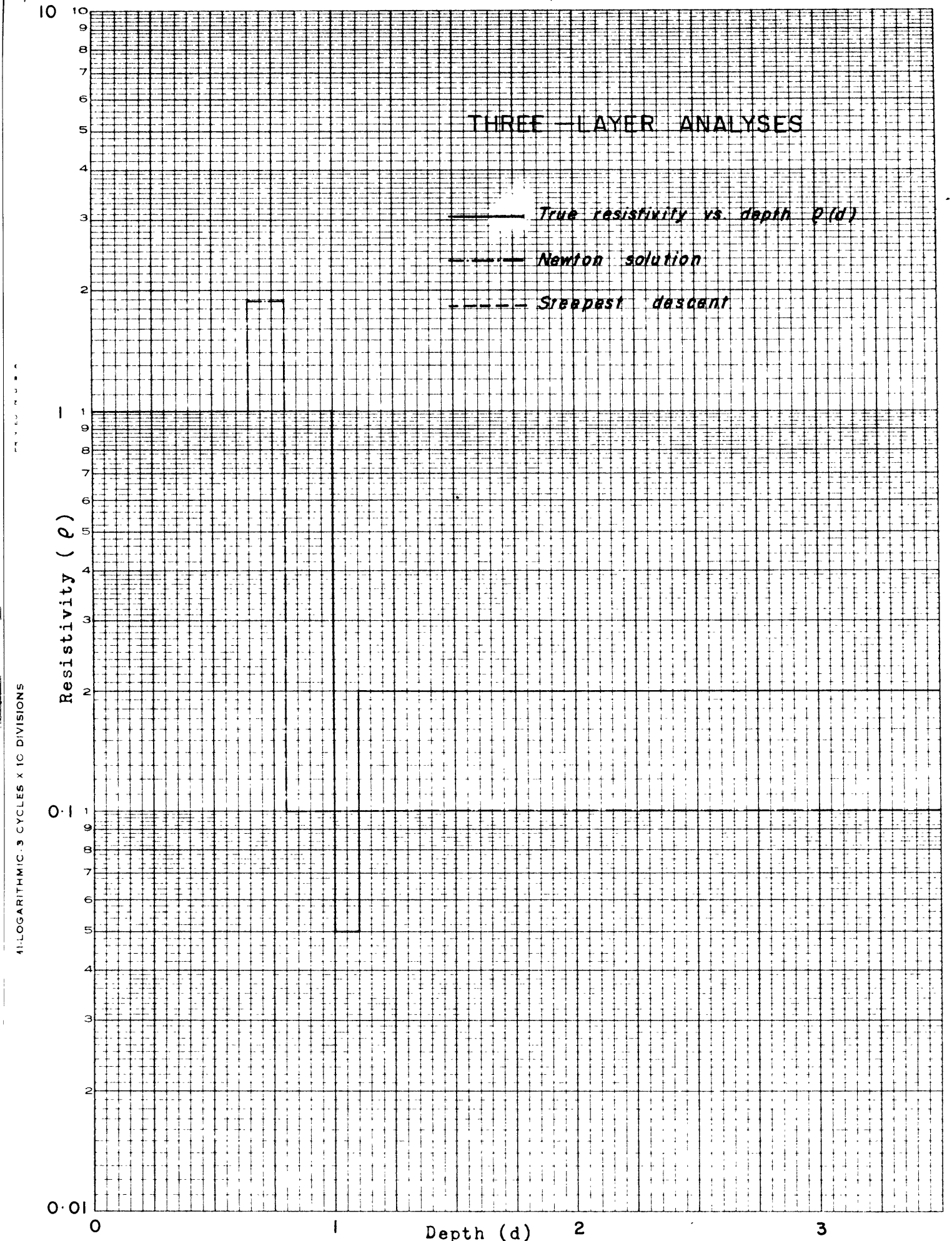

Fig. 21

Cases 17a 17b

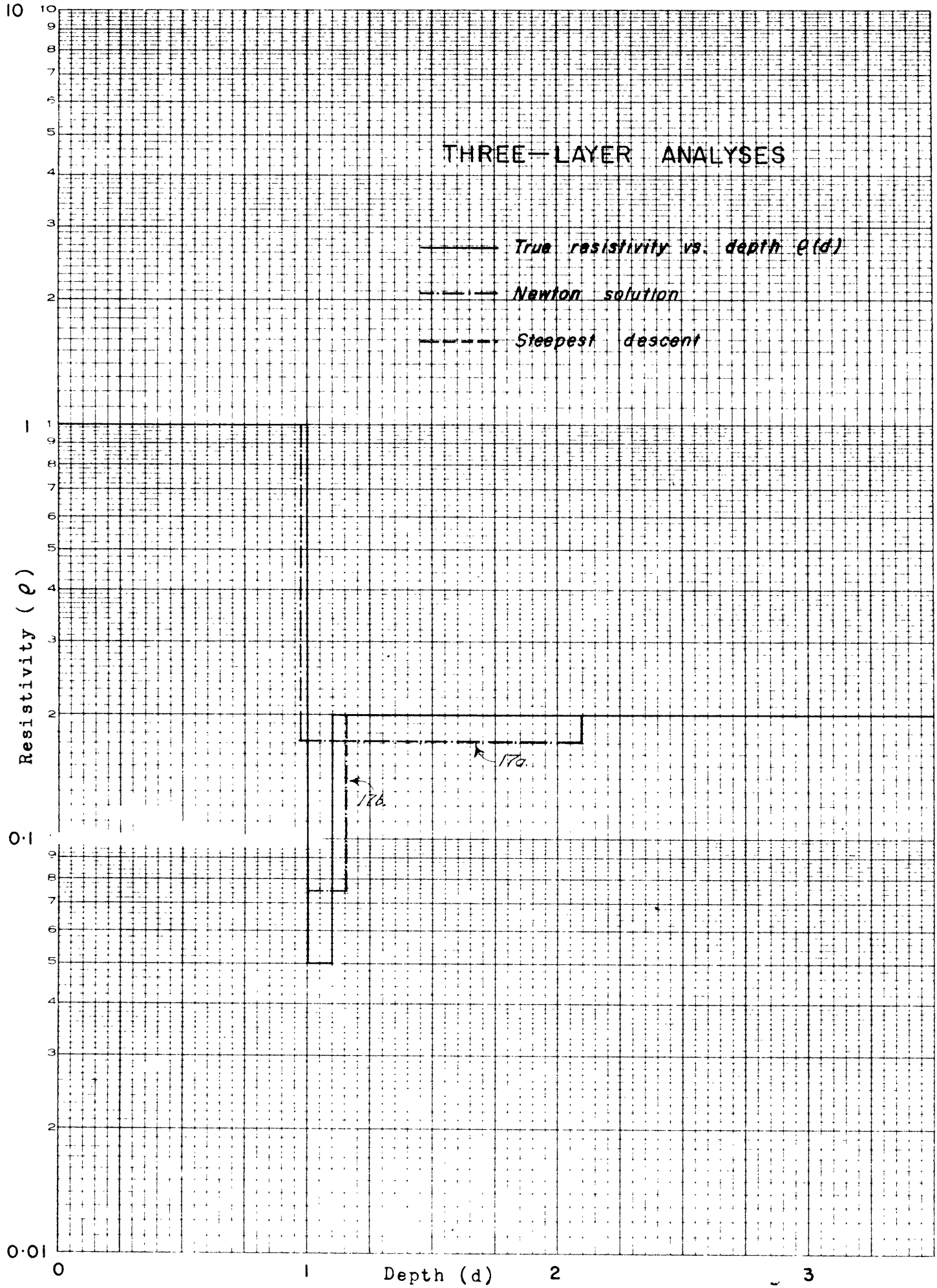

Fig. 22

Case 18

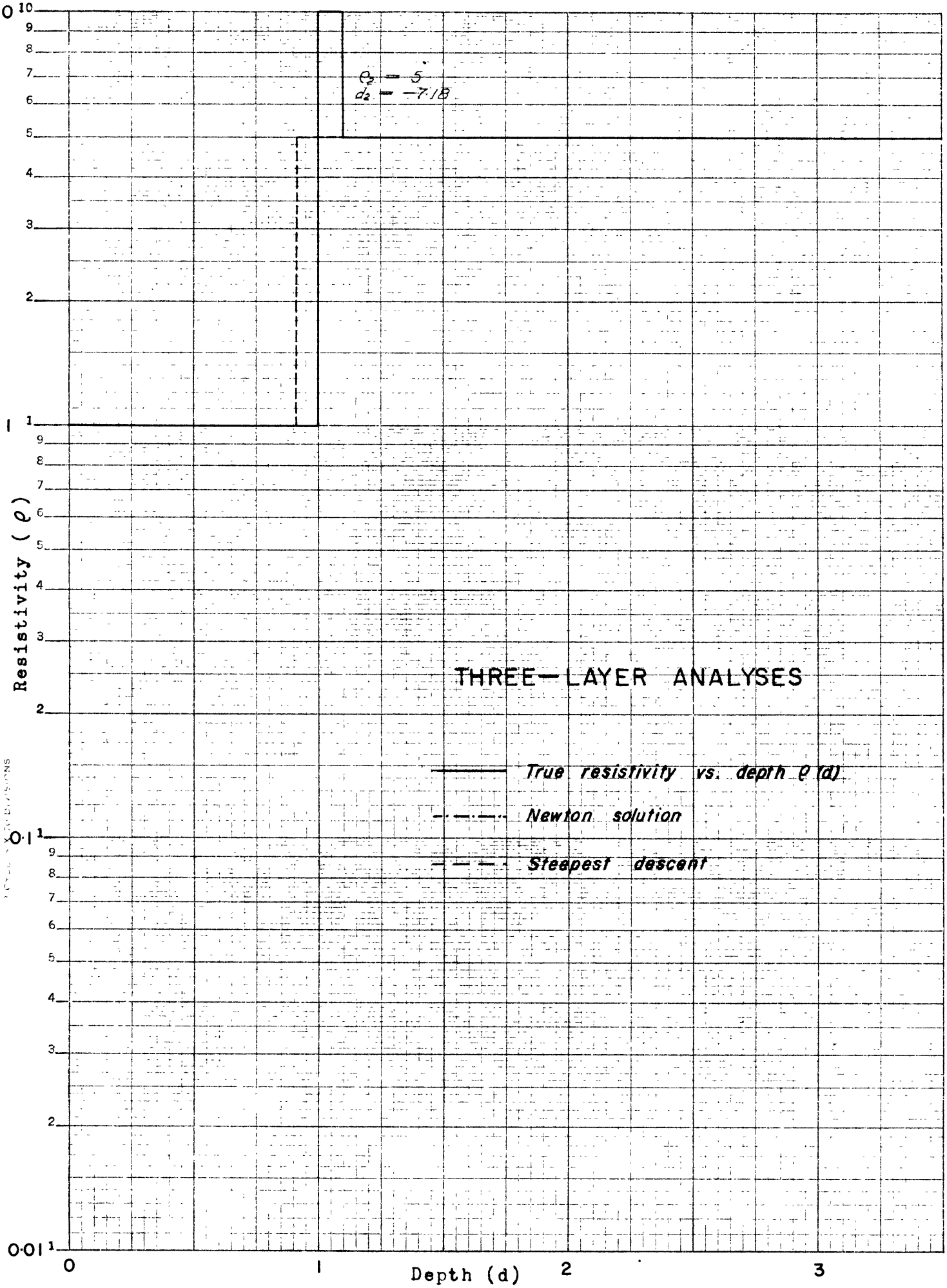

Fig. 23

Cases 19a 19b

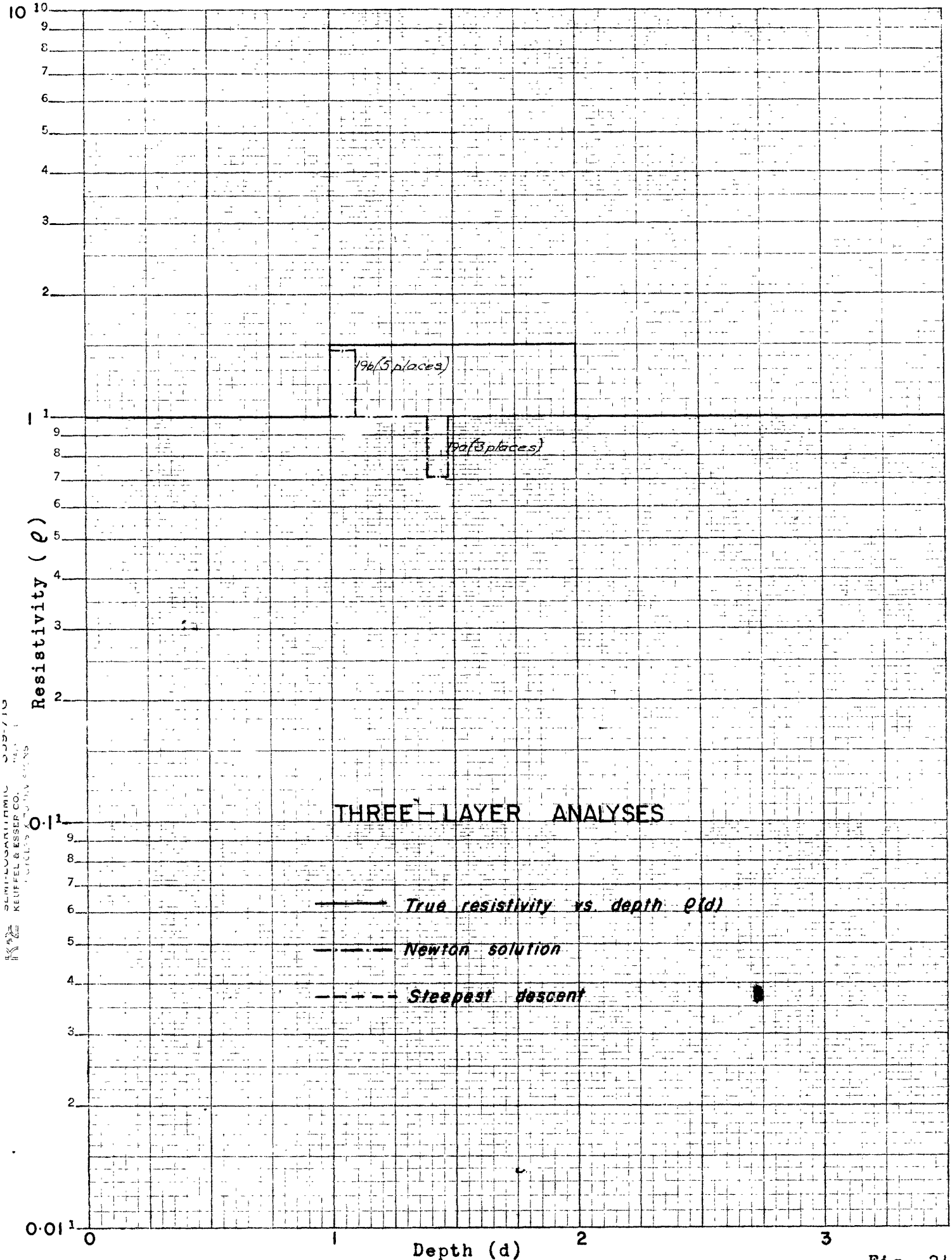

Fig. 24

Cases 20 21 22

CASE	d_1	ρ_1	d_2	ρ_2	ρ_3
20	1	1	0·01	0·1	10
21	1	1	0·01	100	1
22	1	1	0·01	2	10

SLICHTER KERNEL

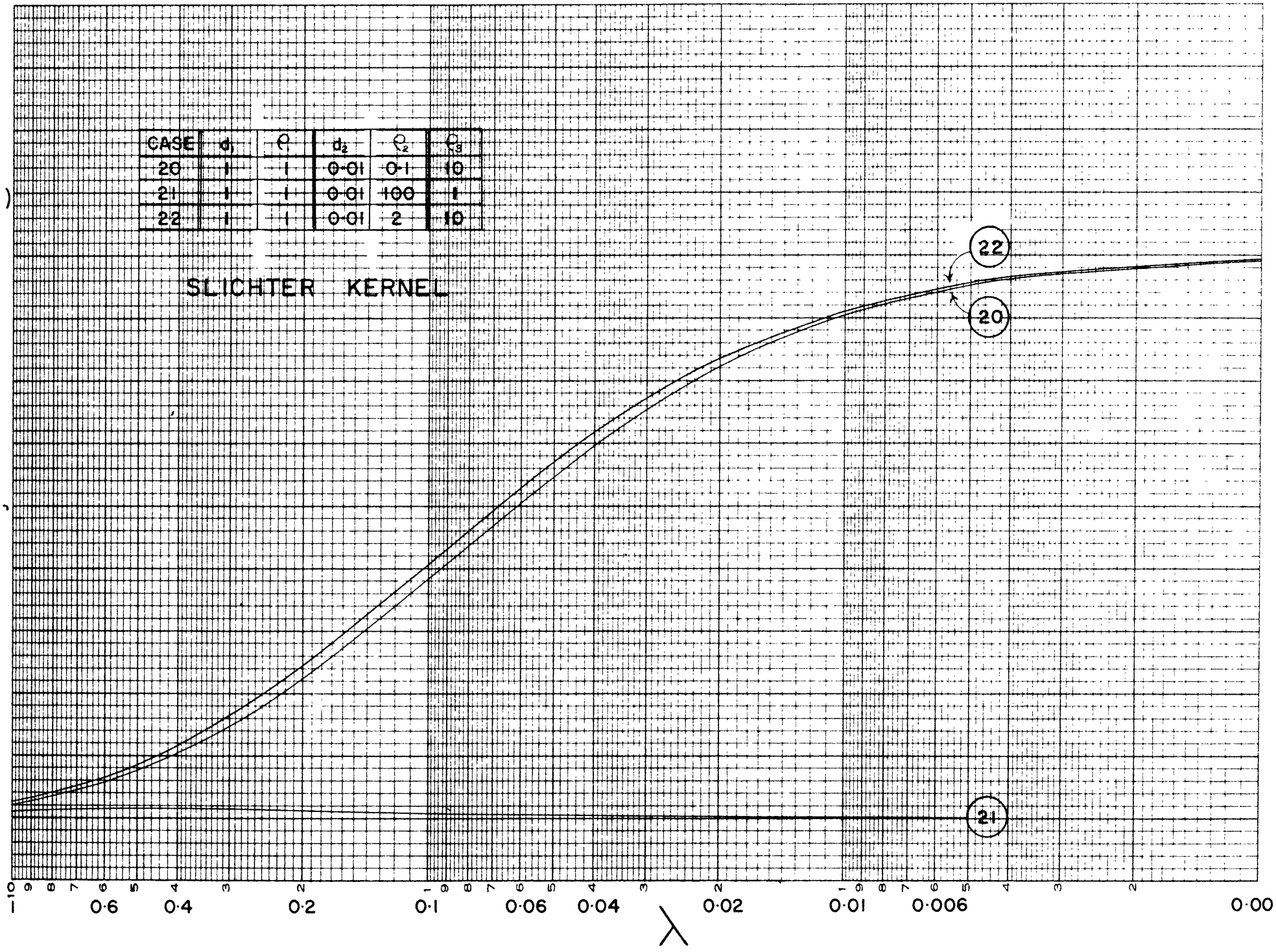

NO. 340-L310 DIETZGEN GRAPH PAPER
MI-LOGARITHMIC-3 CYCLES X 10 DIVISIONS

EUGENE DIETZGEN CO.
PRINTED IN U.S.A.

Fig. 25

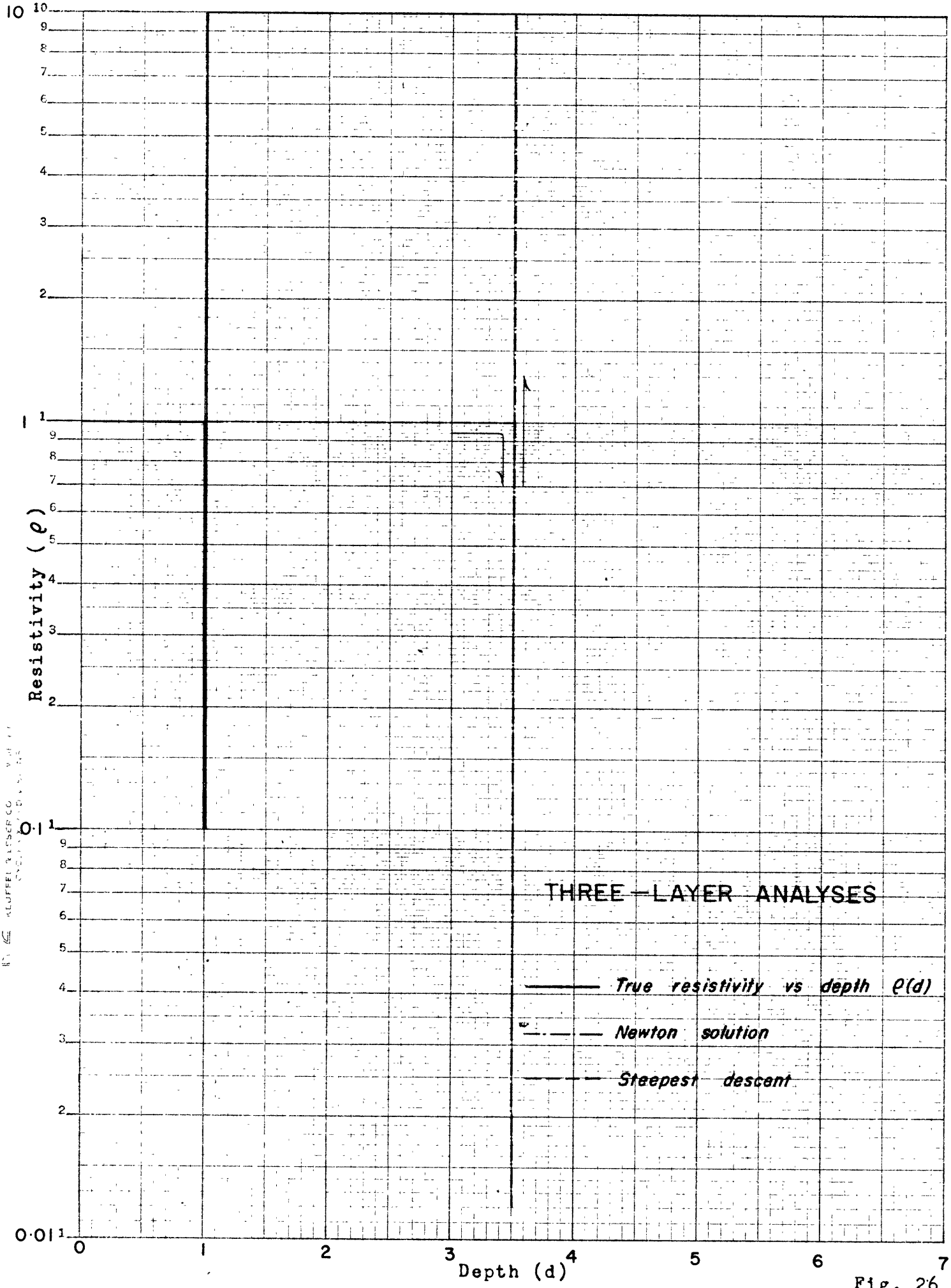
Resistivity (ρ)
10
1
0·1
0·01
Depth (d)
0
1
2
3
4
5
6
7
THREE—LAYER ANALYSES
True resistivity vs depth ρ(d)
Newton solution
Steepest descent

Fig. 26

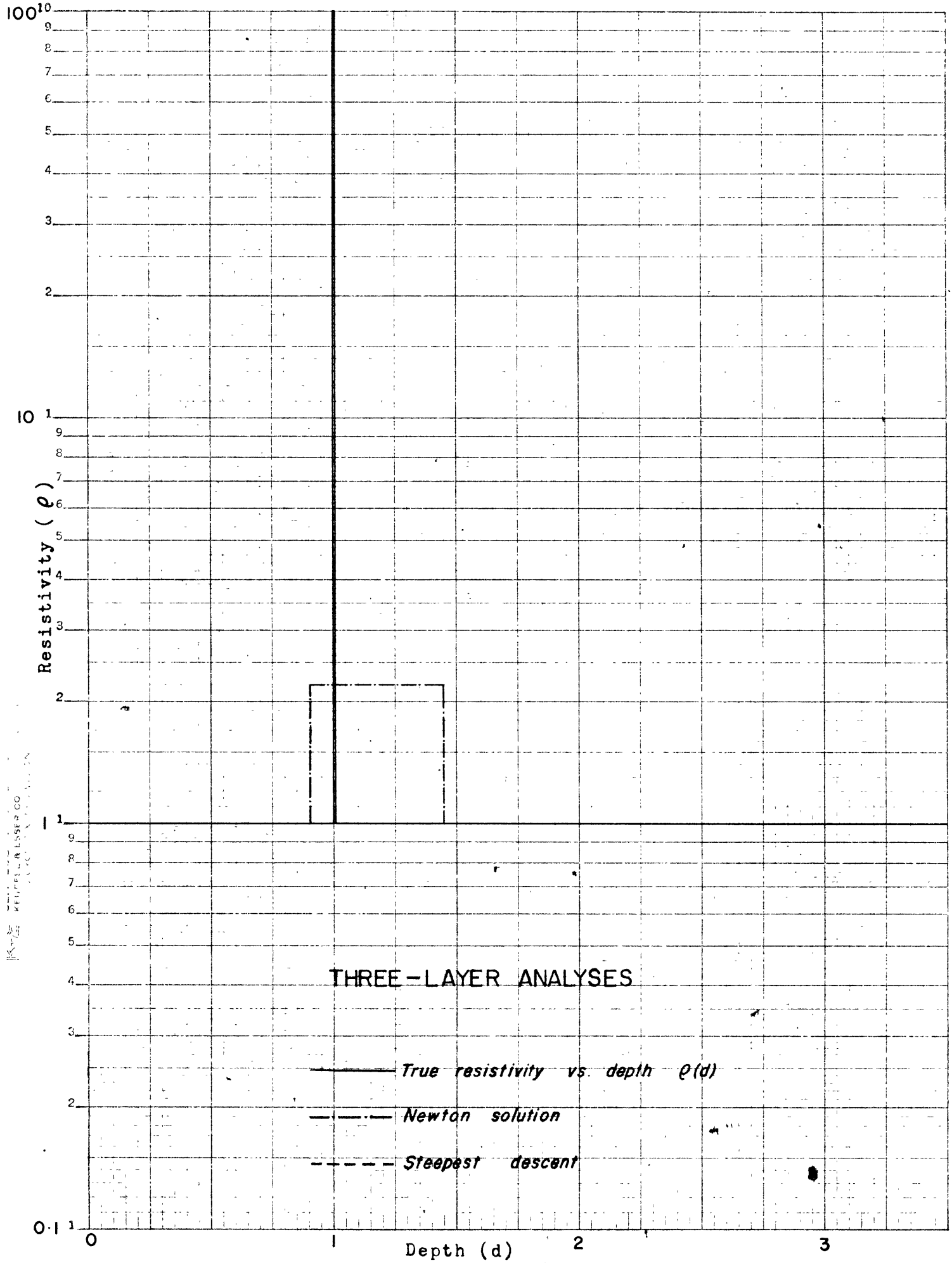
Resistivity (ρ)
Depth (d)
0
1
2
3
THREE-LAYER ANALYSES
True resistivity vs. depth ρ(d)
Newton solution
Steepest descent

Fig. 27

Case 22

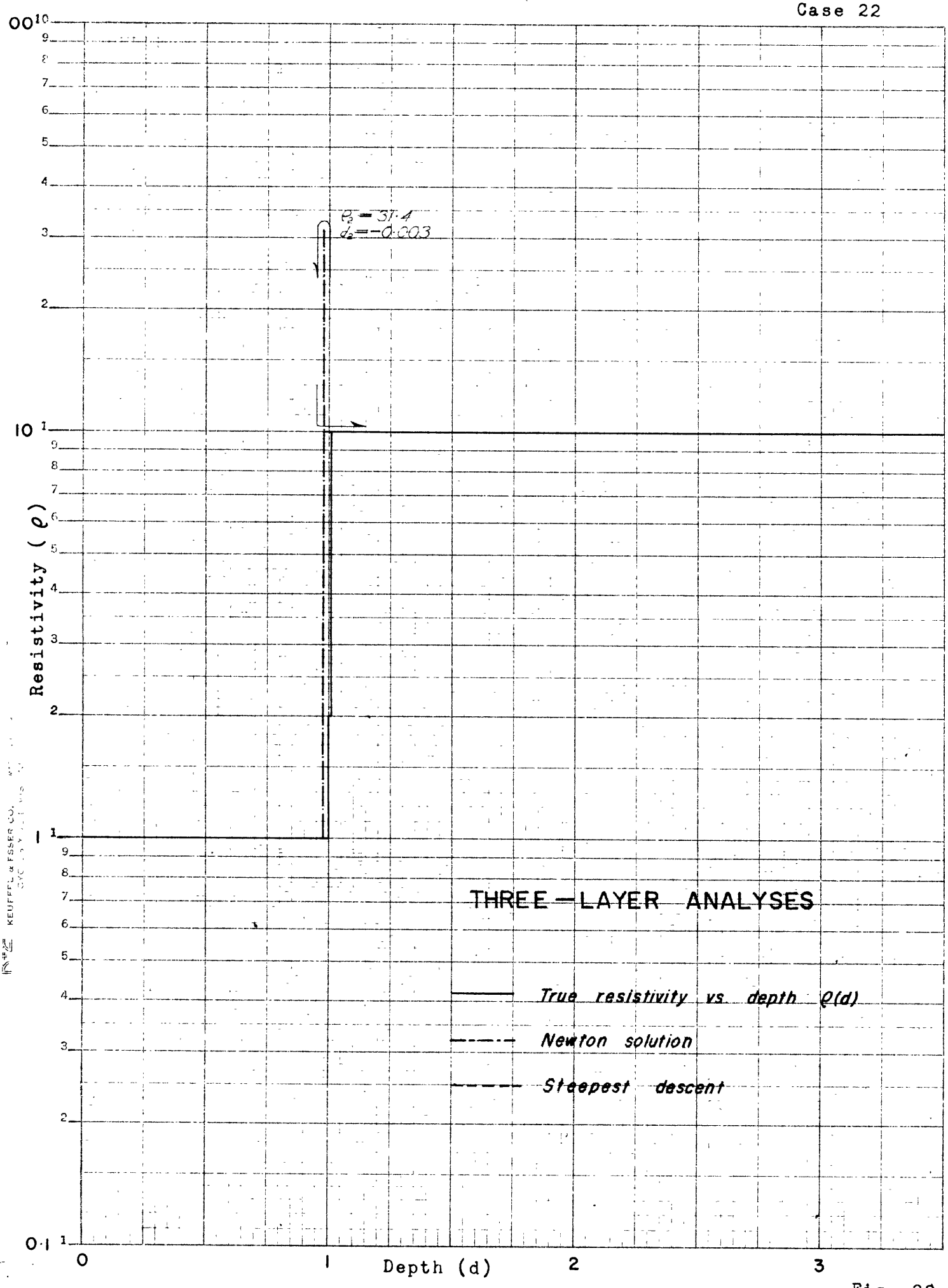

Fig. 28

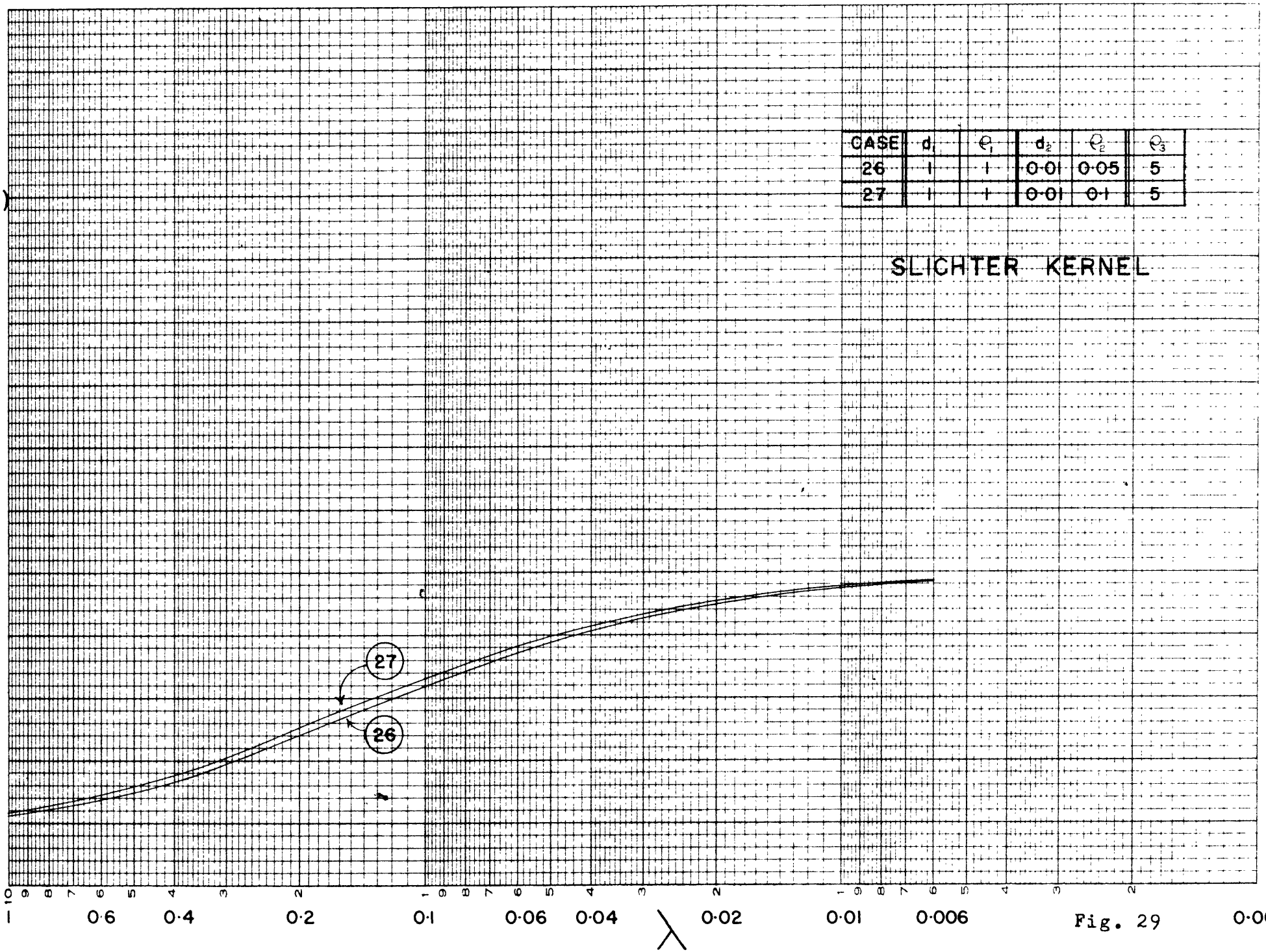
k(λ)
10
8
6
4
2
0
1
0·6
0·4
0·2
0·1
0·06
0·04
λ
0·02
0·01
0·006
0·001
27
26
SLICHTER KERNEL
CASE | d1 | ϱ1 | d2 | ϱ2 | ϱ3
26 | 1 | 1 | 0·01 | 0·05 | 5
27 | 1 | 1 | 0·01 | 0·1 | 5

Fig. 29

Fig. 29

Cases 26a 26b

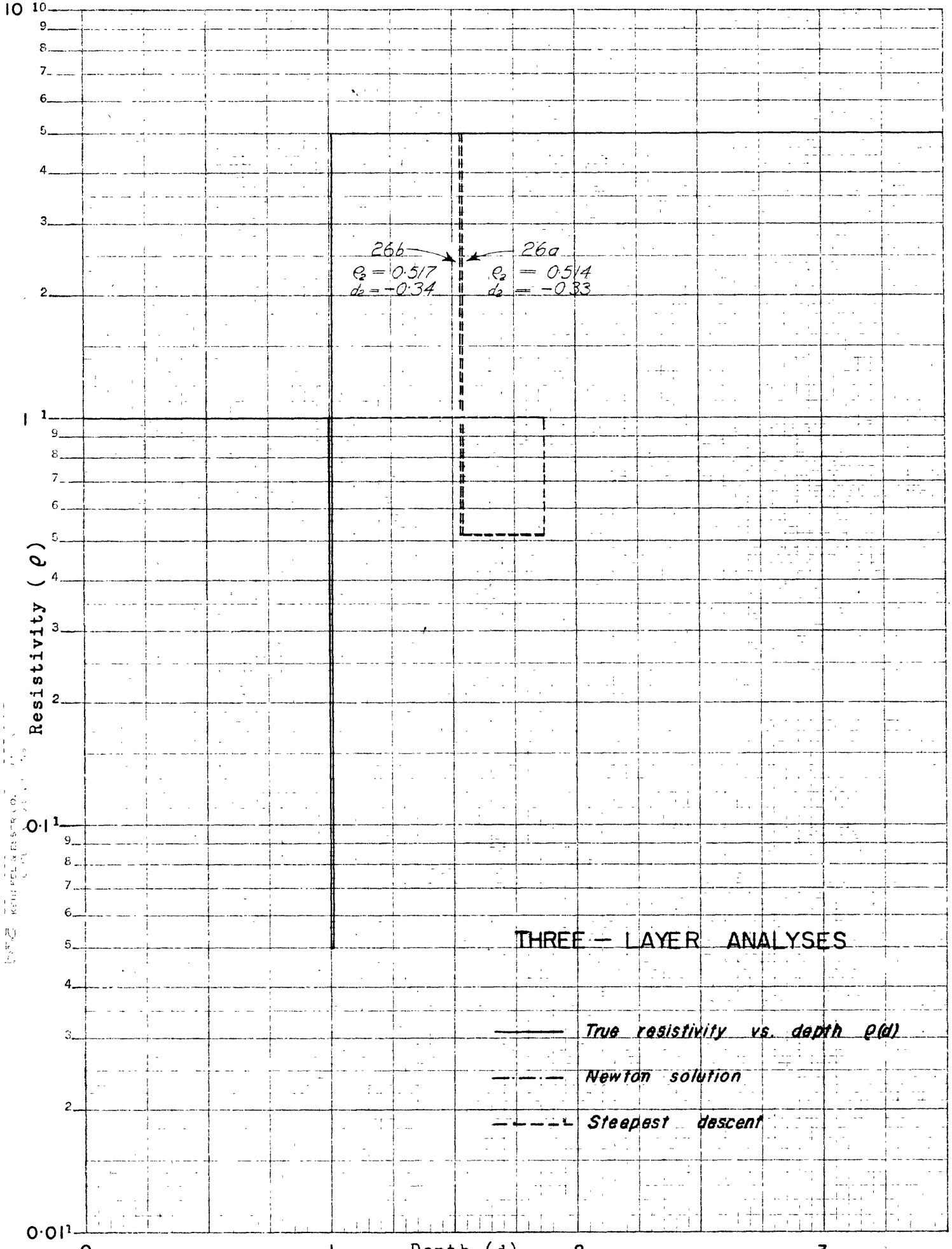

Fig. 30

Case 27

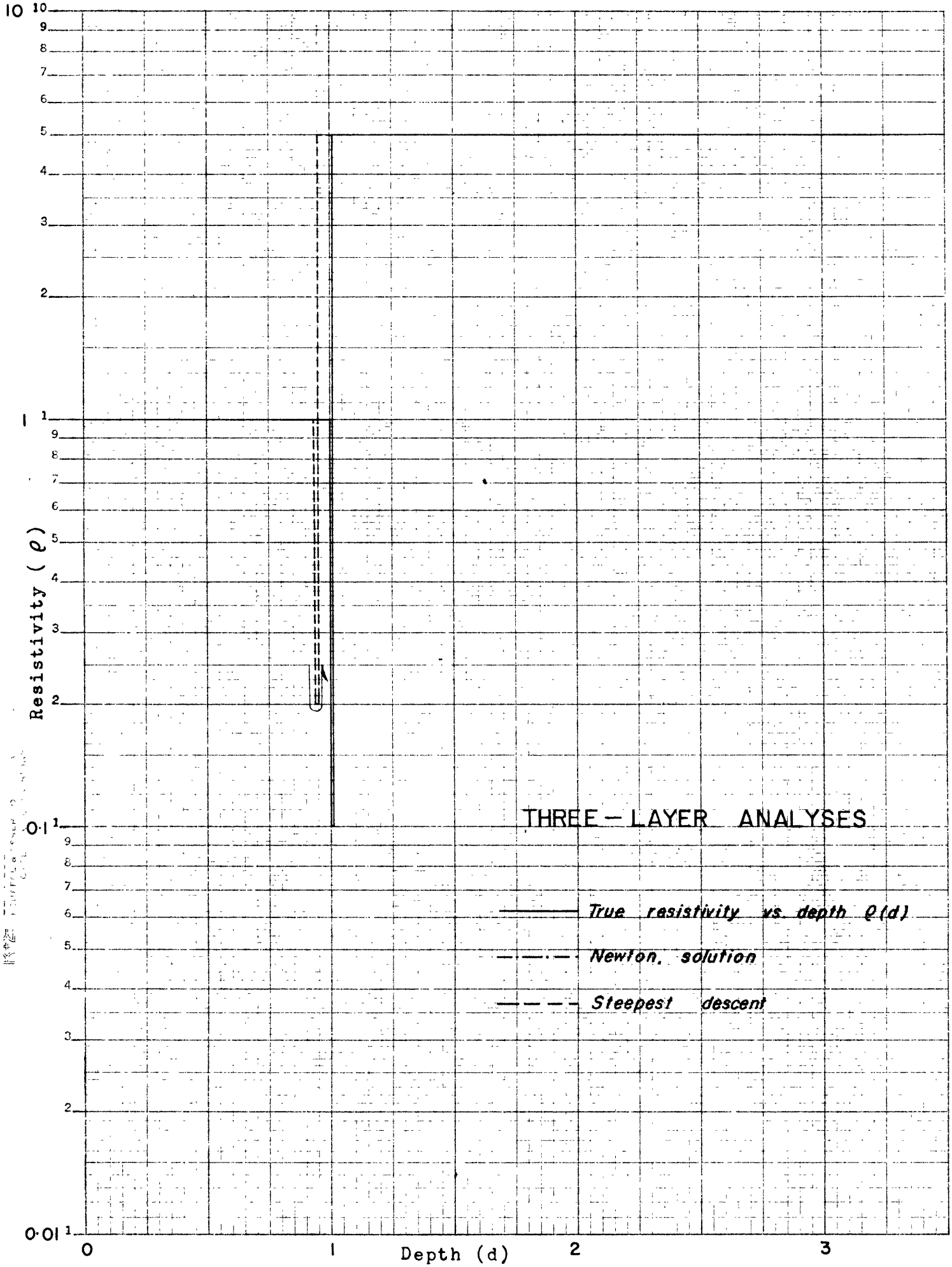

Fig. 31

Cases 23 24 25

CASE	d_1	ρ_1	d_2	ρ_2	d_3	ρ_3	ρ_4
23	1	1	1	100	4	1	0·01
24	1	1	1	0·01	4	1	100
25	1	1	4	10	1	1	0·1

FOUR—LAYER SLICHTER KERNEL

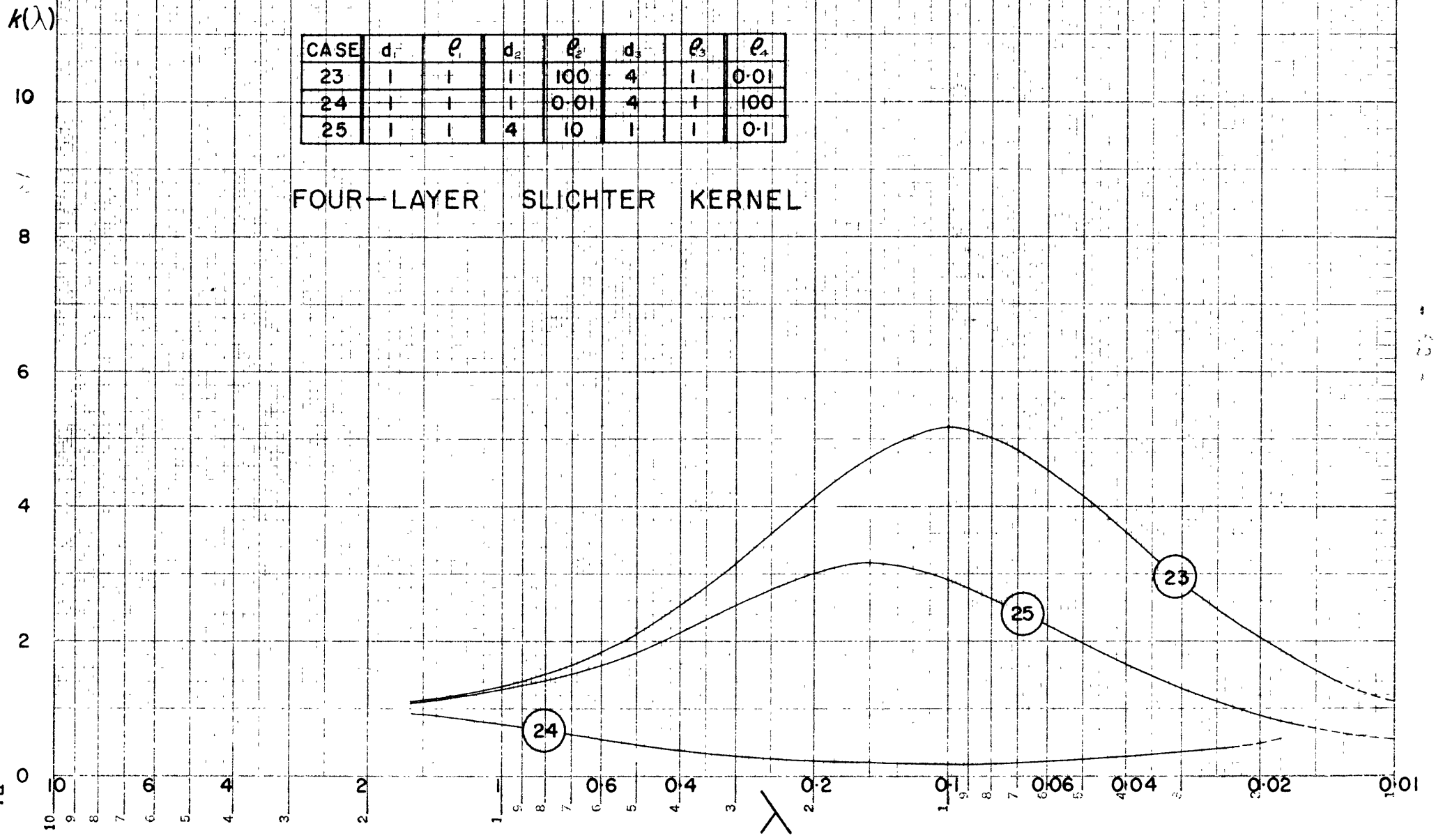

SEMI-LOGARITHMIC 359-71G

Fig. 32

Case 23

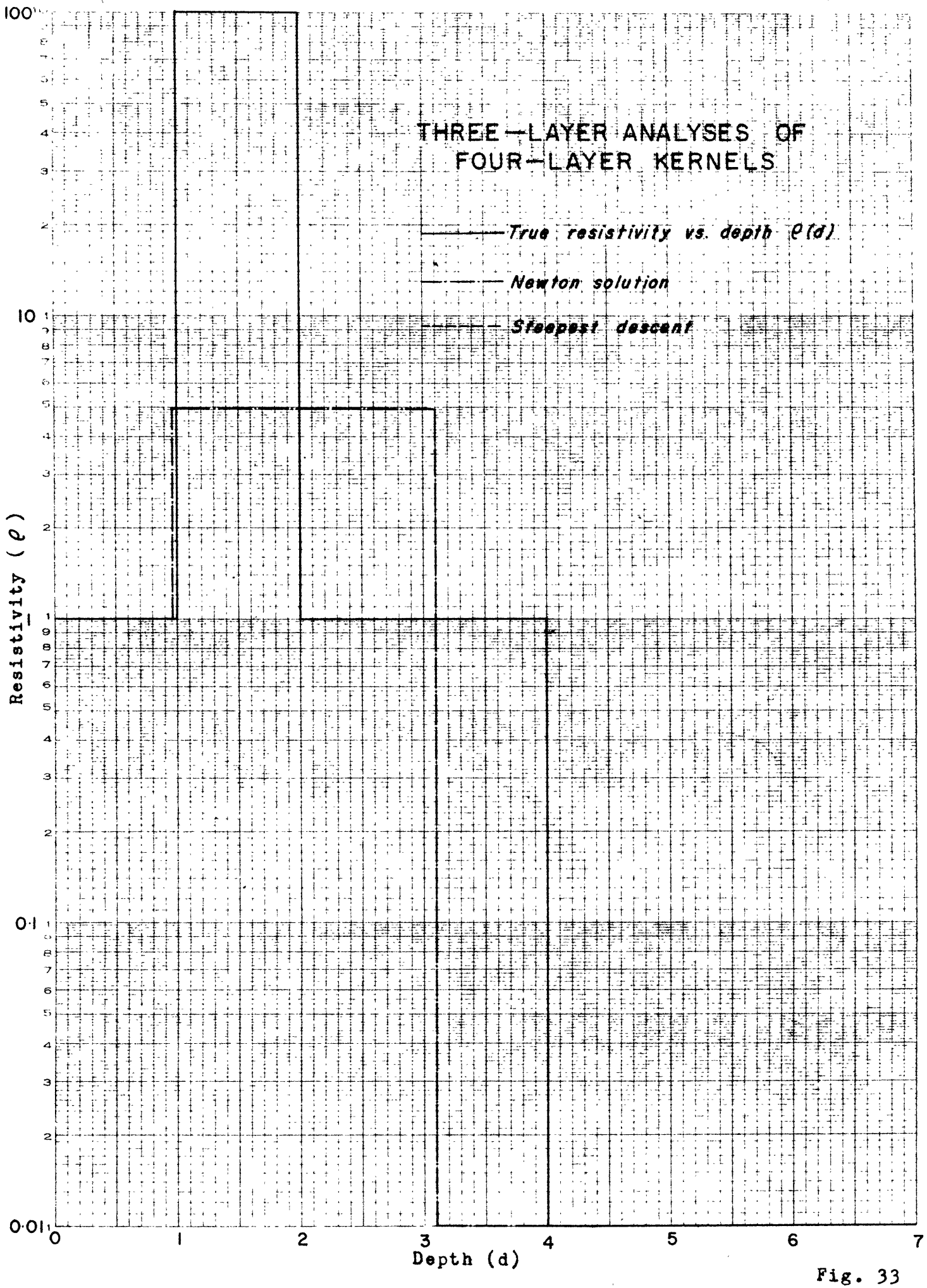

Fig. 33

Case 24

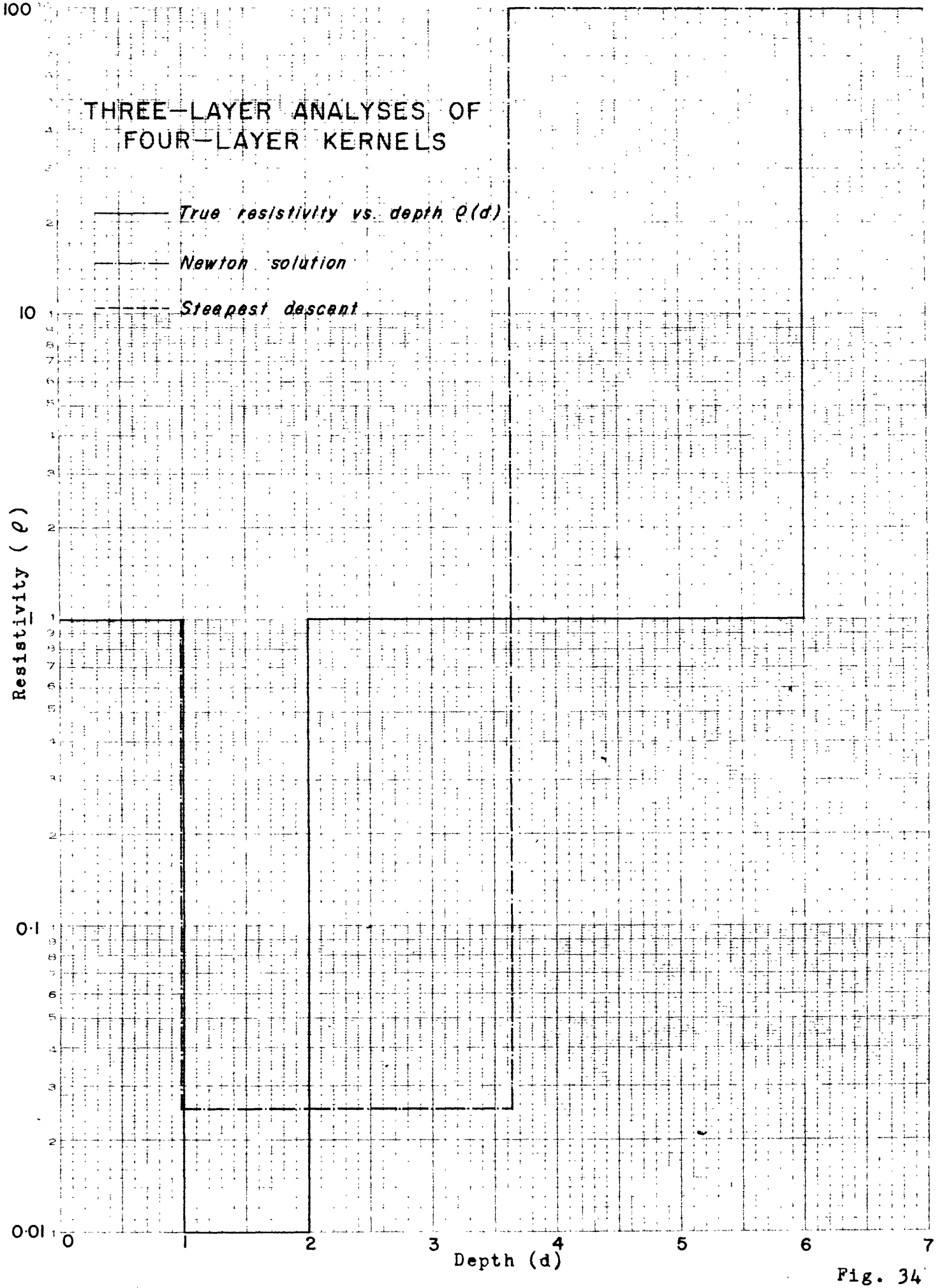

Fig. 34

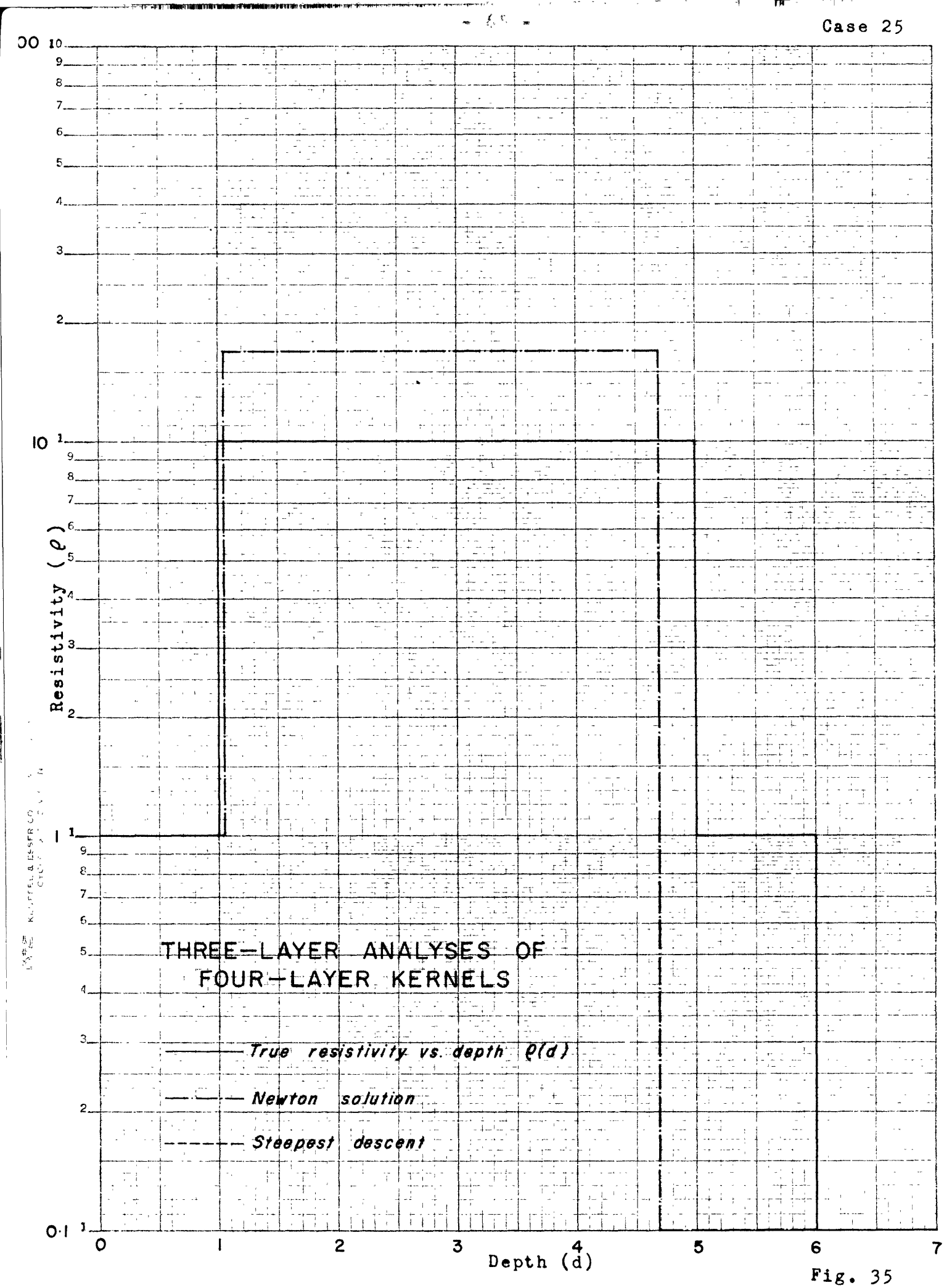
Resistivity (ρ)
Depth (d)
0
1
2
3
4
5
6
7
0.1
1
10
100
THREE-LAYER ANALYSES OF
FOUR-LAYER KERNELS
True resistivity vs. depth ρ(d)
Newton solution
Steepest descent

Fig. 35

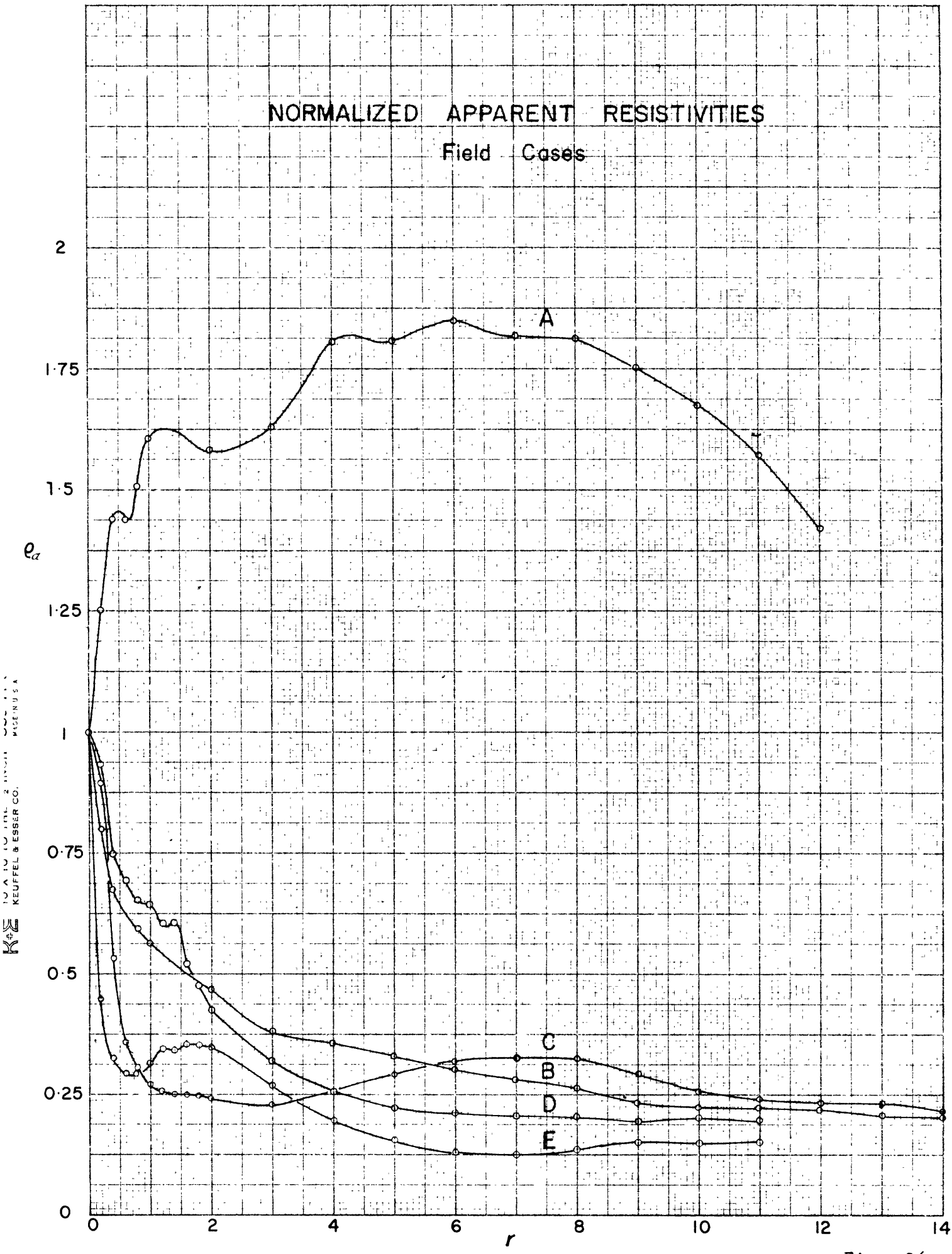
NORMALIZED APPARENT RESISTIVITIES
Field Cases
A
B
C
D
E
ϱ_a
r
2
1.75
1.5
1.25
1
0.75
0.5
0.25
0
0
2
4
6
8
10
12
14
KEUFFEL & ESSER CO.

Fig. 36

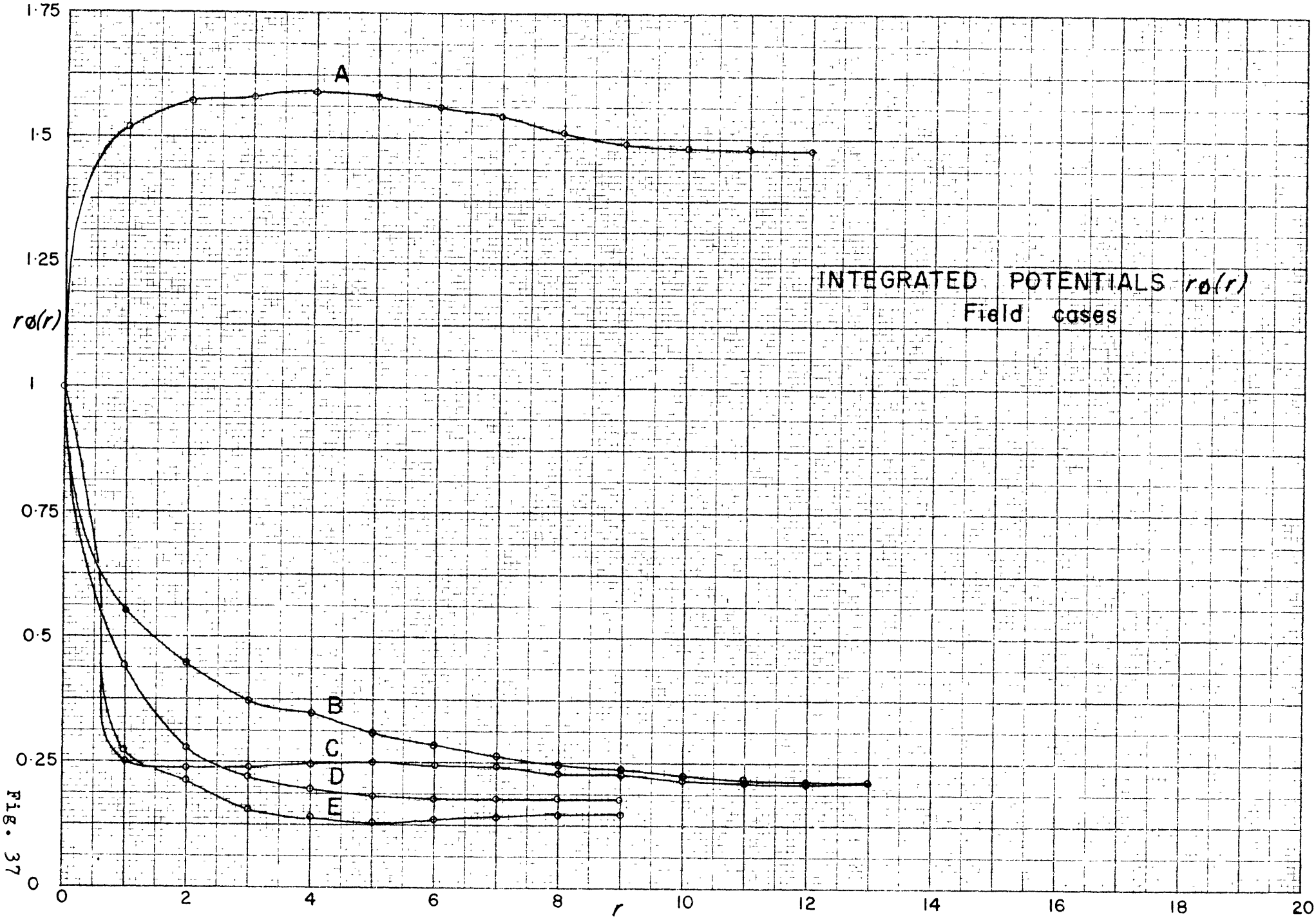

Fig. 37

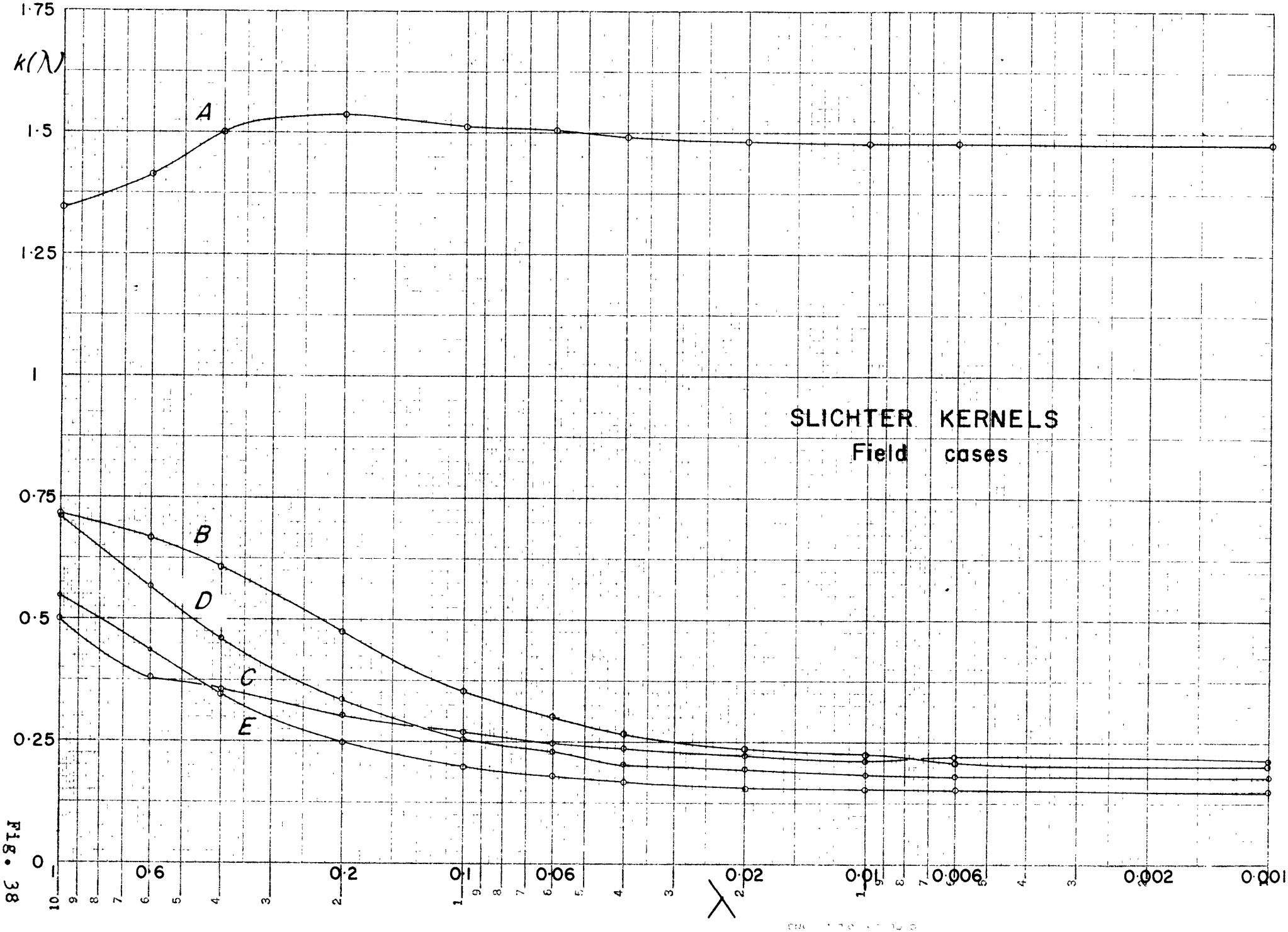

Fig. 38

Field Case A

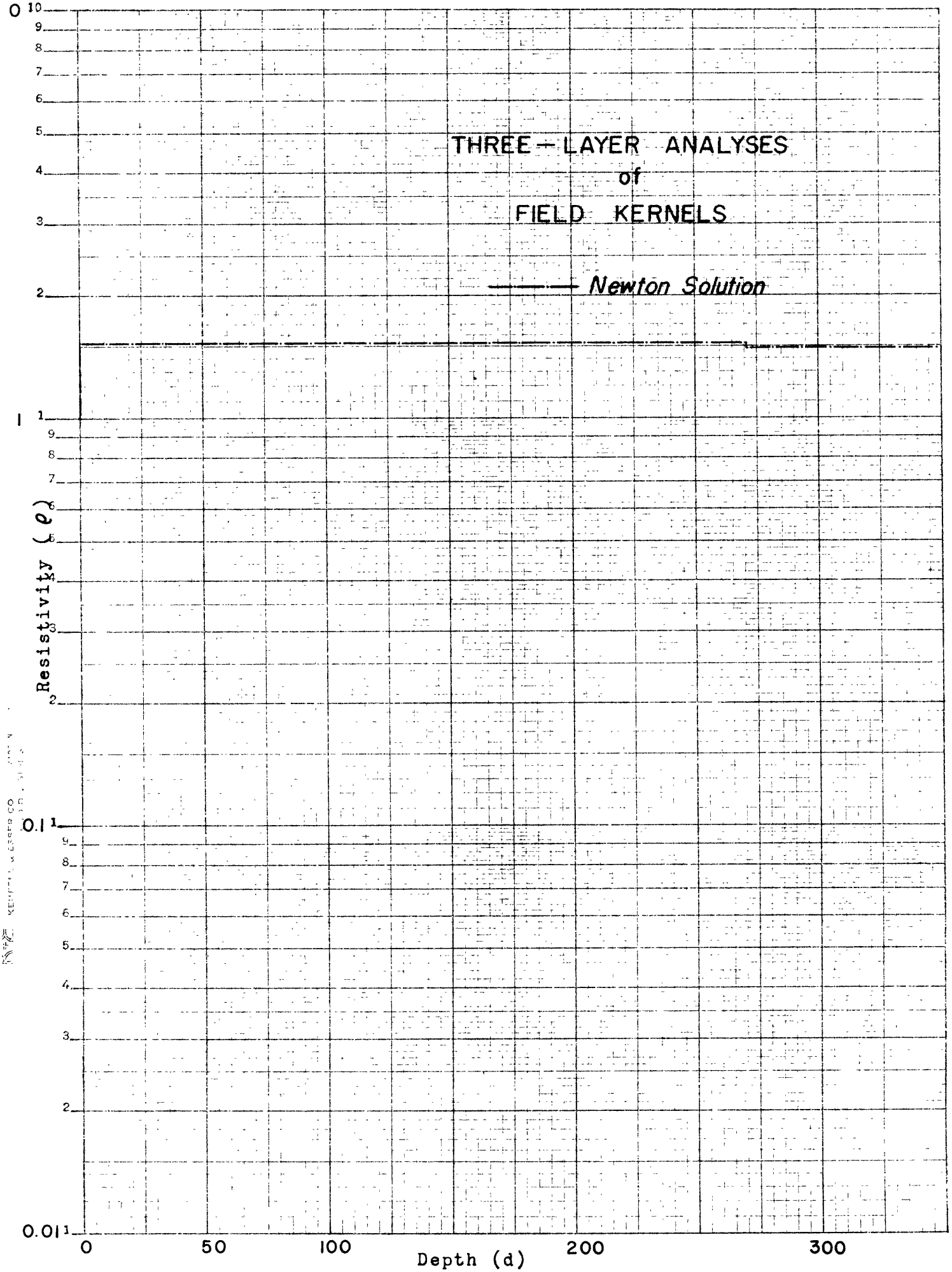

Fig. 39

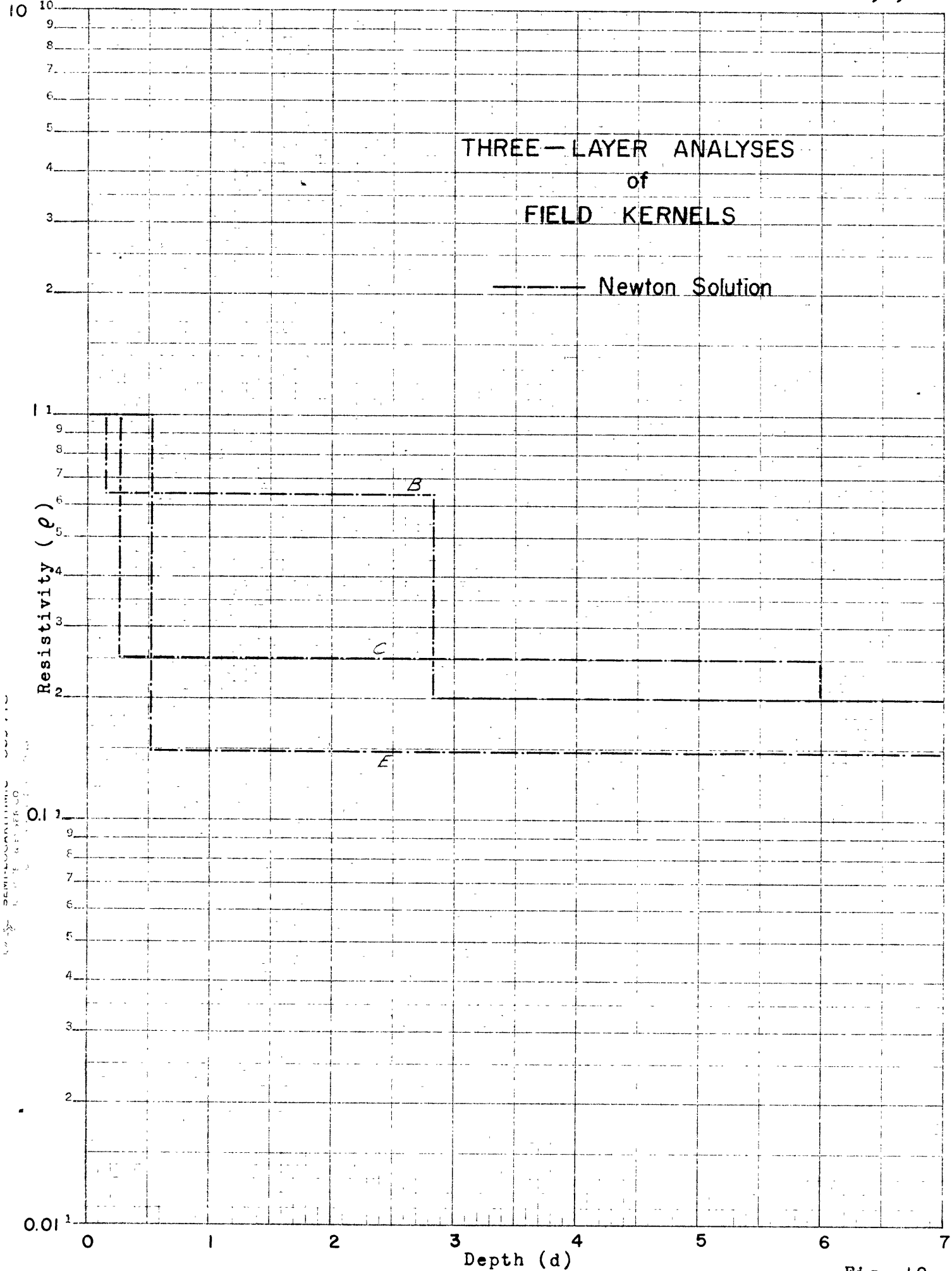
THREE—LAYER ANALYSES
of
FIELD KERNELS
—·—·— Newton Solution
B
C
E
Resistivity (ρ)
10
1
0.1
0.01
0
1
2
3
4
5
6
7
Depth (d)

Fig. 40

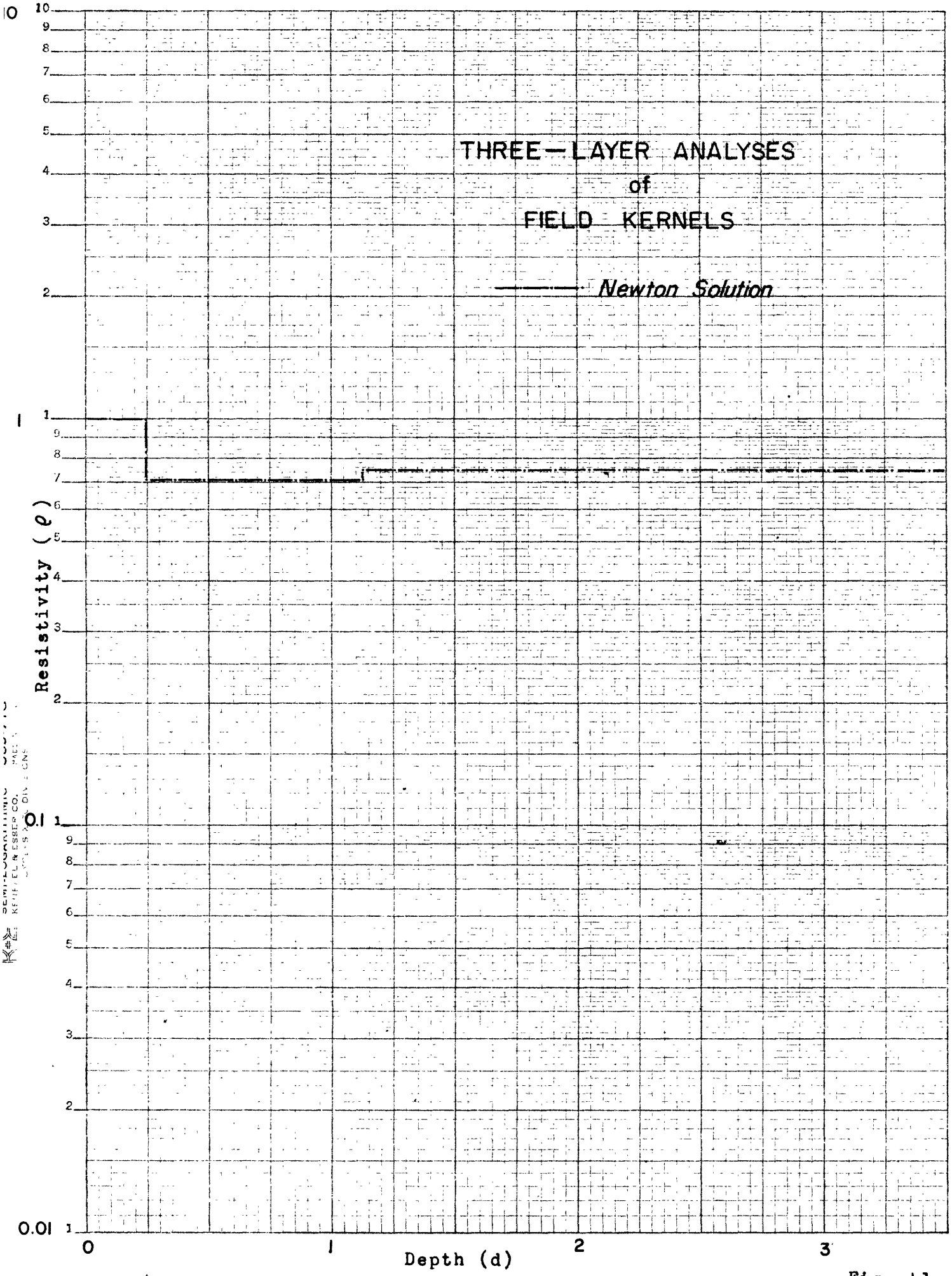
THREE—LAYER ANALYSES
of
FIELD KERNELS
Newton Solution
Resistivity (ρ)
Depth (d)
10
1
0.1
0.01
0
1
2
3

Fig. 41

V BIBLIOGRAPHY - PART ONE

Hallof, P.G. and Ness, N., Personal communication, 1955.

Hildebrand, F.B., Advanced Calculus For Engineers, Prentice-Hall, 1949.

Householder, A.S., Principles of Numerical Analysis, McGraw-Hill Book Co., 1953.

Langer, R.E., "An inverse problem in differential equations" Bull. Amer. Math. Soc., series 2, 39, p 814-820, 1933.

_____, "On the determination of earth conductivity from observed surface potentials", Bull. Amer. Math. Soc., series 2, 42, p 747-754, 1936.

Pekeris, C.L., "Direct method of interpretation in resistivity prospecting", Geophysics, V, no. 1, p 31-42, 1940.

Rogers, G.R., Personal communication, 1951.

von Sanden, H., Practical Mathematical Analysis, Methuen, 1923.

Schlumberger, C., "Abaques de sondage electrique", Geophysical Prospecting, III, Supplement 3, September 1955.

Slichter, L.B., "Interpretation of resistivity prospecting for horizontal structure", Physics, 4, p 307-322; also erratum p 407, 1933.

Stevenson, A.F., "On the theoretical determination of earth resistance from surface potential measurements", Physics, 5, p 114-124, 1934.

Sunde, E.O., Earth Conduction Effects in Transmission Systems, Van Nostrand, 1949.

Vozoff, K., "Newton analysis of earth resistivity measurements", Summary Report no. 41, Project Whirlwind, M.I.T., 1955.

PART TWO

I INTRODUCTION

The resistivity analysis problems fall into the class of inverse boundary value problems which have received very little attention from mathematicians. The cause of this, and as a result of it, they do not yield readily to existing analytical techniques, except in a few very special cases.

In the normal boundary value problem, one has a medium of given geometry and physical properties undergoing a physical disturbance, and wishes to find the effect of the particular medium on the disturbance. In the steady state (D.C.) problems dealt with here, the disturbance is a function of position, and has associated with it a mathematical function, a potential, which permits systematic treatment of the physical problem.

In the normal three dimensional formulation, then, one is given the differential or integral equation which the suitable potential must satisfy within a medium, the conditions which the potential must satisfy at boundaries between media of different properties, and the analytic representation of the boundaries. This information is dictated by physical considerations and is often idealized or simplified for mathematical reasons. From it, one attempts to find the potential everywhere in the medium.

One is sometimes able to write down all possible solutions to the differential equation in the medium. When this totality of solutions is forced to conform to some given boundary cond-

itions on a surface, (by integral equation formulation or by standard differential equation techniques) only a certain combination of the set of possible solutions is found allowable.

The inverse problem is that in which one attempts to determine, quantitatively, the properties of the medium from measurements, at a surface, of the response of the medium to disturbances. Mathematically, it is more difficult, and few examples are to be found in the literature (Slichter, 1954; Jost & Kohn, 1953; Langer, 1933). These are mainly specific examples; there is no general theory such as exists for the direct problem, and each new type must be solved starting from scratch.

II GENERAL THREE-DIMENSIONAL INHOMOGENIETY

DIRECT PROBLEM

Electrical prospecting is a standard method in geophysical exploration. In it one applies currents to the ground, and measures the voltage distribution, usually all at the surface, in order to find regions of anomalous conductivity. Qualitatively, the concept, its application, and interpretation are relatively straightforward. However, in a few cases qualitative interpretation is not sufficient, and it would be quite worthwhile to have available the tools of quantitative interpretation, for which we must go to the mathematical formulation of the problem.

Papers have been appearing on the subject since 1928,

(Ollendorff) but, with one exception, there has been very little mention of the case of general heterogeneity. The exception, a very interesting paper by Stevenson (1934) discusses both the normal and inverse boundary value problems, indicating formal solutions for both.

The following is a mathematical statement of the general problem, indicating two new kinds of solutions.

The statement of conservation of current at any point in space is

$$\nabla \cdot J = -s$$

where s is the magnitude of current source at the point. Then if $\sigma(P)$ is the conductivity at the point P

$$J(P) = \sigma(P)\nabla\phi(P)$$

$$\nabla \cdot J = \sigma\nabla^2\phi + \nabla\sigma \cdot \nabla\phi = -s$$

$$\nabla^2\phi + \nabla S \cdot \nabla\phi + \frac{s}{\sigma} = 0 \qquad (1)$$

$$S = \frac{\nabla\sigma}{\sigma} = \nabla(\log\sigma)$$

Equation (1) is the differential equation which our potential must satisfy. As indicated above, we can handle both the direct and the inverse problems as either differential or integral equations, each being advantageous for specific purposes. The proofs for existence and uniqueness of solutions to the direct problem have been rigorously developed in the work on elliptic differential equations (Bernstein, 1950; Petrovsky, 1954; Murray and Miller, 1954) and will not be given here.

Reciprocity of the Green's Function for the potentials

$\phi(P,Q)$ and $\phi(Q,P)$ (i.e. interchangability of sender and receiver positions) is not obvious for an inhomogeneous medium. It follows directly, however, from the self-adjointness of the differential equation

$$\sigma \nabla^2 \phi + \nabla \sigma \cdot \nabla \phi = 0$$

(Sommerfeld, 1949, p.50). It can also be verified that the normalized differential equation

$$\nabla^2 \phi + \nabla S \cdot \nabla \phi = 0$$

is not self-adjoint. Construction of a solution to the direct problem is not of interest here.

INVERSE PROBLEM

The problem of proving the existence of a solution to the inverse problem apparently does not arise (provided the physical assumptions are satisfied) because the data are obtained from measurements on a real earth. Stevenson's formal construction of a solution (1934) includes a plausibility argument for its uniqueness. This argument is implied in the work here; uniqueness has never been rigorously shown, to this writer's knowledge.

Part of the difficulty in solution of the inverse problem can be seen by reference to the differential equation (1). Both S and ϕ are unknown functions, hence the problem is non-linear. Further, it is non-linear in three dimensions. It will be seen how these facts hinder solution. If equation (1)

is rewritten (source at Q)

$$\nabla^2\phi\ (P,Q) = -\nabla\phi(P,Q)\cdot\nabla S(P) - \frac{s(P)}{\sigma(P)} = \varrho(P,Q) \qquad (2)$$

one can see the obvious resemblance to a Poisson equation, whose solution is (integrating over all space)

$$4\pi\phi(P,Q) = -\int_R G(P,R)\,\varrho\,(R,Q)\,dR \qquad (3)$$

$$= +\int_R G(P,R)\left[\nabla\phi(R,Q)\cdot\nabla S(R) + \frac{s(R)}{\sigma(R)}\right] dR \qquad (3a)$$

(This kind of solution was given by Stevenson and developed independently by T. R. Madden (personal communication). A physical picture of the solution as a distribution of interacting collections of charge, when all changes in resistivity are finite discontinuities, was pointed out by Madden.)

The physical requirement that there be no vertical current flow at the surface can be handled in either of two ways, each requiring a different Green's function. If $r_3 = 0$ is the earth's surface, r_3 positive downwards

$$(a)\ \sigma(r_1,r_2,r_3) = \sigma(r_1,r_2,-r_3)$$

$$G(P,R) = \frac{1}{r_{PR}} = \left[(p_1-r_1)^2+(p_2-r_2)^2+(p_3-r_3)^2\right]^{-\frac{1}{2}}$$

or

$$(b)\quad \sigma(R) = 0 \qquad r_3 < 0$$

$$G(P,R) = \frac{1}{r_{PR}} + \frac{1}{r'_{PR}}$$

$$r'_{PR} = \left[(p_1-r_1)^2+(p_2-r_2)^2+(p_3+r_3)^2\right]^{\frac{1}{2}}$$

It is seen that these are equivalent. Using (a), and recog-

nizing that in the practical problem of isolated sources

$$s(P) = \delta(P,Q)$$

$$4\pi\phi(P,Q) = \int_R \frac{\delta(R,Q)}{\sigma(R) r_{RP}}\, dR + \int_R \frac{\nabla\phi(R,Q)\cdot\nabla S(R)}{r_{PR}}\, dR \qquad (4)$$

The source term simplifies to

$$\int_R \frac{\delta(R,Q)}{\sigma(R) r_{RP}} = \frac{1}{\sigma(Q) r_{PQ}}$$

Thus it is, unfortunately, this three-dimensional, non-linear, inhomogeneous integro-differential equation whose solution we desire. To further complicate the mathematical situation, the equation is singular both in the kernel $(\frac{1}{r})$ and in the limits

$$(-\infty , \infty)$$

Instead of the integro-differential equation, we can write the pair of integral equations

$$4\pi\phi(P,Q) = -\int_R G(P,R)\,\rho(R,Q)\, dR \qquad (3)$$

and

$$\rho(R,Q) = -\frac{\delta(R,Q)}{\sigma(R)} - \int \rho(T,Q)\nabla S(R)\cdot\nabla G(R,T)\, dT \qquad (5)$$

An infinite series solution for the second equation can be written by substituting the entire right hand side of the equation for $\rho(R,Q)$ inside the integral

$$\rho(R,Q) = -\frac{\delta(R,Q)}{\sigma(R)} - \int\left[\frac{-\delta(T,Q)}{\sigma(T)} - \int \rho(U,Q)\nabla S(T)\cdot\nabla G(T,U)\, dU\right]\nabla S(R)\cdot\nabla G(R,T)\, dT$$

$$= \frac{-\delta(R,Q)}{(R)} + \nabla S(R)\cdot\nabla G(R,Q) + \iint\left[\rho(U,Q)\nabla S(T)\cdot\nabla G(T,U)\, dU\right]\nabla S(R)\cdot\nabla G(R,T)\, dT$$

and repeating the process an infinite number of times. The

expressions can be simplified somewhat by writing

$$H(A,B) = \nabla S(A) \cdot \nabla G(A,B)$$

$$\rho(R,Q) = -\frac{\delta(R,Q)}{\sigma(R)} + \frac{H(R,Q)}{\sigma(Q)} + \int H(R,T) \int H(T,U) \rho(U,Q)\, dU dT$$

$$= -\frac{\delta(R,Q)}{\sigma(R)} + \frac{H(R,Q)}{\sigma(Q)} - \int H(R,T) \int \frac{H(T,U)}{\sigma(Q)} dU dT + \int H(R,T) \int H(T,U)\, \frac{H(U,Q)}{\sigma(Q)} dU dT$$

$$+ \int H(R,T) \int H(T,U) \int H(U,V) \int H(V,W) \int (W,Q)\, dW dV dU dT$$

etc., in which the H(A,B) acts as an influence function. It is this form of the expression which suggests the physical picture of a source function composed of interacting charge densities. When conductivity changes occur at surfaces of finite discontinuity, the magnitude of interaction suggests that the surfaces act as layers of charge.

Substituting this expression for ρ into the expression for ϕ

$$4\pi\phi(P,Q) = \frac{G(P,Q)}{\sigma(Q)} - \frac{1}{\sigma(Q)} \int_R G(P,R) H(R,Q)\, dR \qquad (6)$$

$$- \int G(P,R) \int H(R,U) \int H(U,T)\, \rho(T,Q)\, dT dU dR$$

Thus, the potential is expressed as an infinite series, the first term of which varies as $\frac{1}{r}$. The function H(A,B) contains a gradient of $\frac{1}{r_{AB}}$, meaning a variation as $\left(\frac{1}{r_{AB}}\right)^2$. Succeeding terms of the expansion for ϕ, therefore, depend as

a) $\frac{1}{r}$ on the distance between P and locations of conductivity gradients,

b) $\frac{1}{r^2}$ on the distances between locations of conductivity gradients

and c) $\frac{1}{r^2}$ on the distance between the potential source (Q) and locations of conductivity gradients,

all modified by the angular relationships $\nabla S(A) \cdot r_{AB}$. Since all integrals must be dimensionally equivalent, there is no a priori reason to say that the contributions from successive terms must diminish in magnitude. If, however, the conductivity gradients are non-vanishing only over finite ranges, it would be expected that the multiples of $\frac{1}{r^2}$ will force such diminution. It is interesting to note that, despite the apparent dissymmetry in P and Q, $\phi(Q,P)$, must equal $\phi(P,Q)$.

The object, then, is solve the integral equation (6) for $S(R) = \log \sigma(R)$. The equation is insoluble analytically because of the difficulties mentioned previously, the non-linearity being the major obstacle. One may, of course, approximate the solution by trial and error. Such a procedure with a three dimensional function, however, borders on the impractical, even with the best of modern computing facilities.

By neglecting all but the first two terms on the right side of equation (6) we are left with a linear approximation to $\phi(P,Q)$ which is tractable.

$$4\pi\phi(P,Q) \approx \frac{G(P,Q)}{\sigma(Q)} - \frac{1}{\sigma(Q)} \int_R G(P,R)\, H\,(R,Q)\, dR \qquad (7)$$

$$\approx \frac{1}{\sigma(Q) r_{PQ}} - \frac{1}{\sigma(Q)} \int_R \frac{\nabla S(R) \cdot \nabla\left(\frac{1}{r_{RQ}}\right)}{r_{PR}}\, dR$$

$$\approx \frac{1}{\sigma(Q) r_{PQ}} - \frac{1}{\sigma(Q)} \int_R \frac{\nabla S(R) \cdot r_{RQ}}{r_{PR}\, r_{RQ}^3}\, dR$$

It is this approximation which we will attempt to solve for S(R).

The quality of the linear approximation can be studied in a special case in which the direct potential problem is soluble exactly in closed form. That is, in the case of a single vertical discontinuity, where

$$\phi(P,Q) = \frac{1}{4\pi\sigma_1}\left[\frac{1}{r_{PQ}} + \frac{\sigma_1 - \sigma_2}{r'_{PQ}(\sigma_1 + \sigma_2)}\right]$$

for P in medium of σ_1, and

$$\phi(P,Q) = \frac{1}{2\pi r_{PQ}(\sigma_1 + \sigma_2)}$$

for P in medium of σ_2 (see Figure 1)

The approximation in this case is

$$\phi(P,Q) \approx \frac{1}{4\pi\sigma_1 r_{PQ}} - \frac{1}{4\pi\sigma_1} \lim_{b\to a} \int_{-\infty}^{\infty} dr_1 \int_{-\infty}^{\infty} dr_3 \int_{a}^{b} \frac{(S_1 - S_2)(r_2 - q_2)\,dr_2}{(a-b)\,r_{PR}\,r_{QR}^3}$$

$$\theta(P,Q) = (S_1 - S_2)(a - q_2) \int_{-\infty}^{\infty} dr_1 \int_{-\infty}^{\infty} dr_3 \Big/ \left[(p_1 - r_1)^2 + (p_2 - a)^2 + (p_3 - r_3)^2\right]^{\frac{1}{2}} \left[(q_1 - r_1)^2 + (q_2 - a)^2 + (q_3 - r_3)^2\right]^{\frac{3}{2}}$$

$$= (S_1 - S_2)(a - q_2) \int_{-\infty}^{\infty} dr_1 \int dr_3 \left[(p_1 - r_1)^2 + r_3^2 + (p_2 - a)^2\right]^{\frac{1}{2}} \left[(q_1 - r_1)^2 + r_3^2 + (q_2 - a)^2\right]^{\frac{3}{2}}$$

A major point of difference is the manner in which the conductivities enter. In the exact solution the conductivities enter in algebraic functions which have finite limits as the contrast increases. The same is true of the sphere in an otherwise homogeneous medium. In the approximate expression there is no saturation of effect with increasing contrast, which is a strong indication of the importance of succeeding terms in the expansion. That this saturation actually occurs was observed

by Hallof (1955) in model experiments with finite sized conductors. He found that the factor*

$$\frac{3(\sigma_1 - \sigma_2)}{\sigma_1 + 2\sigma_2}$$

gave much closer agreement with experimental results than did

$$\log \frac{\sigma_1}{\sigma_2}$$

A first glance at the succeeding terms of the expansion (equation 6) gives the impression that, in the case of a single surface of discontinuity, these terms are identically zero. However, if they are set up for a region of finite thickness, δ, of gradient $(S_1 - S_2)/\delta$, and the limiting operation $(\delta \to 0)$ is performed, it becomes quite clear that these terms remain finite, and there is an interaction effect within the surface.

One might speculate that a comparison of the exact solution with the terms of the expansion may point the way to exact solutions of the integrals in the expansion.

The question arises of the amount of information which is necessary for a solution. The conductivity is a three dimensional function, whereas the potentials $\phi(P,Q)$ on the surface from a fixed source, Q_o, on the surface are $\phi(p_1,p_2,0;Q_o)$, a two-dimensional function. The logical step is to measure $\phi(P,Q)$ with a one-dimensional variation of Q, i.e. measure $\phi(p_1,p_2,0;q_1,0,0)$ for example, with p_1, p_2, and q_1, each varying over the entire range $(-\infty, \infty)$. This is only a plausibility argument, and is the one given by Stevenson. (It should be emphasized that the mathematics

* A factor which he was able to justify theoretically.

and many of the arguments up to this point follow very closely the work of Stevenson, who, unfortunately, carried the solution no farther.) For the development of the first kind of solution the validity of the argument is assumed. A more logical argument will follow from the limiting case of the second kind of solution.

First Kind of Solution

Morse, (1953, p. 926, ff) presents a series solution which is applicable to equation (7). Let us first put it in form

$$4\pi\sigma(Q)\phi(P,Q) - \frac{1}{r_{PQ}} = \theta(P,Q) = \int_R \frac{\nabla S(R) \cdot r_{RQ}}{r_{PR}\, r_{RQ}^3} dR \quad (8)$$

Next, the procedure is to represent the functions θ and S by series or integrals valid over their entire range; θ with coefficients determinable numerically or analytically, and S with coefficients determinable by comparison with those of θ. Trying the integrals first, let

$$S(R) = \int_K A(K) e^{-iK \cdot R}\, dK$$

S is represented as the Fourier transorm of the function A(K), and when either S(R) or A(K) is known, the other is uniquely defined. Then

$$\theta(P,Q) = \int \frac{r_{RQ} \cdot \int -iKA(K) e^{-iK \cdot R} dK}{r_{PR}\, r_{RQ}^3}\, dR$$

$$= \int \frac{1}{r_{PR}\, r_{RQ}^3} \int -ir_{RQ} \cdot KA(K) e^{-iK \cdot R}\, dK dR$$

Assuming that S(R) is well enough behaved, the order of

integration can be reversed

$$\theta(P,Q) = \int - iA(K) \int \frac{r_{RQ}\cdot K}{r_{PR}\, r_{RQ}^3} e^{-iK\cdot R} dR dK$$

$$= - i \int A(K) F(P,Q,K)\, dK$$

$$F(P,Q,K\cdot) = \int \frac{r_{RQ}\cdot K}{r_{PR}\, r_{RQ}^3} e^{-iK\cdot R}\, dR$$

and A(K) would be determined by a suitable inverse transform type of operation on $\theta(P,Q)$, the operator determined by the form of F(P,Q,K). It was found impossible to evaluate the integral F(P,Q,K) in terms of simple functions, however. If a series representation is used instead, in the hope that the result might be an infinite series of tractable functions one obtains similar results, viz; let

$$S(R) = \sum_{j=0}^{\infty} \sum_{k=0}^{\infty} \sum_{l=0}^{\infty} A_{jkl}\, f_j(r_1) g_k(r_2) h_l(r_3) w_1(r_1) w_2(r_2) w_3(r_3)$$

where the f_j, g_k, and h_l are sets of functions orthogonal over the infinite range, and the w_i are chosen to force convergence of the series by approximating the variation in the r_i coordinate. Then

$$\theta(P,Q) = \int \frac{r_{PQ}\cdot \nabla \left[\sum_j \sum_R \sum_l A_{jkl} f_j g_k h_l w_1 w_2 w_3 \right]}{r_{PR}\, r_{RQ}^3} dR$$

$$= \sum_j \sum_R \sum_l A_{jkl} \int \frac{w_1 w_2 w_3\, r_{RQ}\cdot \nabla [f_i g_j h_l]}{r_{PR}\, r_{RQ}^3} dR$$

$$= \sum_j \sum_R \sum_l A_{jkl} \int \left[(r_1 - q_1) f_j' g_k h_l + (r_2 - q_2) f_j g_k' h_l + (r_3 - q_3) f_j g_k h_l' \right] \frac{w_1 w_2 w_3}{r_{PR}\, r_{RQ}^3} dR$$

provided that the integrals converge.

$$\theta(P,Q) = \sum_j \sum_k \sum_l A_{jkl} F_{jkl}(P,Q)$$

$$F_{jkl}(P,Q) = \int \frac{w_1 w_2 w_3}{r_{PR} r_{RQ}^3} \left[(r_1 \cdot q_1) f_j' g_k h_l + (r_2 \cdot q_2) f_j g_k' h_l + (r_3 \cdot q_3) f_j g_k h_l' \right] dR$$

By setting the $w_i = 1$, one could conceivably devise sets of functions f, g, and h which would yield an $F_{jkl}(P,Q)$ in terms of standard functions. A great deal of effort was devoted to this problem, however, and it appears to be impossible.

It would seem more advisable, if one must deal with functions of the type $F(P,Q,K)$ or $F_{jkl}(P,Q)$, to calculate their mappings in three dimensions. Although the mappings need be calculated only once, a threefold infinity is necessary, again removing the task from the realm of immediate practicality.

Second Kind of Solution

If we can assume further (i.e. in addition to the linearity) that the conductivity does not vary beyond a limited region of space, and that the region can be considered as being made up of homogeneous blocks of given geometry but unknown conductivity, a solution can be written which gives results from finite calculations. This approach has many interesting possibilities, in that the blocks can simulate

many common geologic geometries for which the mathematical problem has not been solved (vertical strata under overburden, for example) in addition to the general three-dimensional variation. However, it will have to be applied with care if it is to be a good approximation as well as a practicable solution. A general description will be given before going into detail.

Let the space of variable conductivity be considered as divided into a three-dimensional array of cubes, the logarithm of the conductivity of the typical cube being

$$S_{ijk} \qquad i = 1, 2, - - - l;\ j = 1, 2, - - - m;$$
$$k = -n, -n+1, - - - , -1, +1, +2, - - -, n-1, n$$

and

$$S_{ijk} = S_{i,j,-k}$$

by virtue of our earlier assumptions. Then from equation (8)

$$\theta(P,Q) = \iiint_R \frac{\nabla S(R) \cdot \left(\frac{1}{r_{RQ}}\right)}{r_{PR}}\, dR$$

$$= \iiint_R \frac{H(R,Q)}{r_{PR}}\, dR$$

Obviously, all contributions to the integral come from the interfaces between cubes. Considering an element of area of an interface, normal $\hat{n}$, across which there is a change of conductivity $\triangle S$,

$$H(R,Q) = \frac{\triangle S}{r^3_{RQ}}\, \hat{n} \cdot r_{RQ}$$

If we sum over all interfaces $\left[1xmx(n+1) + 1x(m+1)xn + (1+1)xmxn = 3(1xmxn) + 1xm + 1xn + mxn\right.$ in all

$$\theta(P,Q) = \sum_{\alpha} \Delta S_{\alpha}\, \hat{n}_{\alpha} \cdot \iint_{\alpha} \frac{r_{RQ}}{r_{RQ}^{3}\, r_{PR}}\, dA \qquad (9)$$

Here dA is the element of area on interface α. For a given geometry, the values of the integrals are constants and can be calculated for all α. The unknowns, then, are the ΔS , or the S_{ijk}, of which there are a given number. Since the number of observations, $\theta(P,Q)$, is arbitrary, it is seen that a solution can be written in terms of a set of linear equations if we choose the number of observations equal to the number of unknowns.

These equations in terms of conductivities would be

$$\theta(P,Q) = \sum D_{ijk}\ (P,Q)\ S_{ijk}$$

$$D_{ijk}\ (P,Q) = 2\left\{ \hat{i} \cdot \left[\iint_{\alpha_1} \frac{r_{RQ}\, dA}{r_{RQ}^{3}\, r_{RP}} - \iint_{\alpha_2} \frac{r_{RQ}\, dA}{r_{RQ}^{3}\, r_{RP}} \right] \right.$$

$$+ \hat{j} \cdot \left[\iint_{\alpha_3} \frac{r_{RQ}\, dA}{r_{RQ}^{3}\, r_{RP}} - \iint_{\alpha_4} \frac{r_{RQ}\, dA}{r_{RQ}^{3}\, r_{RP}} \right]$$

$$\left. + \hat{k} \cdot \left[\iint_{\alpha_5} \frac{r_{RQ}\, dA}{r_{RQ}^{3}\, r_{RP}} - \iint_{\alpha_6} \frac{r_{RQ}\, dA}{r_{RQ}^{3}\, r_{RP}} \right] \right\}$$

where α_1 is the surface bounding cubes $\left[(i-1),\ j,\ k\right]$ and (i,j,k), α_2 is that bounding cubes (i,j,k) and $(i+1),\ j,\ k$, α_3 is that

between i, (j-1), k and (i,j,k), etc. The factor of two arises from the symmetry of conductivity distribution about the plane $r_3 = 0$.

In the limiting case of a triple infinity of cubes we will obviously require a like number of observations. Thus we are led back to the necessity for a double infinity of receiving points (P coordinate), and the single infinity of source points (Q coordinate), or vice-versa, a double infinity of sources and a single infinity of receivers.

In setting up a routine for practical interpretation, based on this last approach, our choice of geometry is dictated by several considerations. These are

a) There is a normal decrease in resolving power with depth. In the limit, very little detailed information can be expected from depths much greater than the maximum sender-receiver distance.

b) The minimum "wavelength" of lateral conductivity variations which can be discerned is limited by the minimum spacing of surface stations.

Field examples will seldom, if ever, satisfy the assumption of no conductivity variations outside of a restricted volume. Since the resistivity measurements are assumed to extend well beyond the area of direct interest, conductivity variations outside of this area can possibly be represented well enough by a few large blocks. It will be noted, however, that some definition will be lost within the volume of interest if we are forced

to consider changes outside for two reasons; the amount of data is the same for a greater volume, and the approximations at the edges will be poor.

It would be best to illustrate the use of this method with a simple two-dimensional example. However, the coefficients D_{ijk} are still in the process of integration, by P.G. Hallof and M. Ness (1955).

III HORIZONTALLY STRATIFIED MEDIA

If the geological situation is such that the conductivity can be assumed to be a function of depth only, considerable simplification appears in the mathematics. This approach is of interest where there are flat-lying sediments, at water tables in gravel-filled valleys, and in a few other situations, (gross earth structure, for example).

The theoretical problem, for a point source on the surface, has been discussed at great length and with considerable elegance by several writers. Langer (1933) and Slichter developed solutions to the direct and inverse problems for the case of a smoothly-varying $\sigma(z)$. Their inverse solution, in terms of a Taylor series expansion, approaches the true solution asymptotically if σ is, indeed, smooth. It was hoped that the solution would behave similarly in the case of a discontinuity in σ, but this was soon shown not to be the case. Because of this difficulty, as well as the general laboriousness of the entire procedure, the work is generally conceded to be of little

practical value. A later paper by Langer treated the above case with a single discontinuity, but was even more laborious.

DIRECT PROBLEM

A direct solution to the case of discontinuous variations (i.e. homogeneous, isotropic layers) was first given by J.C. Maxwell, and another was developed much later by Ollendorf, and by Stefanesco and Schlumberger.

Within the layered medium, the potential must satisfy several conditions.

a) Within a layer, Laplace's equation must hold

$$\nabla^2\phi = 0$$

b) Across the boundaries between layers, ϕ must be continuous

$$\phi_i(z) = \phi_{i+i}(z)$$

and c) The normal component of current across boundaries must be continuous.

$$\sigma_i \frac{\partial \phi_i(z)}{\partial z} = \sigma_{i+i} \frac{\partial \phi_{i+i}(z)}{\partial z}$$

There are the additional requirements, of course, that there be no vertical current flow at the surface, and that the potential go to zero at infinite distance from the source. The former was mentioned in the discussion on general inhomogeniety, and is handled in the same way; either by adjusting the Green's Function, or by assuming an image space symmetric about the surface.

This problem can be looked at, physically, in two ways giving equivalent solutions which differ in mathematical form. Maxwell, considering this as similar to the electrostatic problem, presented his expression for surface potential in terms of infinite series of images, multiply reflected about the planes of discontinuity. For a two layer case, source at (0,0,0)

$$2\pi O(r) = \frac{1}{\sigma_1}\left\{\frac{1}{r} + 2\sum_{n=1}^{\infty}\frac{(-\mu_{12})^n}{[\,r^2+4\,{}^2d^2\,]^{\frac{1}{2}}}\right\}$$

where

$$\mu_{12} = \frac{\rho_1-\rho_2}{\rho_1+\rho_2}$$

ρ_1 = resistivity of upper medium

$\sigma = 1/\rho_1$

d = thickness of upper medium

ρ_2 = resistivity of lower medium

∞ = thickness of lower medium

For a greater number of layers, one must deal with reflections of the original source in each of the interfaces, as well as the multiple reflections of each of these images from all interfaces (see Figure 2 for the three-layer case). The expression for surface potential becomes unwieldy very rapidly.

This image formulation of the solution has, thus far, not been of much aid in solving the inverse problem, although a

great deal of effort has been expended to this end (e.g. see Evjen, 1938). Formulae and tables for calculating surface potentials from images are given by Hummel (1929) and Roman (1931).

An integral solution of the direct problem, first presented by Ollendorf (1928), results immediately from the simplification of the integral formulation for the general problem. It differs in concept from the image approach in that the flow of current is thought of as sustaining charge distributions on the surfaces of discontinuity. The potentials are obtained by the usual method of volume integration of the product of charge density and Green's Function.

In the exact treatment, the charge density depends on the geometrical factors, the magnitude of the discontinuity, and the location and magnitude of all other discontinuities. The linear approximation, used by Stevenson (1934) for the layered case (and applied here to the general case) neglects interaction within discontinuities and between adjacent discontinuities.

Our general differential equation of potential

$$\sigma \nabla^2 \phi + \nabla\sigma \cdot \nabla\phi = -\delta(P,Q)$$

modified for a homogeneous medium, is

$$\sigma \nabla^2 \phi = -\delta(P,Q)$$

At any non-source point, this reduces to Laplace's equation

$$\nabla^2 \phi = \frac{\partial^2 \phi}{\partial r^2} + \frac{1}{r}\frac{\partial \phi}{\partial r} + \frac{1}{r^2}\frac{\partial^2 \phi}{\partial \eta^2} + \frac{\partial^2 \phi}{\partial z^2} = 0$$

whose solution is obtained immediately by assuming separability

and non-dependence of the solution on η. This procedure (in our circular-cylindrical coordinate system) gives us two equations. Assuming

$$\phi(r,z) = R(r)Z(z)$$

$$\frac{\partial^2 R}{\partial r^2} + \frac{1}{r}\frac{\partial R}{\partial r} + \lambda^2 R = 0$$

and

$$\frac{\partial^2 Z}{\partial z^2} - \lambda^2 Z = 0$$

The first of these two is a Bessel equation, satisfied by Bessel's functions of the first and second kind, of zero order $J_o(\lambda r)$ and $Y_o(\lambda r)$. The second expression is satisfied by the exponentials $e^{+\lambda z}$ and $e^{-\lambda z}$. Thus the solution in any layer is of the form

$$\left[A_i(\lambda)e^{+\lambda z} + B_i(\lambda)e^{-\lambda z}\right]\left[J_o(\lambda r) + Y_o(\lambda r)\right]$$

The Y_o term does not apply because it becomes infinite everywhere on the axis, whereas our potential must remain finite. This reduces the form of the solution to

$$\left[A_i(\lambda)e^{+\lambda z} + B_i(\lambda)e^{-\lambda z}\right] J_o(\lambda r)$$

Since it is valid for all real, positive values of λ, the most general solution can be written

$$\phi_i(r,z) = \int_o^\infty \left[A_i(\lambda)e^{+\lambda z} + B_i(\lambda)e^{-\lambda z}\right] J_o(\lambda r)\, d\lambda$$

which, at the surface is

$$\phi_i(r,0) = \int_o^\infty \left[A_i(\lambda) + B_i(\lambda)\right] J_o(\lambda r)\, d\lambda = \int_o^\infty k(\lambda) J_o(\lambda r)\, d\lambda$$

The function $k(\lambda)$ is the Slichter Kernel.

The $A_i(\lambda)$ and $B_i(\lambda)$ are different in each layer, their values determined by the boundary conditions. Thus in the bottom medium

$$A_n(\lambda) = 0$$

in order that the potential go to zero as z goes to infinity. At the boundary between layers (n) and (n-1) at depth $z = h_{n-1}$

$$\phi_n(r,z) = \phi_{n-1}(r,z)$$

and $$\sigma_n \frac{\partial \phi_n(r,z)}{\partial z} = \sigma_{n-1} \frac{\partial \phi_{n-1}(r,z)}{\partial z}$$

or $$B_n(\lambda)e^{-\lambda h_{n-1}} = A_{n-1}(\lambda)e^{+\lambda h_{n-1}} + B_{n-1}(\lambda)e^{-\lambda h_{n-1}}$$

and

$$\sigma_n B_n(\lambda)e^{-\lambda h_{n-1}} = \sigma_{n-1}\left[A_{n-1}(\lambda)e^{+\lambda h_{n-1}} - B_{n-1}(\lambda)e^{-\lambda h_{n-1}}\right]$$

In this fashion, all of the A_i and B_i are determined in terms of the conductivities and B_n. At the surface, z = 0,

$$\phi(r,0) = \int_0^\infty \left[A_1(\lambda) + B_1(\lambda)\right] J_0(\lambda r)\, d\lambda$$

The requirement of no vertical current flow at the surface implies

$$A_1(\lambda) = B_1(\lambda)$$

For a uniform earth, this same requirement forces B to be a constant ($\lambda = 0$) and

$$\phi(r,z) = B \int_0^\infty e^{-\lambda z} J_0(\lambda r)\, d\lambda = B\,(r^2+z^2)^{\frac{1}{2}} \text{ (Hankel transform)}$$

in agreement with equation (6) if $B = \frac{1}{2\sigma\pi}$. Similarly, for the

two layer case the surface potential is easily shown to be

$$2\pi\phi(r,0) = \frac{1}{\sigma_1}\int_0 \frac{1-\mu_{12}e^{-2\lambda d}}{1+\mu_{12}e^{-2\lambda d}} J_o(\lambda r)d\lambda = \frac{1}{\sigma_1}\int_0^\infty k_{12}(\lambda)J_o(\lambda r)\, d\lambda,$$

another Hankel transform, equivalent to Maxwell's expression

$$2\pi\phi(r,0) = \frac{1}{\sigma_1}\left[\frac{1}{r} + \frac{2}{r}\sum_{n=1}^{\infty} \frac{(-\mu_2)^n}{\left[1+\frac{4n^2d}{r^2}\right]^{\frac{1}{2}}}\right]$$

For n horizontal layers, the writing of the Slichter Kernel can be quite messy, obviously. It has been systematized in two different ways. Stefanesco and Schlumberger (1930) have presented it in determinant notation. Sunde (1949, p.55) uses a substitution system. The latter notation has been adopted in this thesis:

$$2\pi\phi(r,0) = \int_0^\infty k_{12\cdots n}\ J_o(\lambda r)\ d\lambda$$

$$k_{12\cdots n} = \frac{1-\mu_{12\cdots n}e^{-2\lambda d}}{1+\mu_{12\cdots n}e^{-2\lambda d}}$$

$$\mu_{12\cdots n} = \frac{\rho_1-\rho_2 k_{23\cdots n}}{\rho_1+\rho_2 k_{23\cdots n}}$$

$$k_{(m-1)m\cdots n} = \frac{1-\mu_{(m-1)m\cdots n}e^{-2\lambda d_{m-1}}}{1+\mu_{(m-1)m\cdots n}e^{-2\lambda d_{m-1}}}$$

$$\mu_{(m-1)m\cdots n} = \frac{\rho_{m-1}-\rho_m k_{m(m+1)\cdots n}}{\rho_{m-1}+\rho_m k_{m(m+1)\cdots n}}$$

$$k_{(n-1)n} = \frac{1-\mu_{(n-1)n}e^{-2\lambda d_{n-1}}}{1+\mu_{(n-1)n}e^{-2\lambda d_{n-1}}}$$

$$\mu_{(n-1)n} = \frac{\rho_{n-1}-\rho_n}{\rho_{n-1}+\rho_n}$$

The direct boundary value problem can be considered solved.

INVERSE PROBLEM

The Numerical Approach

The inverse problem for the case of horizontal stratification has been attacked in a variety of ways. Because of the complexity of the expressions involved, however, a general method for numerical analysis has not previously been devised. Such a method, and its results, are presented here.

The procedure developed requires an enormous amount of numerical computation, and would have been completely impractical before the advent of high-speed digital computers. The calculations are comparatively simple and repetitive, making them ideally suited to computer application. An interesting aspect of the type of analysis is that it is quite general - - an iterative, numerical curve fitting - - and is applicable to other problems in geophysical analysis, notably gravity interpretation. It is this approach of course which is proposed in the interpretation of three-dimensional resistivity problems.

Some objection might be raised to the use of the Slichter kernel for analysis, rather than the apparent resistivity or the potential. That is, the Slichter kernel can be obtained only by an integration, whereas the other quantities are available with almost no further effort from the field data. The counter to this argument is that the relationship between the various parameters (resistivities and thicknesses), and the measured quantities is an integral one. If numerical analysis

is to be done, an integration must be made somewhere in the process. Considering the ease and convenience of interpretation by curve-matching, it is therefore quite difficult to justify numerical work from the practical standpoint unless the results are far superior.

Consider the expression for the surface potential

$$\phi(r,0) \equiv \Phi(r) = \frac{1}{2\pi\sigma_1} \int_0^\infty k(\lambda) J_0(\lambda r)\, d\lambda \qquad (10)$$

σ_1 = surface resistivity = 1

This can be considered a Hankel transform of $k(\lambda)/\lambda$. The inverse transform would then read

$$k(\lambda) = \lambda \int_0^\infty r\phi(r)\, J_0(\lambda r)\, dr \qquad (11)$$

Thus we have a means of obtaining the Slichter kernel from observational data, the choice of λ being completely arbitrary. Next, an assumption is made of the number of layers. This point deserves rather careful consideration for several reasons, and is discussed below. Once the choice is made, however, one has a functional (transcendental) form which the observed kernel must fit, under proper choice of the parameters d_i and ρ_i. The present method fits the functional form to the observed kernel, in the least square sense, by adjusting the values of the parameters.

Before proceeding, some discussion of the practical aspects is in order. Computational procedures for obtaining $\phi(r)$ from

field resistivity data are presented in the Appendix, as is the numerical integration of equation (11) from field potentials. The practical application of this procedure requires that, beyond some finite distance from the source, the function $r\phi(r)$ assumes a constant value. This is equivalent to the assumption that the lowermost layer be a basement, i.e. that it have infinite depth extent. Geologically, this is an impossible assumption to satisfy. For analytical purposes, it will suffice that the "basement" layer be several times thicker than the combined thicknesses of the layers above it. The minimum thickness required of the (assumed) lowermost layer, in order that the layers below it do not influence the result, will depend on the thicknesses and resistivities of all layers in the geologic section and the accuracy of the analysis. On the other hand, practical limitations are imposed on the maximum dimensions with which one can deal. Greatest of these is the dearth of extended areas of laterally uniform geology. The result of these various factors is that it is possible to encounter areas underlain by uniform horizontal layers which are not susceptible to treatment by the analysis presented here.

The problem arises of the number of layers to be assumed. The answer is often obvious from the form of the kernel. If some doubt exists, an excessive number can be assumed, resulting in layers of zero thickness, or conductivities equal to those of adjacent layers. The limited accuracy of the data can be thought of as imposing a certain maximum "resolving power" on

the method, such that only layers of outstanding thickness or resistivity can be discerned. The net effect of this is to average together adjacent layers of like resistivity, and ignore thin layers. More discussion of these effects will follow.

The problem of fitting the "observed" kernels with their functional form is described mathematically as the solution of a set of non-linear transcendental equations, as the following will show. As stated previously, the Slichter kernel $k(\lambda_j)$ can be evaluated, by integration, for arbitrary values of $\lambda = \lambda_j$; (j= 1, 2, - - -, m). Assuming n layers, an expression can be written for the kernel, using the same values of $\lambda = \lambda_j$, the (2n-1) unknowns* remaining in functional form. There results the set of equations to be satisfied

$$\begin{aligned} k_{12\cdots n}(\lambda_1) - k(\lambda_1) &= 0 \\ k_{12\cdots n}(\lambda_2) - k(\lambda_2) &= 0 \\ - - - - - - - - - - - - & \\ k_{12\cdots n}(\lambda_m) - k(\lambda_m) &= 0 \end{aligned} \qquad (12)$$

the $k(\lambda_j)$ being constants. Obviously, this is a set of non-linear equations in (2n-1) unknowns, and can be solved exactly if m = 2n - 1. Because of the errors which exist in the $k(\lambda_j)$, it has appeared desirable to use an excess number of data points $k(\lambda_j)$, such that $m > 2n-1$, and to obtain a least square fit, viz

$$\sum_{j=1}^{m} [k_{12\cdots n}(\lambda_j) - k(\lambda_j)]^2 = \text{minimum} \qquad (13)$$

* Consisting of n resistivities and (n-1) thicknesses. In practice, the uppermost and lowermost resistivities are known from the asymptotes of the apparent resistivity curve.

Two methods of numerical analysis were applied to the problem. The first was a Newton-Least Squares analysis, described in general terms in von Sanden (1923). The application with detailed description of results is described in Vozoff (1955a). Although the results were generally satisfactory, several difficulties arose with the method as originally programmed. one of these was the necessity of solving a (2n-3) x (2n-3) matrix which, in the type of example used, was often near-singular. This being an intrinsic difficulty of the Newton method, it was deemed necessary to apply a second method. A Steepest Descent approach (e.g. see Householder, 1953) was chosen and modified as described below.

In the normal steepest descent problem, one has a set of equations to be satisfied, here, equations (12)

$$K_j = k_{12\cdots n}(\lambda_j) - k(\lambda_j) = 0 \qquad j = 1, 2, - - -, m$$

These, in turn, are satisfied by

$$K = \sum_{j=1}^{m} K_j^2 = 0 \qquad m = 2n-3$$

Let the (2n-3) unknowns be termed ξ_α , $\alpha = 1, 2, - - -, (2n-3)$. Then K can be considered a continuous function in (2n-3) space, and to arrive at the point

$$K = K(\xi_\alpha) = 0$$

from some starting point

$$K = K(\xi_\alpha^{(0)})$$

(ξ_α the correct values of the unknowns, $\xi_\alpha^{(0)}$ first approximations to these values), we must proceed along the vector ∇K.

The components of this vector are

$$K_\alpha = \frac{\partial K}{\partial \xi_\alpha} \Big/ \left[\sum_\beta \left(\frac{\partial K}{\partial \xi_\beta}\right)^2 \right]^{\frac{1}{2}}$$

A general procedure such as described will bring us to a minimum provided that the starting point is on a closed hypersurface within which a minimum exists. Since the gradient direction will not, in general, be constant within the volume traversed, it will be necessary to proceed to a minimum value along a calculated gradient, then to calculate a gradient at the new position, using the new position coordinates as second approximations to the solution, and to repeat the process until the minimum is reached. Normally, this is done changing one variable at a time. Thus

$$K\left(\xi_\alpha^{(i+1)}\right) = K\left(\xi_\alpha^{(i)} - MK_\alpha^{(i)}\right), \text{ etc.} \qquad (14)$$

the value of M taken to minimize $K\left(\xi_\alpha^{(i+1)}\right)$ at each iteration. M might be estimated by one of several kinds of approximations, or determined by trial and error.

The procedure actually employed embodied several modifications. All parameters were changed simultaneously. It was a least-squares fit rather than an exact fit, and used m=10, n=3. Equation (13) would be

$$K = \sum_{j=1}^{10} \left[k_{123}(\lambda_j) - k(\lambda_j) \right]^2 = \text{minimum} \qquad (15)$$

In order to explain and avoid the extrapolation difficulties which arose in the Newton method, some calculations were done

to determine the shape of the error surfaces.** It was found that negative second derivatives were not uncommon at points distant from the minimum. In the vicinity of the minimum, the second derivatives were always positive (Figure 4). This observation, coupled with the fact that the minimum of the curve is always greater than zero would seem to make the Newton method singularly unsuitable for the particular problem.*** The least-squares modification is probably of some help in the latter respect, because it seeks to minimize a function rather than find its root. It is difficult to see how it would avoid the complications arising from negative second derivatives.

The steepest descent approach, on the other hand, takes into consideration both first and second derivatives, and really does not require a null value.

The coefficient M was first estimated by approximating the ratio of first to second derivatives of K along the path defined by ∇K, i.e.

$$M' = \frac{K_s}{K_{ss}} = \frac{\sum_i \frac{\partial K}{\partial \xi_i} \frac{d\xi_i}{ds}}{\sum_i \frac{\partial^2 K}{\partial \xi_i^2} \left(\frac{d\xi_i}{ds}\right)^2} \qquad (16)$$

** These are the multi-dimensional surfaces whose projections are curves of K as a function of one variable, all others held fixed. In the case of only two variables (a,b) they would be three-dimensional surfaces K(a,b) (see Fig. 3).

*** See Hildebrand, 1949 p. 364.

Trial values of K were then calculated, using c_1M', c_2M', and equation (14). The constants c_1 and c_2 are near unity, and unequal. The values thus obtained, and the previous value of K (ξ_α^{i}), corresponding to M' multiplied by zero, could be used to interpolate for a new value of M. Two kinds of interpolations were used, depending on proximity to the minimum. This procedure was arrived at empirically, because it was suited to the shapes of the error surfaces. Letting the two trial values of K be θ_1 and θ_2, when $|\theta_1-\theta_2|<K(\xi_\alpha^{(i)})$ a linear interpolation to $\theta = 0$ was used, but when $|\theta_1-\theta_2| \geq K(\xi_\alpha^{(i)})$ a parabolic interpolation to θ = minimum was used. That is, at the beginning of the calculation it was found in general that

$$|\theta_1-\theta_2|<K$$

In this case it was assumed

$$\theta_1 = c_1\alpha+\beta$$

$$\theta_2 = c_2\alpha+\beta$$

and the equations were solved for the value of c giving,

$$\theta = 0$$

This was

$$c = -\frac{\theta_1-\theta_2}{c_1-c_2}$$

As the solution was approached, a point was reached at which

$$|\theta_1 - \theta_2|\geq K$$

and thence a parabolic interpolation was used. Assuming

$$\theta_1 = c_1^2\alpha + c_1\beta + \gamma$$

$$\theta_2 = c_2^2\alpha + c_2\beta + \gamma$$

$$0_3 \quad K(\xi_\alpha^{(i)}) = \gamma \qquad (c_3 = 0)$$

and solving for that value of c which causes Θ to be minimized

$$c = - \frac{c_1^2(\theta_2-\theta_3) + c_2^2(\theta_3-\theta_1)}{\theta_1 c_1 - \theta_2 c_2 + \theta_3(c_1-c_2)}$$

In the analyses done numerically, c has generally ranged between $\frac{1}{2}$ and 3/2.

The iteration then proceeded, using

$$M = cM'$$

in equation (14).

Because of the flexibility of the procedure, computation time could probably have been saved by replacing equation (16) by

$$M' = \frac{K}{K_s}$$

the Newton estimate or, alternatively, the interpolations might have been found unnecessary if a more nearly accurate expression was used for the third order iteration.

The procedure used here, effectively an interpolation within an interpolation, would seem to be highly inefficient at first glance because three times as many values of K are calculated as are actually necessary for a normal iteration. It was found that this was justified since K decreased four to five times as fast as it did without the inner interpolation.

The resistivity problem differs from the classical steepest descent problem in that the variables of the former are not all dimensionably equivalent. This implies that, in any particular

field case, the numerical values of the resistivities may generally be of a different order than those of the thicknesses. As a result, in many cases the process would ignore one variable completely in the early iterations, changing this variable only after all possible reduction of K had been made with the others. This was especially outstanding in theoretically derived kernels of thin, highly resistive, second layer; ρ_2 was ignored entirely at first.

This tendency was reduced considerably by the artifice of modifying the components of gradient from

$$K_\alpha = \frac{\partial K}{\partial \xi_\alpha} \Big/ \left[\sum_\beta \left(\frac{\partial K}{\partial \xi_\beta} \right)^2 \right]^{\frac{1}{2}}$$

to

$$K_\alpha = \xi_\alpha \frac{\partial K}{\partial \xi_\alpha} \Big/ \left[\sum_\beta \xi_\beta^2 \left(\frac{\partial K}{\partial \xi_\beta} \right)^2 \right]^{\frac{1}{2}}$$

In the initial discussion on steepest descent it was stated that the iteration would proceed to the local minimum. The obvious question is: How do we know this is the desired solution? That is, are there other solutions to our equations, and, if so, how many and of what nature? From the standpoint of the pure mathematician these questions must go unanswered, since, as far as can be ascertained, mathematics has not yet provided an answer in our case of transcendental equations in several variables. The possibilities of embarrassment which might arise from a multiplicity of roots are diminished somewhat by the physical restrictions on the solution. Negative

values are inadmissable, and complex values will never appear in numerical computation with real numbers. In the numerical work done, a second solution was obtained in one case. This solution had negative resistivities and thicknesses, although the corresponding minimum value of K was less than that for the true solution. Both minima lay within the roundoff error of the kernels.

Computation

A numerical study of the method was carried out to

a) determine accuracies necessary for definite analysis

b) observe the behavior of the method under conditions of excess layers, lateral resistivity variations, and random errors in data

c) compare this method with other methods of analysis.

For this purpose, a program was written to analyze kernels as three-layer cases on the M.I.T. Whirlwind computer. Input data were

a) the number and values of λ_j

b) values of ρ_1 and ρ_3

c) estimates of ρ_2, d_1 and d_2

d) the kernel values $k(\lambda_j)$.

A considerable amount of machine algebra was saved by dealing with

$$f_3(\lambda) = 1 \Big/ \left[1 + k_3(\lambda) \right] - \tfrac{1}{2}$$

and

$$f_{123}(\lambda) = 1 \Big/ \left[1 + k_{123}(\lambda) \right] - \tfrac{1}{2} = \mu_{123} t_1 / 2$$

$$t_1 = e^{-2\lambda d_1}$$

rather than with $k_3(\lambda)$ and $k_{123}(\lambda)$.

The part played by λ in the analysis is perhaps worthy of comment. The parameter λ is, in a sense, equivalent to the wave number of hyperbolic (wave) equations, and has the dimensions of $\frac{1}{r}$. Because of the character of the function $J_o(\lambda r)$, the major contribution to the Slichter kernel

$$k(\lambda) = \lambda \int_o^\infty r\phi(r)\, J_o(\lambda r)\, dr$$

is from small values of the argument (λr). At large values of λ, the contribution from small values of r is dominant, whereas decreasing values of λ put increasing emphasis on the information from greater r. As a result, although the behavior at small r is always important because of the nature of the physical problem, one could probably increase the accuracy of analyses of deeper features by using more of the smaller values of λ in the analysis. This is equivalent in a sense to increasing the size of units of r, i.e., increasing spread dimensions in the field. Examination of the curves in Figure 5 shows that kernels of cases satisfying our assumptions vary rapidly in only a restricted range (usually several decades), and approach constant values at large and small λ. It is, of course, this region of rapid variation that is used for interpretation.

Results and Discussion

With the Newton Method, some 30 cases were analyzed, including five integrated from field measurements, two derived from the four-layer formula, and the rest from the three-layer formula. The last were restricted to the difficult case of a thin second layer. Of the 30 cases, the Newton Method could not handle two and had difficulty with others. Causes of difficulty were a too thin second layer, and very low resistivity contrast between adjacent layers (giving near-degeneracy further aggravated by the small second layer thickness).

Several of the more difficult cases were chosen for analysis with the new technique. Results are presented for four of these, together with two of the field cases, and two additional examples of the difficult category (Tables 2 and 3, Figures 5-17).

For thick d_2 ($d_2 \geq .5$) it was found that the Newton method gave better solutions than did the steepest descent.

One interesting result noted in all the work is that in these thin-layered cases a very definite relationship is found to hold, in successive iterations, between the resistivity and thickness of the second layer. That is, if

$$d_2 << 1$$

then

$$\frac{d_2}{\rho_2} = c_1 \quad \rho_3 >> \rho_2$$

and

$$d_2 \rho_2 = c_2 \qquad \rho_3 << \rho_2$$

where c_1 and c_2 are approximately equal to the values obtained using the exact values of ρ_2 and d_2. This is so even if each of the solutions for ρ_2 and d_2 are far from the correct values. That this could be so, and is a kind of indeterminacy can be shown as follows. The expressions for $\frac{\partial k}{\partial \rho_2}$ and $\frac{\partial k}{\partial d_2}$ are

$$\frac{\partial k}{\partial \rho_2} = - \frac{\rho_1 t_1}{I^2} \left[\frac{\rho_2 - \rho_3}{\rho_2 + \rho_3} t_2^2 + 4 \frac{\rho_2 \rho_3}{(\rho_2 + \rho_3)} t_2 - 1 \right]$$

$$\frac{\partial k}{\partial d_2} = + 4 \frac{\lambda \rho_1 \rho_2 \mu_{23} t_1 t_2}{I^2}$$

$$t_1 = e^{-2\lambda d_1}$$

$$t_2 = e^{-2\lambda d_2}$$

where I is another large algebraic term in the same variables. Let $d_2 << 1$. Then if $\frac{\rho_2}{\rho_3} << 1$, and neglecting terms in

$$\left.\begin{matrix} \left(\frac{\rho_2}{\rho_3}\right)^n \\ (\lambda d_2)^n \end{matrix}\right\} \quad n \geqslant 2$$

$$\frac{\rho_2}{\rho_3} \lambda d_2$$

we find

$$\frac{\partial k}{\partial \rho_2} \approx + \frac{4 \lambda d_2 \rho_1 t_1}{I^2}$$

$$\frac{\partial k}{\partial d_2} \approx - \frac{4 \lambda \rho_1 t_1 \rho_2}{I^2}$$

The determinants can be considered Jacobians, the first as

$$\frac{\partial(f_1,k)}{\partial(\rho_2,d_2)}$$

$$f_1 = f_1\ (d_2/\rho_2)$$

and the second as

$$\frac{\partial(f_2,k)}{\partial(\ _2,d_2)}$$

$$f_2 = f_2\ (d_2\rho_2)$$

The implication is that these functions, f_1 and f_2, must exist, hence k (and therefore K also) cannot vary if ρ_2 and d_2 are changed so as to keep the appropriate function fixed (d_1 assumed constant). The problem of a thin second layer might be reduced to a two-variable problem, at least for a portion of the computations.

Two examples of this indeterminate condition are illustrated in Table 1. Both sets of kernels are identical to within one percent, and the usual accuracy of field data.

The maximum difference between the second pair of kernels occurs between $\lambda = 1.0$ and $\lambda = 0.4$. Comparison of several other such kernels, whose values were known to greater accuracy, has shown that the maximum difference nearly always lies within this range ($d_1=\rho_1=1$ in all cases).

Hence, if a greater concentration of kernels in the range $1.0>\lambda>.4$ were to be used in the analyses, better definition of the second layer should be expected (assuming that the errors are sufficiently small). If the references to optical termi-

	k(λ)			
λ	ρ_2=10; d_2=.1 k(λ)	ρ_2=100; d_2=.01 k(λ)	△	
1.0	1.09	1.09	0.00	
.6	1.15	1.15	0.00	
.4	1.16	1.16	0.00	$\rho_1=d_1=1$
.2	1.13	1.13	0.00	
.1	1.08	1.08	0.00	$\rho_3=1$
.06	1.05	1.05	0.00	
.04	1.04	1.04	0.00	$\rho_2 d_2=1$
.02	1.02	1.02	0.00	
.01	1.01	1.01	0.00	
.006	1.01	1.01	0.00	

	k(λ)			
λ	ρ_2=.1; d_2=.1 k(λ)	ρ_2=.01; d_2=.01 k(λ)	△	
1.0	.915	.914	.001	
.6	.872	.870	.002	
.4	.862	.861	.001	$\rho_1=d_1=1$
.2	.886	.885	.001	
.1	.926	.925	.001	$\rho_3=1$
.06	.950	.950	.000	
.04	.965	.964	.000	$d_2/\rho_2=1$
.02	.981	.981	.000	
.01	.990	.990	.000	
.006	.994	.994	.000	

TABLE 1

Illustrating near-indeterminacy in three-layer cases.

nology in describing these analytical methods can be carried a bit farther, this latter procedure would be analogous to a focusing.

Table 2 illustrates the effectiveness of the Steepest Descent analysis in the case of small d_2. Column A indicates the number of decimal places to which the kernel data were accurate. Column E shows the sum of squares error due to round-off in each case.

Regarding the effect of using $f_3(\lambda)$ rather than $k_{123}(\lambda)$ for analysis, the Whirlwind computer performed arithmetic operations maintaining about nine decimal places of accuracy. Storage accuracy was seven decimal places. Thus in the worst case of $k(\lambda)$ near unity, the use of $f_3(\lambda)$ caused no loss of accuracy when the data were accurate to four places or less.

Other errors introduced in algebraic manipulations, and in the approximation used to calculate the inverse exponentials, are quite small, usually less than 10^{-6} at any point.

In cases 5, 6, 10, and 11 the final K is quite close to E, and departure of the solutions from their true values results almost entirely from rounding off the kernels. Cases 26 and 27 do not have such satisfactory results, as might be expected with $d_2 = .01d_1$. Little improvement was obtained by using six places rather than four places accuracy in Case 26. There is the possibility that the minimum is a secondary one but several analyses from different initial estimates led to solutions essentially the same. Another minimum closer to the true solution seems unlikely.

The examples of field data analyses in Table 3 have thick d_2 and are thus not particularly difficult. The apparent resis-

tivity curves indicate that Case B can probably be approximated by the three-layer representation, although small lateral resistivity variations occur near the source. The smoothing obtained by integrating the potentials from the original (difference) measurement is not sufficient to remove the effect of these lateral inhomogeneities. This difficulty might possibly be eased by taking, in the field, measurements about several adjacent centers, and averaging. Alternatively, individual analyses might be made, and the solutions averaged.

Case C appears to consist of at least four layers. It would appear that a four or five layer analysis would be a fairer test of the methods in both cases.

The use of multiple senders suggests another possible, related, approach to the resistivity analysis problem. The field cases presented here are from "hardrock" regions, i.e., regions of characteristically complex geology. If, on the other hand, a large number of cases were collected at various stations in a region of relatively simple geology (a large, unmetamorphosed sedimentary basin, for example) one could possibly apply restrictions on the allowable variation of parameters between stations, and, using an excess of data, obtain a consistent picture of the entire area. This procedure would take somewhat longer than a single analysis, but not a great deal longer, because the first solution would presumably be a close approximation to the others.

The analyses of four layer kernels, by the Newton Method, gives an interesting result. It appears that the analyses

yield the quantity $\rho_2 d_2$ or ρ_2/d_2 (as applicable) characteristic of the second layer only, ignoring the third layer. Individually, the ρ_2 and d_2 indicate that the solution smooths the second and third layers together, as might be expected.

In concluding, a comparison should be made of the present results with those obtained by curve matching with the same data. Unfortunately, the only existing curves for $d_2 < 1$ are those of the Schlumbergers (1955). These curves are of $d\phi(r)/dr$ in terms of apparent resistivities, and thus are not suitable for direct comparison. It should be stated that the measurement required to obtain this type of curve has the obvious disadvantage of amplifying lateral discontinuities. Preliminary comparisons of potentials with their corresponding kernels indicate that the kernel is always a more sensitive indicator of resistivity variations. This implies that interpretation of kernels is to be preferred to interpretation of potentials, especially when comparing curves (see Figures 16 and 17).

TABLE 2 THREE-LAYER ANALYSES OF THREE-LAYER KERNELS

	Theoretical Values				Solutions					
Case	ρ_1 d_1	ρ_2 d_2	ρ_3	$d_2\rho_2$ d_2/ρ_2	ρ_1 d_1	ρ_2 d_2	ρ_3 K	E*	$d_2\rho_2$ d_2/ρ_2	A**
5	1. 1.	.05 .5	5.	10.	1. .962	.101 1.01	5. $6.\times10^{-6}$	2×10^{-7}	10.	3
6	1. 1.	10. .5	.2	5.0	1. .923	4.26 1.20	.2 $5.\times10^{-7}$	3×10^{-7}	5.11	3
10	1. 1.	10. .1	.1	1.	1. .742	1.42 .893	.1 1.7×10^{-7}	2×10^{-7}	1.27	3
10a	1. 1.	10. .1	.1	1.	1. .987	19.3 .0524	.1 $7.\times10^{-7}$	2×10^{-7}		3
10b	1. 1.	10. .1	.1	1.	1. 1.22	19.6 .0443	.1 $9.\times10^{-5}$			3
11	1. 1.	10. .1	.2	1.	1. .988	19.5 .0516	.2 $6.\times10^{-7}$	5×10^{-7}	1.01	3
26a	1. 1.	.05 .01	5.	.2	1. 1.87	.514 -.33	5. $3.\times10^{-6}$	8×10^{-10}		4
26b	1. 1.	.05 .01	5.	.2	1. 1.87	.517 -.34	5. 2.6×10^{-6}	9×10^{-13}		6
27	1. 1.	.1 .01	5.	.1	1. .930	.120 .0198	5. $9.\times10^{-8}$	7×10^{-13}	.165	6

* Minimum significant error due to roundoff of data.

** This column indicates number of places accuracy of kernel used.

TABLE 3

THREE-LAYER ANALYSIS OF FIELD KERNELS

Case	First Estimate			Solution		
	ρ_1	ρ_2	ρ_3	ρ_1	ρ_2	ρ_3
	d_1	d_2	K	d_1	d_2	K
B	1.	.6	.2	1.	.629	.2
	.15	3.	$3.\times10^{-4}$	.174	2.72	1.3×10^{-5}
C	1.	.25	.2101	1.	.251	.2101
	.3	6.	3.3×10^{-4}	.272	5.97	1.7×10^{-4}

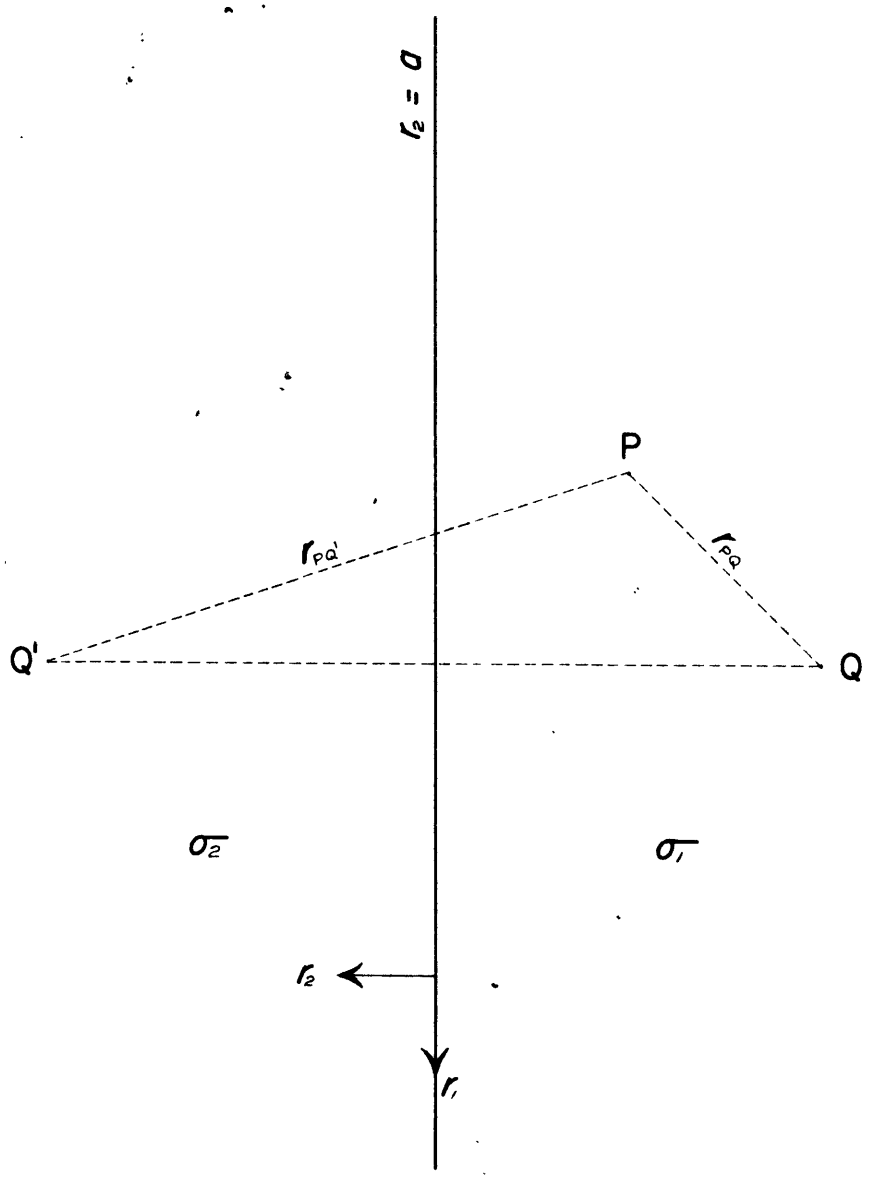

SHOWS CASE OF SINGLE VERTICAL DISCONTINUITY

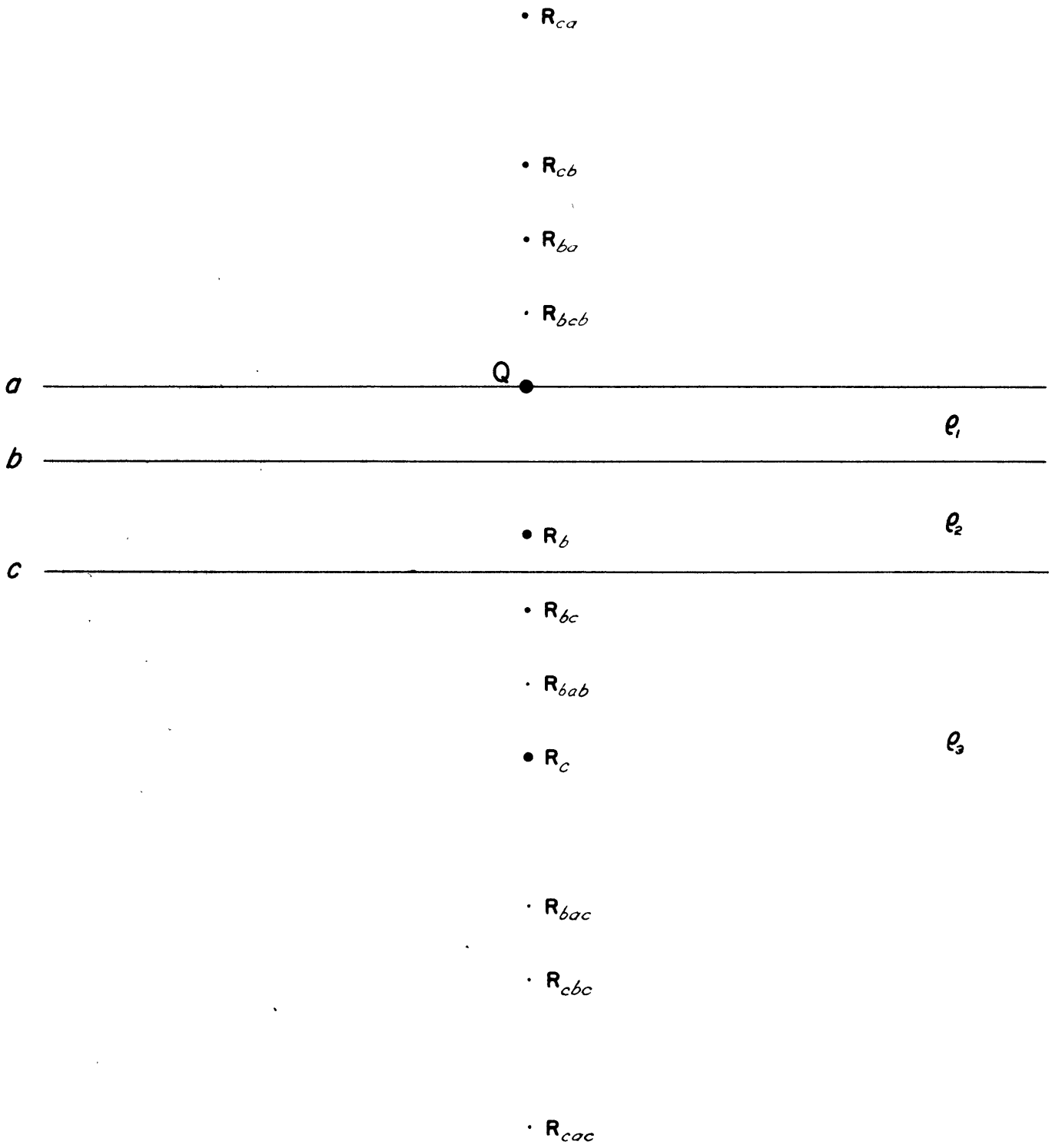

MAXWELL IMAGES OF FIRST THREE ORDERS

FIG. 2

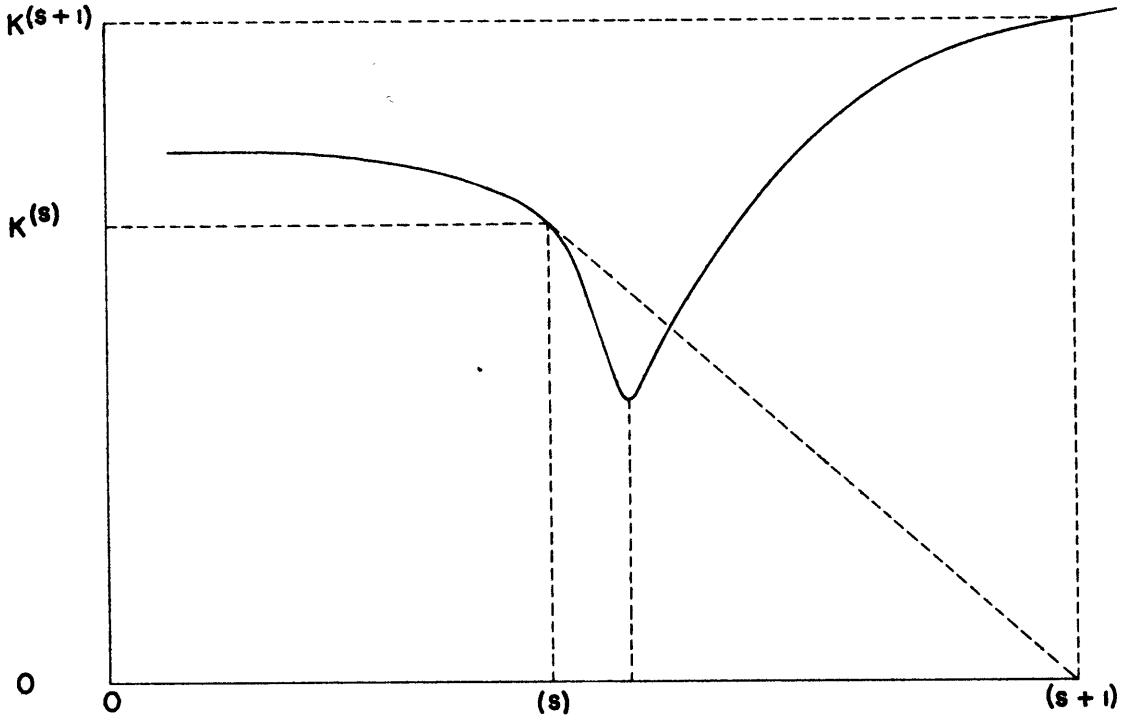

Fig. 3——Result of a First Order Newton Extrapolation on the Type of Error Surface Encountered

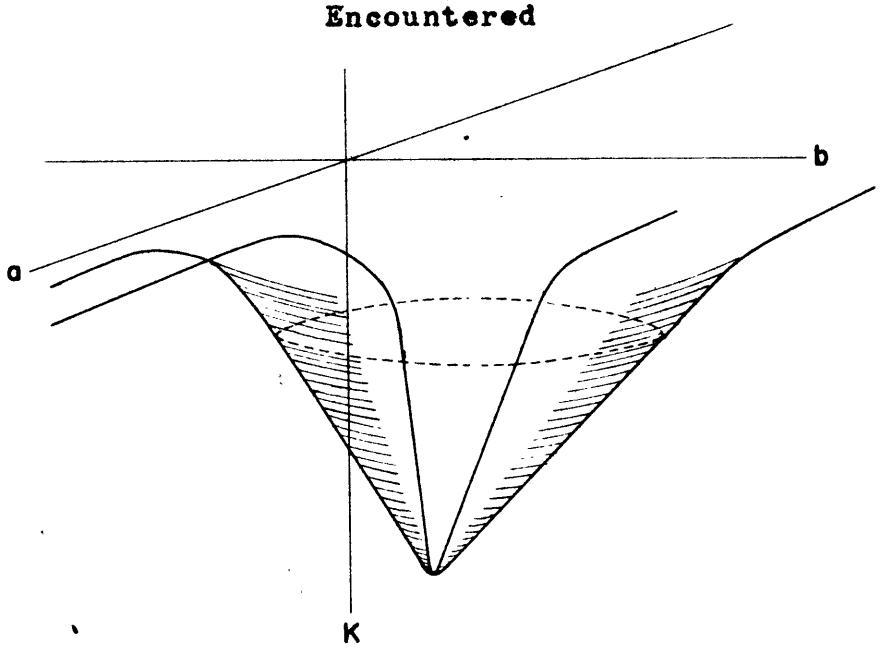

Fig. 4——Error Surface K(a,b,) for a two-variable case

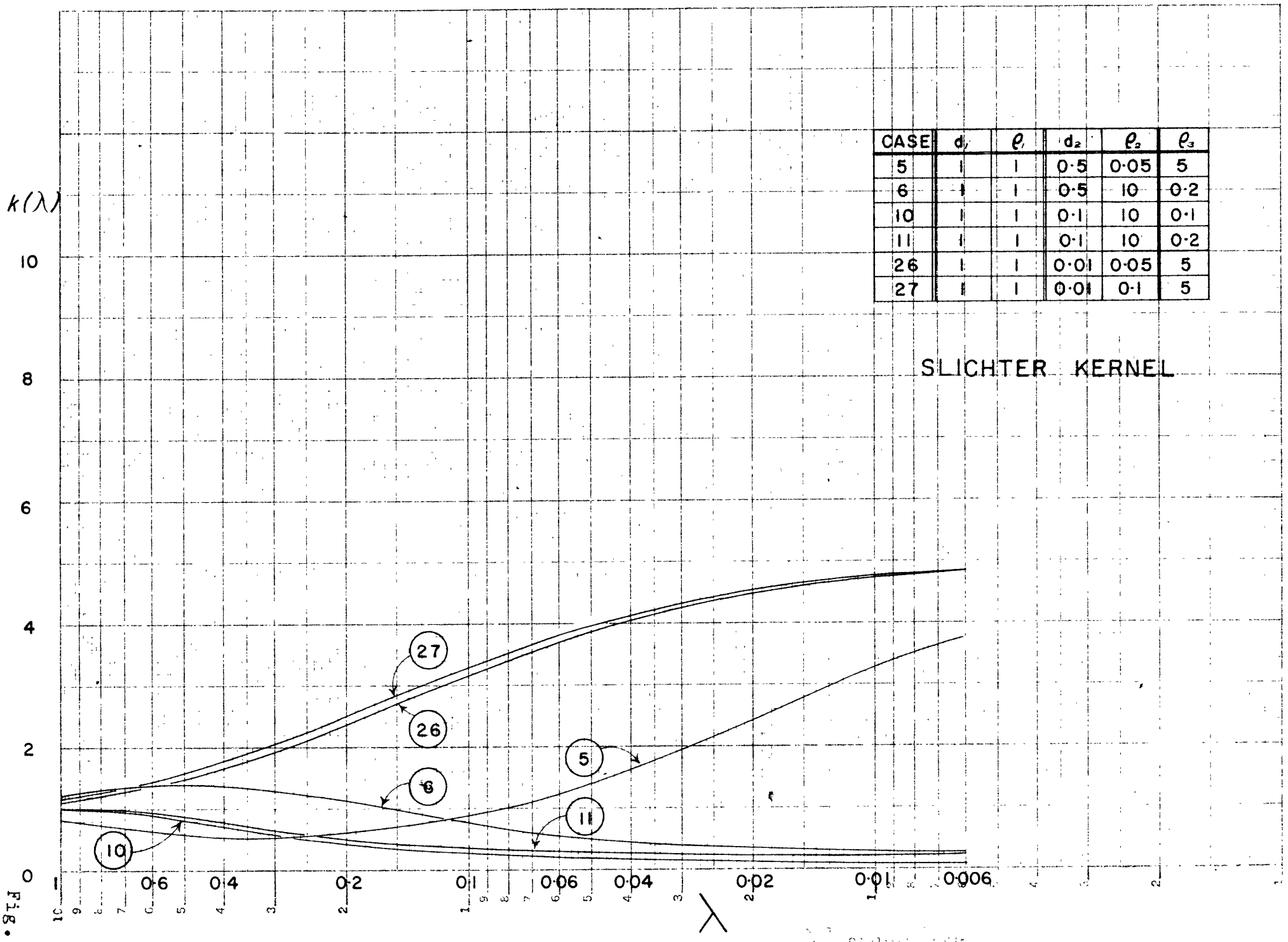

CASE	d_1	ρ_1	d_2	ρ_2	ρ_3
5	1	1	0·5	0·05	5
6	1	1	0·5	10	0·2
10	1	1	0·1	10	0·1
11	1	1	0·1	10	0·2
26	1	1	0·01	0·05	5
27	1	1	0·01	0·1	5

SLICHTER KERNEL

FIG. 5

Case 5

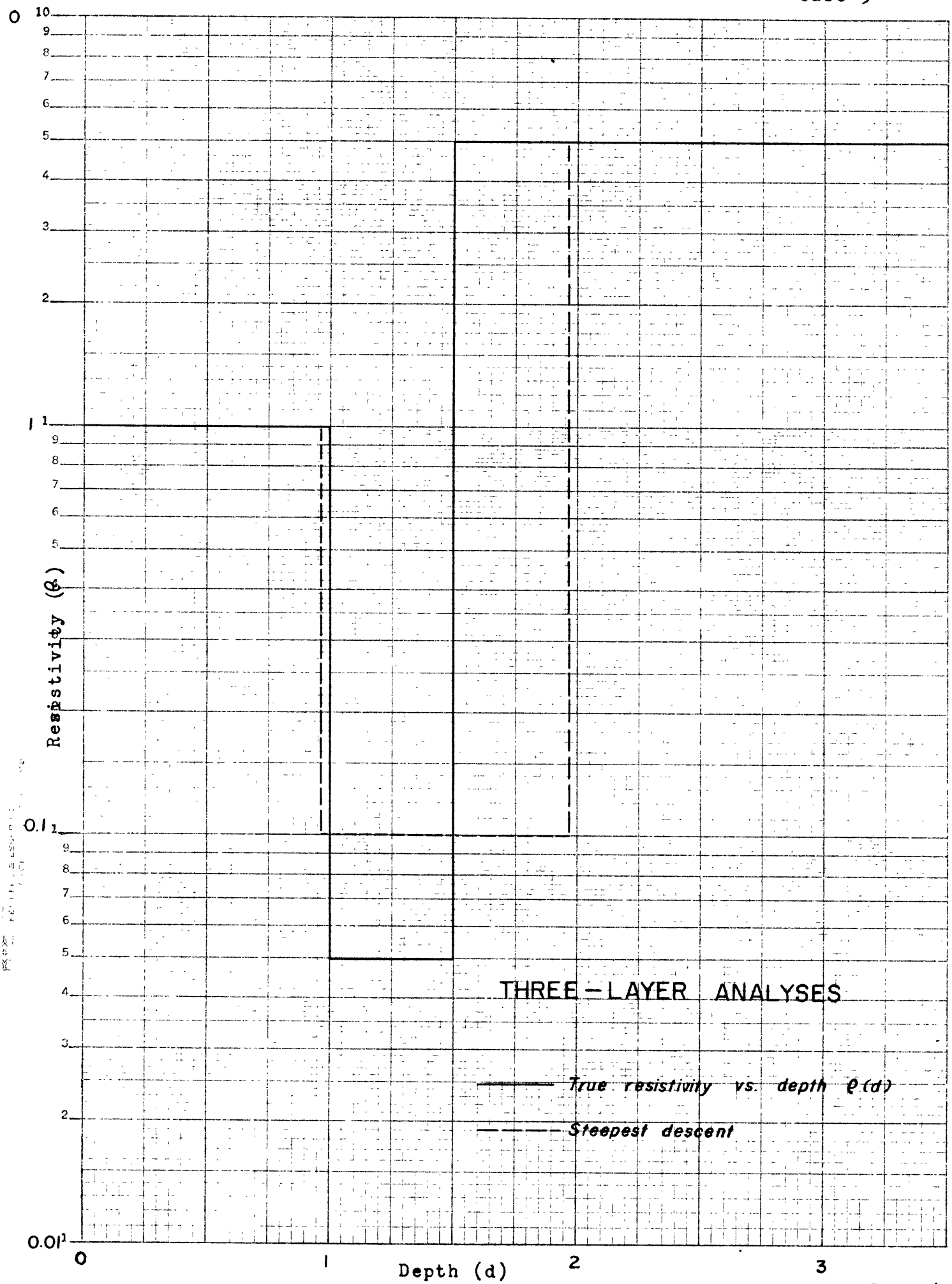
Resistivity (ρ)
Depth (d)
THREE – LAYER ANALYSES
True resistivity vs. depth ρ(d)
Steepest descent

Fig. 6

Case 6

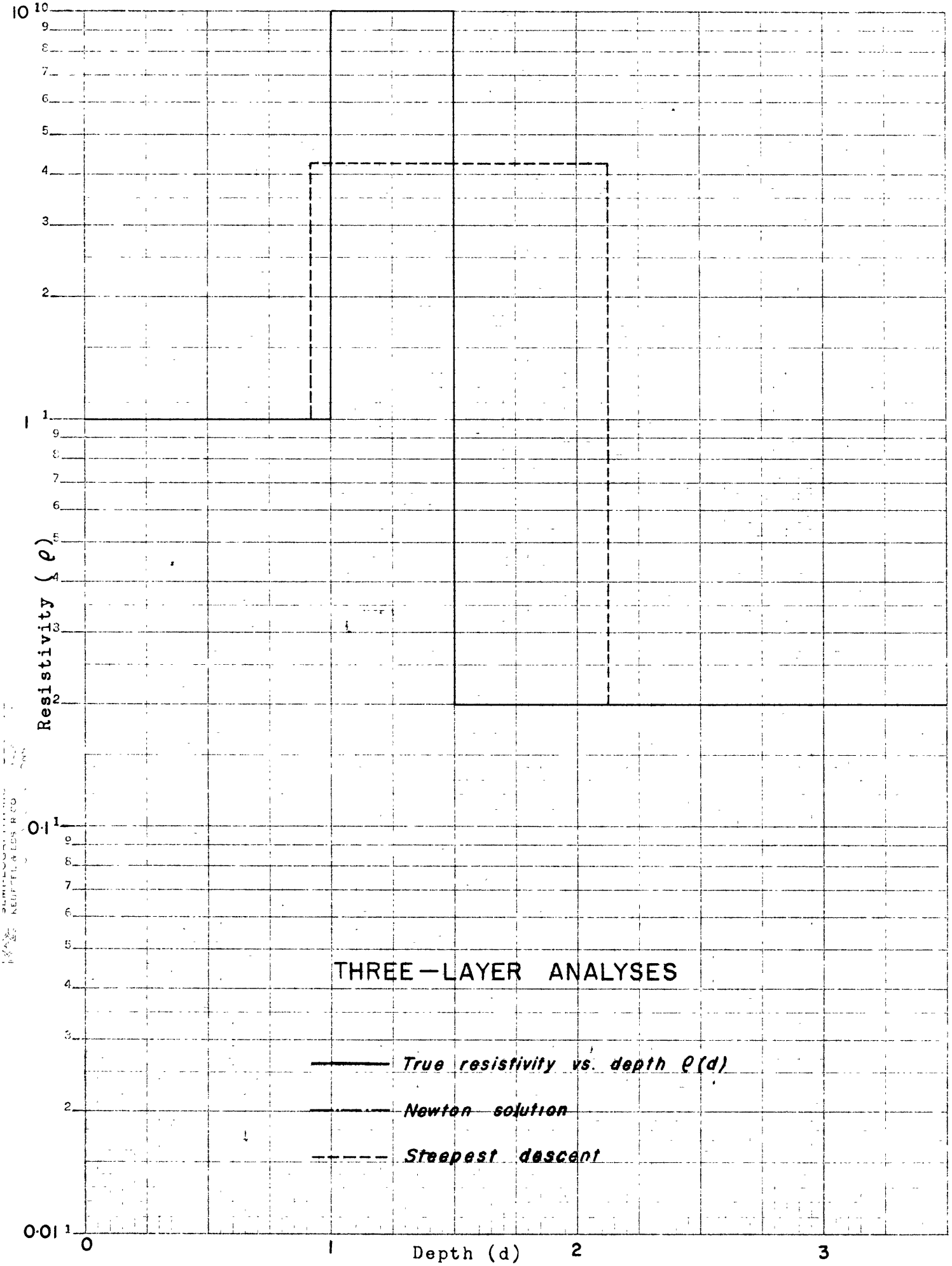
10
1
0·1
0·01
Resistivity (ρ)
0
1
2
3
Depth (d)
THREE—LAYER ANALYSES
True resistivity vs. depth ρ(d)
Newton solution
Steepest descent

Fig. 7

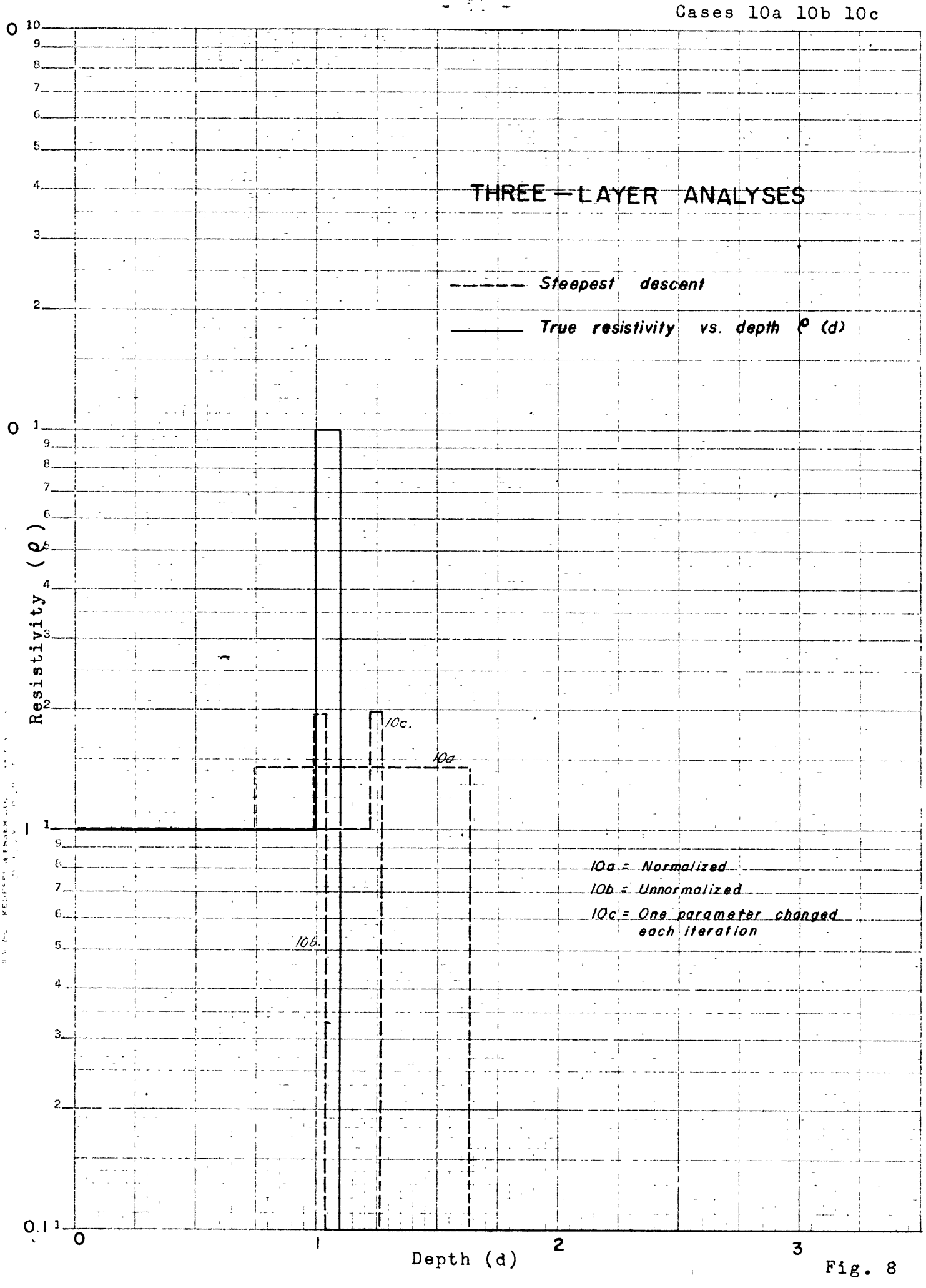
Cases 10a 10b 10c
THREE – LAYER ANALYSES
Steepest descent
True resistivity vs. depth ρ (d)
Resistivity (ρ)
Depth (d)
10c.
10a
10b.
10a = Normalized
10b = Unnormalized
10c = One parameter changed each iteration

Fig. 8

Case 11

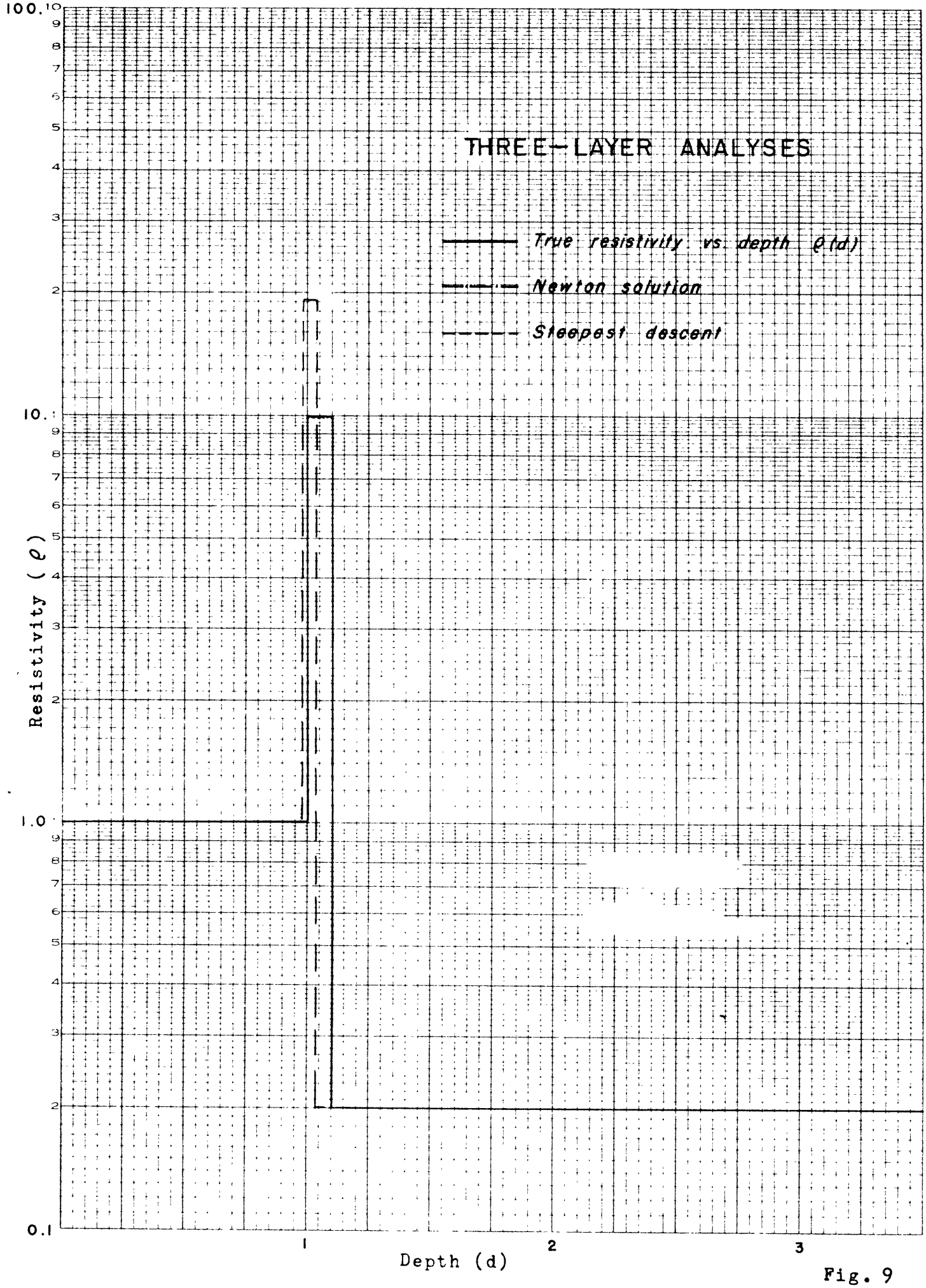
THREE-LAYER ANALYSES
True resistivity vs depth ρ(d)
Newton solution
Steepest descent
Resistivity (ρ)
100.
10.
1.0
0.1
1
2
3
Depth (d)

Fig. 9

Cases 26a 26b

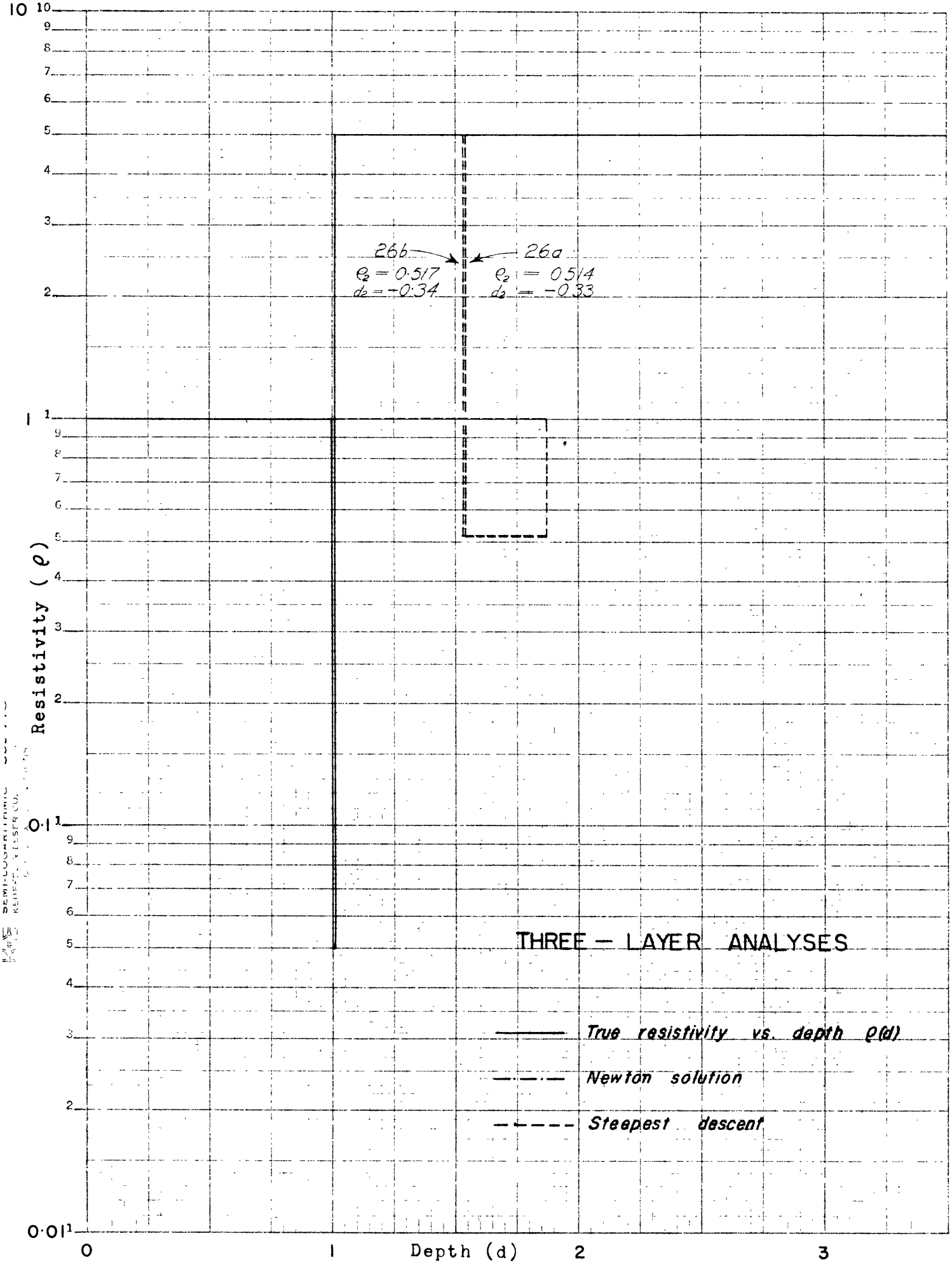

Fig. 10

Case 27

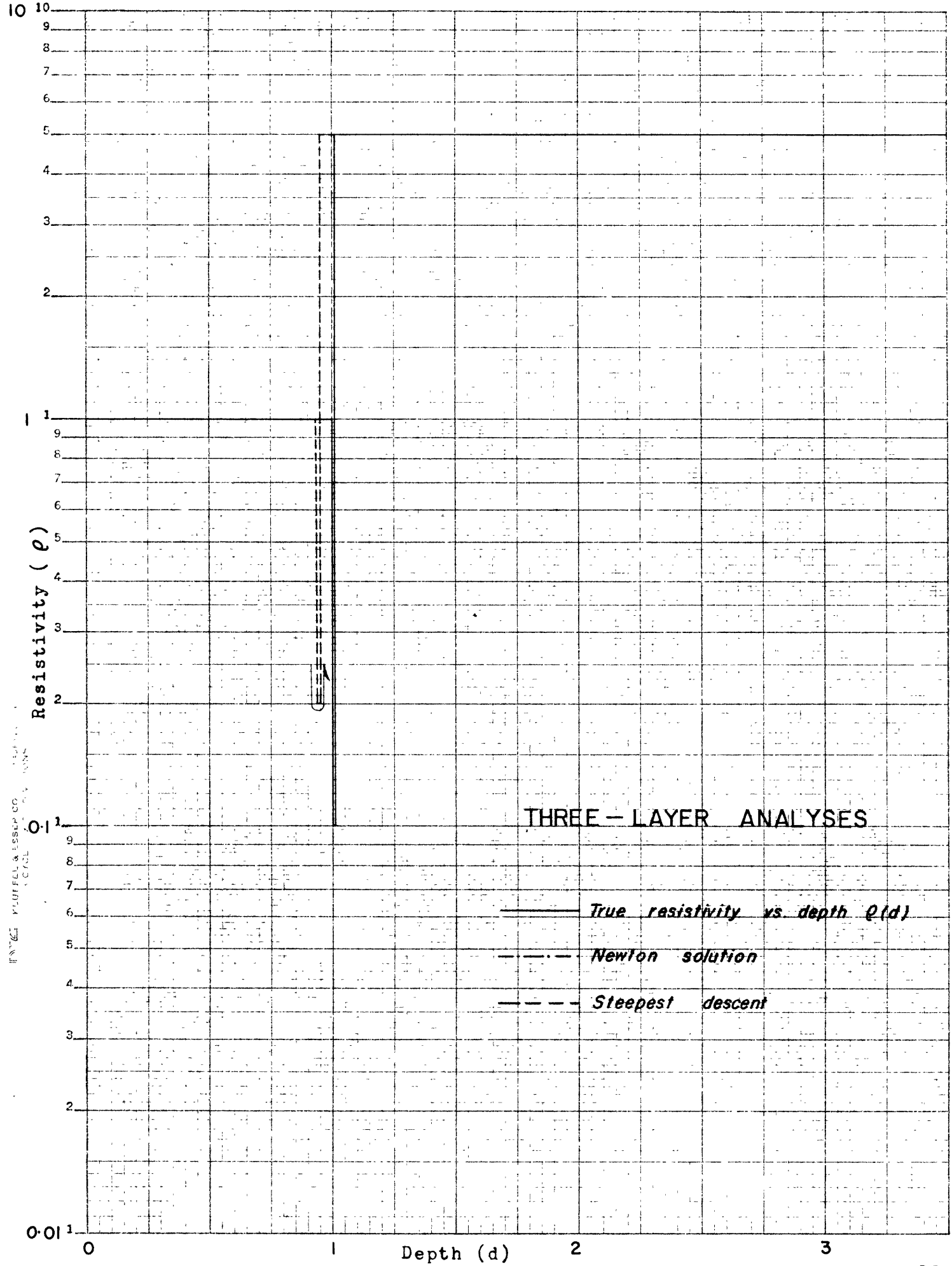

Fig. 11

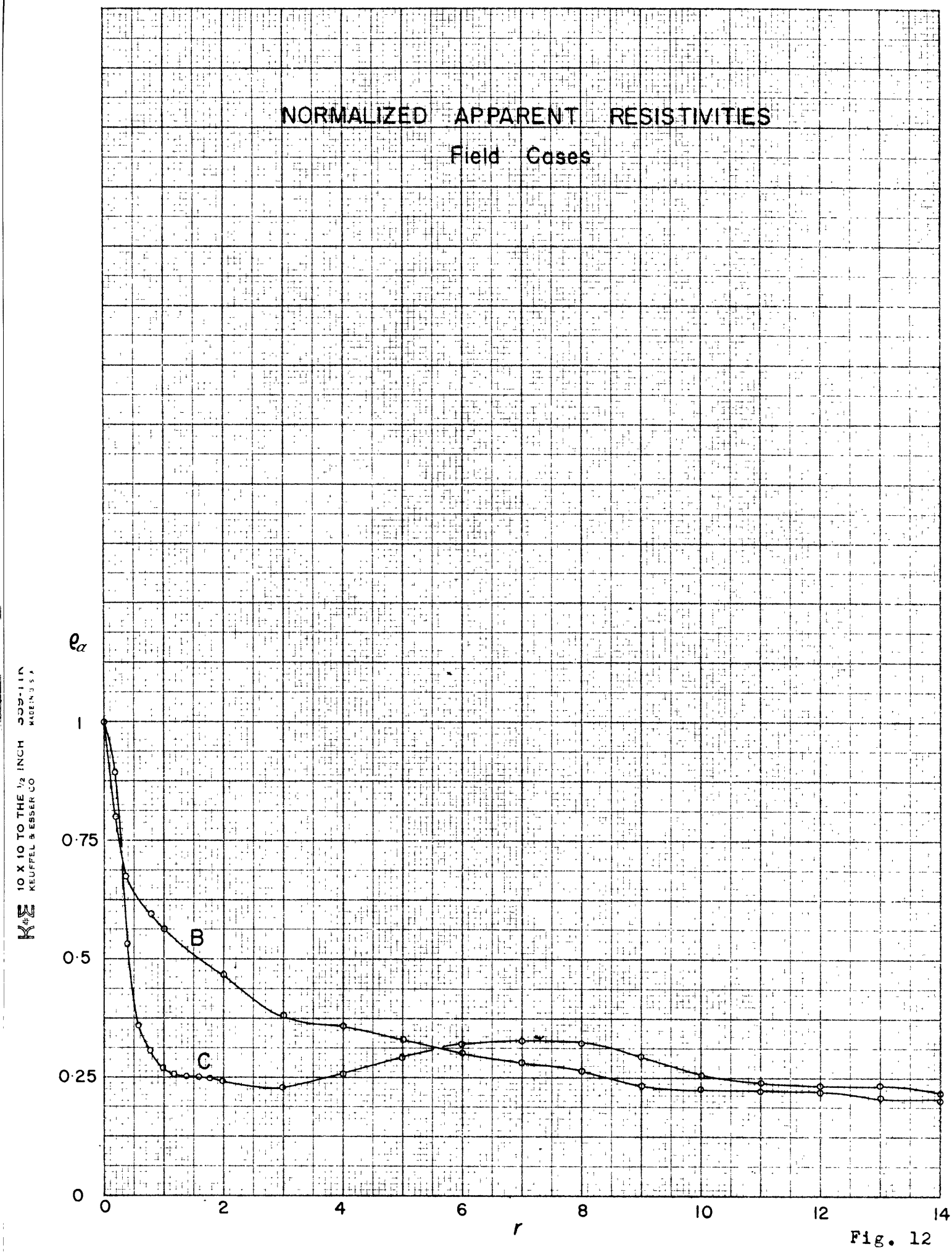
NORMALIZED APPARENT RESISTIVITIES
Field Cases
ρ_a
1
0.75
0.5
0.25
0
B
C
0
2
4
6
8
10
12
14
r
10 X 10 TO THE ½ INCH
KEUFFEL & ESSER CO

Fig. 12

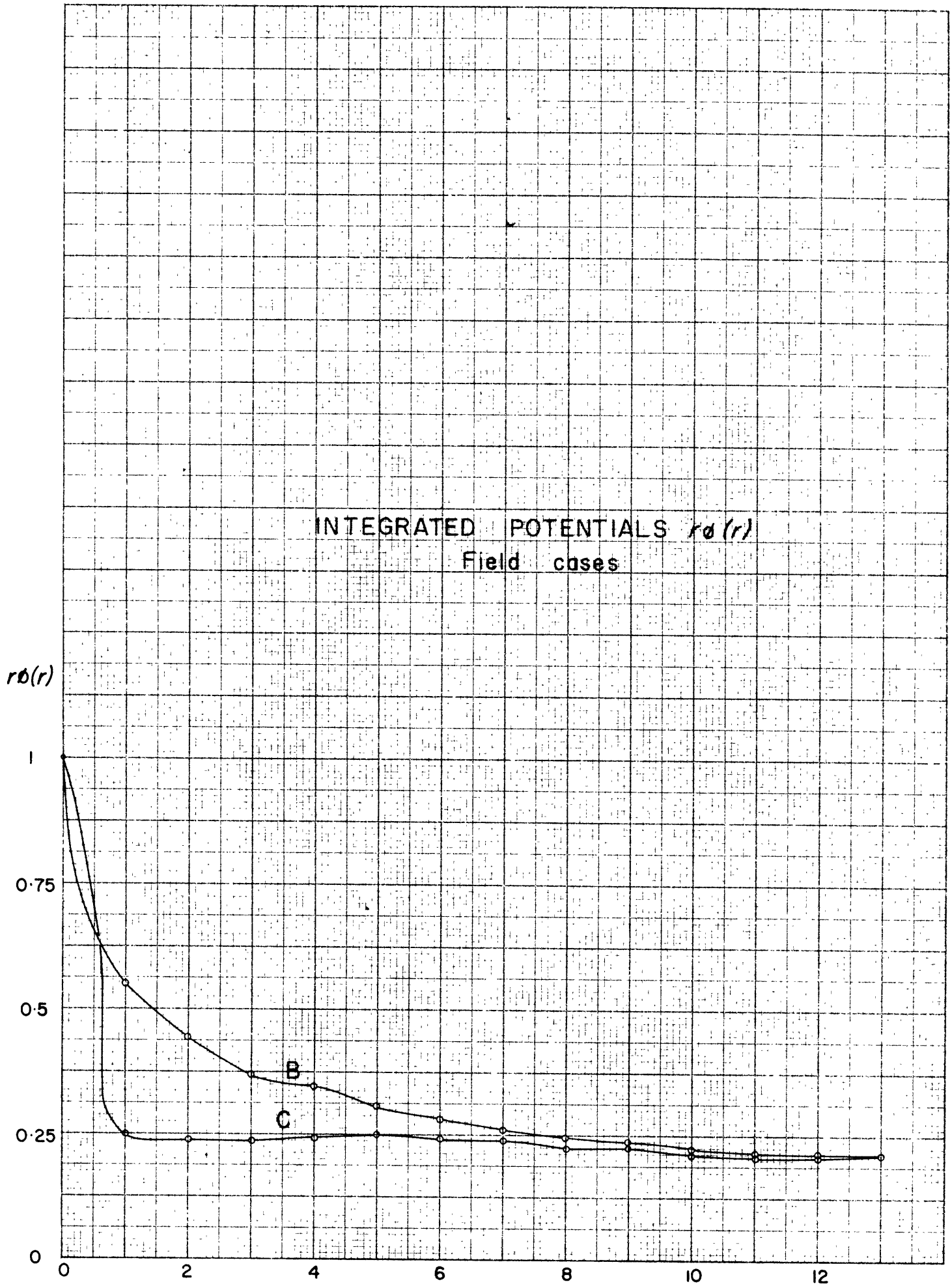
INTEGRATED POTENTIALS rø(r)
Field cases
rø(r)
1
0·75
0·5
0·25
0
0
2
4
6
8
10
12
B
C
10 X 10 TO THE ½ INCH 359-11K
KEUFFEL & ESSER CO.

Fig. 13

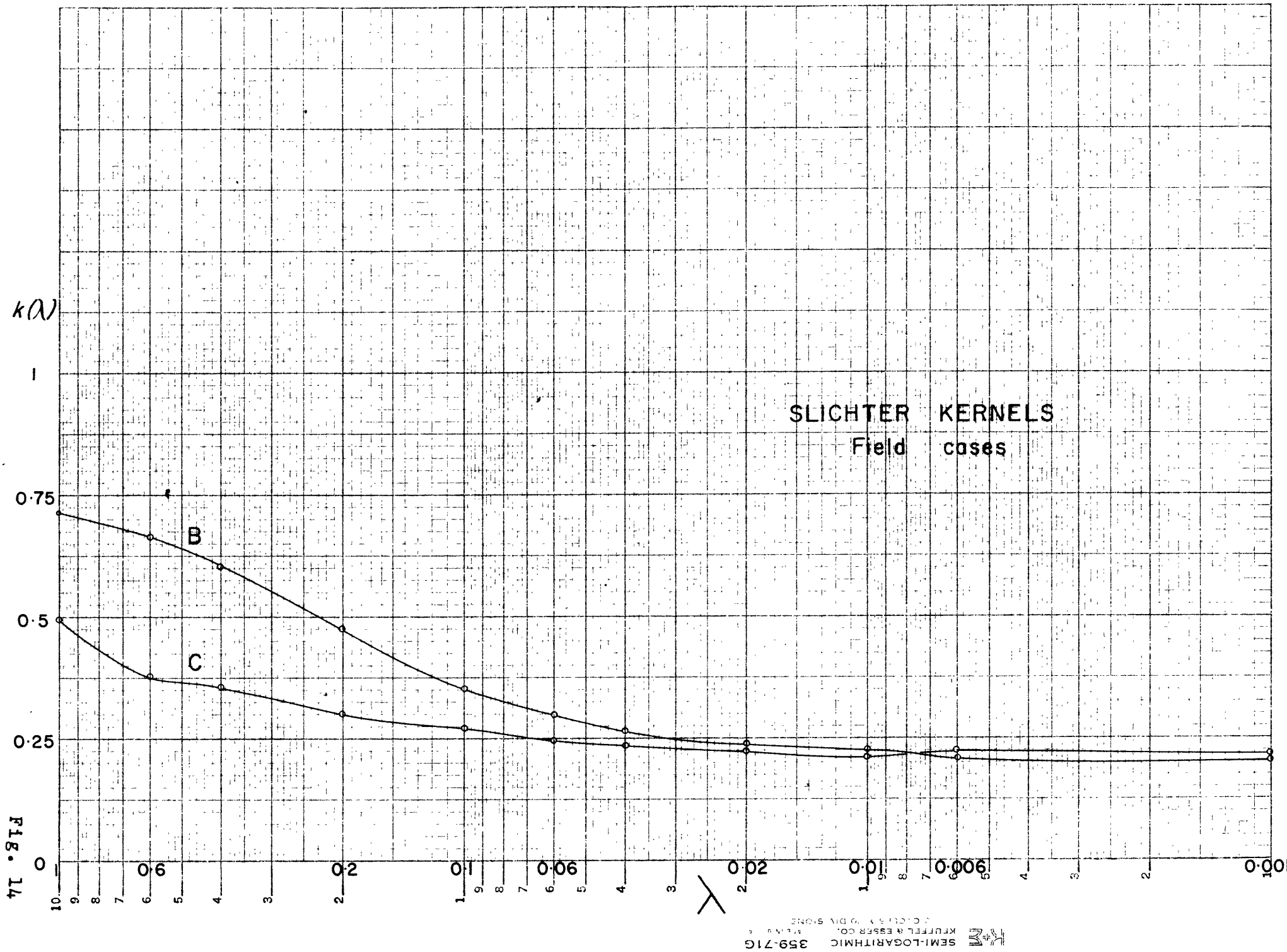
SLICHTER KERNELS
Field cases
k(λ)
1
0·75
0·5
0·25
0
B
C
0·6
0·2
0·1
0·06
0·02
0·01
0·006
0·001
λ
SEMI-LOGARITHMIC 359-71G
KEUFFEL & ESSER CO.

Fig. 14

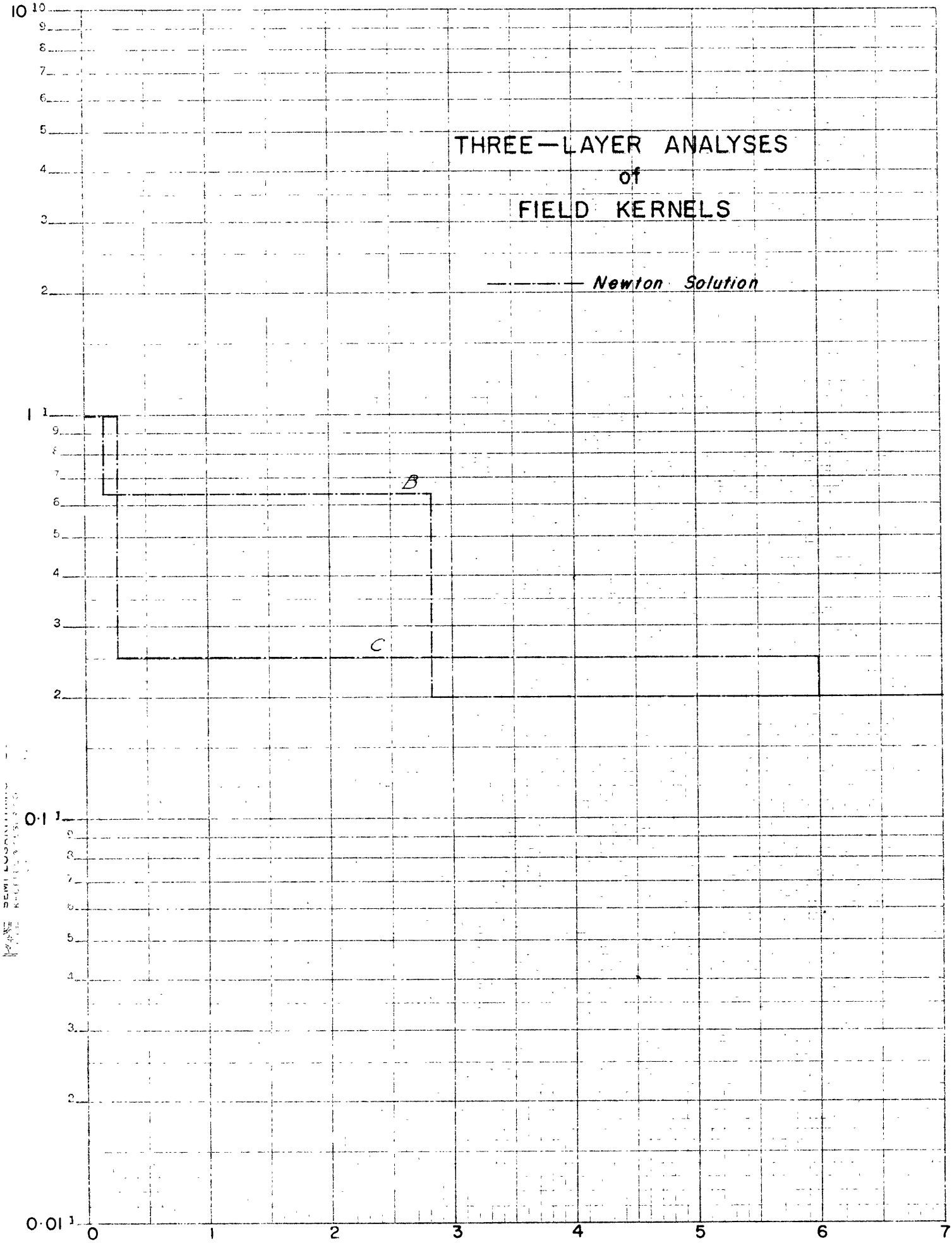
THREE—LAYER ANALYSES
of
FIELD KERNELS
Newton Solution
B
C
10
1
0·1
0·01
0
1
2
3
4
5
6
7

Fig. 15

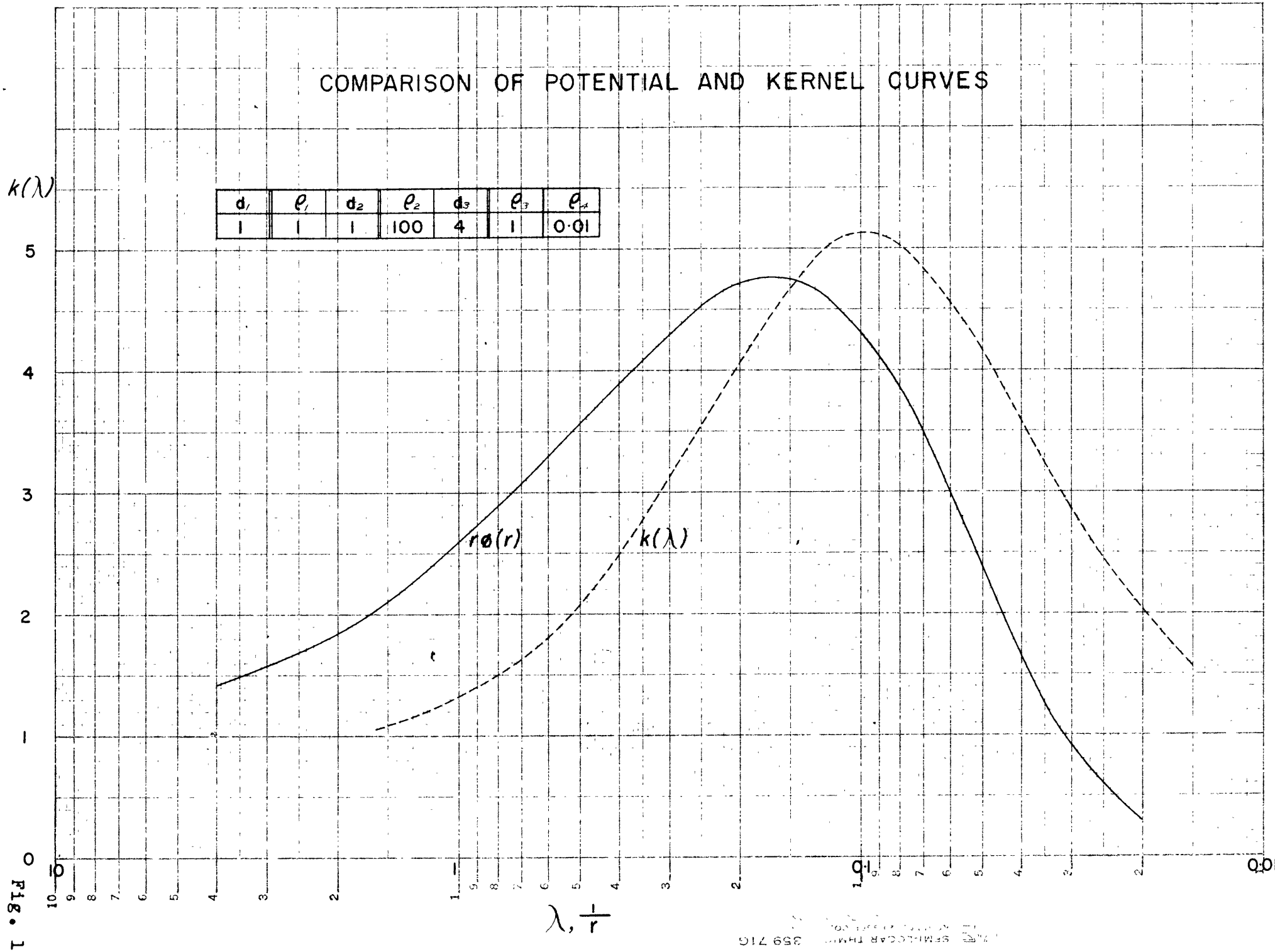
COMPARISON OF POTENTIAL AND KERNEL CURVES
k(λ)
d1 ρ1 d2 ρ2 d3 ρ3 ρ4
1 1 1 100 4 1 0·01
rø(r)
k(λ)
0
1
2
3
4
5
10
9
8
7
6
5
4
3
2
1
0·1
0·01
λ, 1/r

Fig. 16

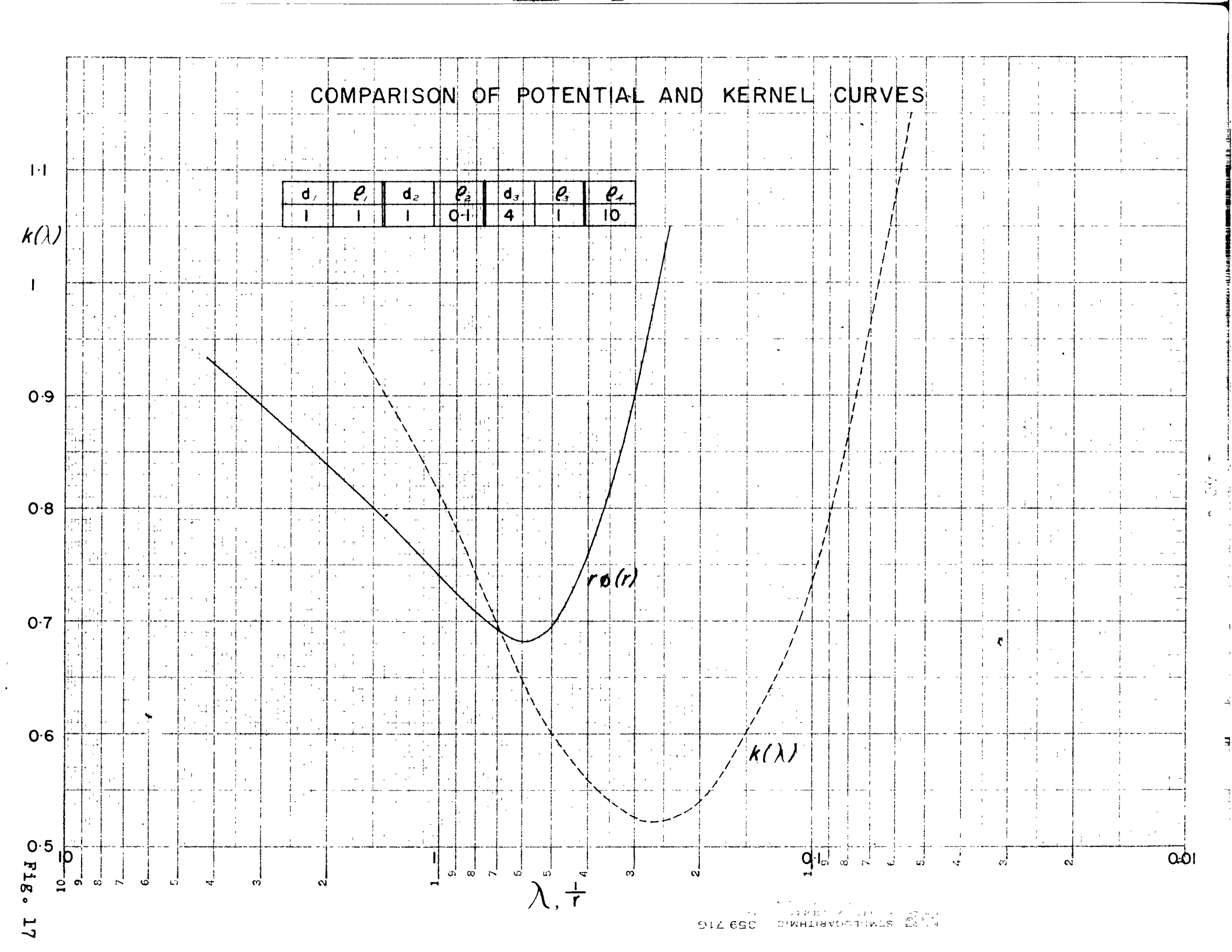
COMPARISON OF POTENTIAL AND KERNEL CURVES
d1 ρ1 d2 ρ2 d3 ρ3 ρ4
1 1 1 0·1 4 1 10
k(λ)
1·1
1
0·9
0·8
0·7
0·6
0·5
rφ(r)
k(λ)
λ, 1/r
10
1
0·1
0·01

FIG. 17

IV BIBLIOGRAPHY - PART TWO

Bernstein, D. L., Existence Theorems in Partial Differential Equations, Princeton Univ. Press, 1950.

Evjen, H. M., "Depth factors and resolving power of electrical measurements", Geophysics III, no. 2, p 78-95, 1938.

Householder, A. S., Principles of Numerical Analysis, McGraw-Hill Book Co., 1953.

Hallof, P. G., and Ness, N., Personal communication. 1955.

Hummel, T. N., "Potential distribution about various bodies in a homogeneous medium", Gerlands Beitrage zur Geophysik, 21, 1929.

King, L. V., "On the flow of electric current in semi-infinite stratified media", Proc. Roy. Soc. A-139, p 237-277, 1933.

Langer, R. E., "An inverse problem in differential equations", Bull. Amer. Math. Soc., series 2, 39, p 814-820, 1933.

_____, "On the determination of earth conductivity from observed surface potentials", Bull. Amer. Math. Soc., series 2, 42, p 747-754, 1936.

Madden, T. R., Personal communication, 1955.

Maxwell, J. C., Electricity and Magnetism, 1891, reprinted by Dover, 1954.

Mooney, H. M., and Wetzel, W. W., The Potentials About a Point Electrode and Apparent Resistivity Curves for a Four-Layer Earth, to be published by Univ. of Minnesota Press.

Morse, P. M., and Feshbach, H., Methods of Theoretical Physics, McGraw-Hill Book Co., 1953.

Murray, F. M., and Miller, K. S., Existence Theorems for Ordinary Differential Equations, New York Univ. Press, 1954.

Ollendorff, F., Erdstrome, Springer Verlag, 1928.

Pekeris, C. L., "Direct method of interpretation in resistivity prospecting", Geophysics, V, no. 1, p 31-42, 1940.

Petrovsky, I. G., Lectures on Partial Differential Equations, Interscience, 1954.

BIBLIOGRAPHY - PART TWO

Roman, K., How to Compute Tables for Determining Electrical Resistivity of Underlying Beds and Their Application to Geophysical Problems, U. S. Bur. Mines, Tech. Paper 502, 1931.

von Sanden, H., Practical Mathematical Analysis, Methuen, 1923.

Schlumberger, C., "Abaques de sondage electrique" Geophysical Prospecting, III, Supplement 3, September 1955.

Slichter, L. B., "Interpretation of resistivity prospecting for horizontal structure," Physics, 4, p 307-322, also erratum, p 407, 1933.

_____, "Seismic interpretation theory for an elastic earth", Proc. Roy. Soc., A. 224, p 43-63, 1954.

Sommerfeld, A., Partial Differential Equations in Physics, Academic Press, 1949.

Stefanesco, S., C. Schlumberger and M. Schlumberger, "Sur la distribution electrique potentielle autour d'une prise de terre ponctuelle dans un terrain a couches horizontales, homogenes et isotropes", Le Journal de Physique et le Radium, 1, p 132, 1930.

Stevenson, A. F., "On the theoretical determination of earth resistance, from surface potential measurements", Physics, 5, p 114-124, 1934.

Sunde, E. D., Earth Conduction Effects in Transmission Systems, Van Nostrand, 1949.

Vozoff, K., a, "Newton analysis of earth resistivity measurements", Summary Report no. 41, Project Whirlwind, M. I. T., 1955.

_____, b, "Steepest descent analysis of resistivity data", Summary Report no. 42, Project Whirlwind, M. I. T., 1955.

APPENDIX

NUMERICAL INTEGRATION OF THE SLICHTER KERNEL

It is desired to perform numerically the following integration:

$$k(\lambda) = \lambda \int_0^\infty r\theta(r) J_0(\lambda r)\, dr$$

Here $r\phi(r)$ is constant for

$$r > r_c$$

by virtue of the assumption that below some depth d

$$d = d_1 + d_2 + \ldots + d_{n-1}$$

the resistivity is constant, and $\phi(r)$ diminishes as $1/r$.

The general field procedure is to measure changes in $\phi(r)$ between fixed intervals from the source. When the point r_c is reached, the potential can be evaluated by the following algebra.

$$\phi(r_i)\, /r_{i+1} = \phi(r_{i+1})\, /r_i$$

$$\phi(r_i) - \phi(r_{i+1}) = \triangle\phi_i$$

$$r_{i+1} - r_i = \triangle r, \text{ the measuring interval}$$

$$r_i > r_c$$

$$\phi(r_i) = -\triangle\phi_i\, r_{i+1}\, /r_i\, (1 - r_{i+1}/r_i)$$

Starting with the value of $\phi(r_i)$

$$\phi(r_{i-1}) = \phi(r_i) + \triangle\phi_{i-1}$$

$$\phi(r_{i-2}) = \phi(r_{i-1}) + \triangle\phi_{i-2}, \text{ etc.,}$$

and the potential curve can be integrated inwards to $i = 1$. The (usually smooth) $r\phi(r)$ curve can be extrapolated to $r = 0$. In the work done, $r\phi(r)$ was determined at 20 equally-spaced points, including $r = 0$ and $r = r_c$. These were replaced by two

sets of fifth order polynomials (Milne 1949, p 265, ff.) one fitted to the first six points, the other to the last 15. The reason for this was that changes in $r\phi(r)$ are usually much more rapid near the origin. The polynomials gave two series, each representing $r\phi(r)$ in their respective intervals

$$r_i\phi(r_i) \approx c_o + c_1P_5^1 + c_2P_5^2 + c_3P_5^3 + c_4P_5^4 + c_5P_5^5 \equiv P_1$$

$$i = 0,1,2,3,4,5$$

$$r_i\phi(r_i) \approx d_o + d_1P_5^1 + d_2P_5^2 + d_3P_5^3 + d_4P_5^4 + d_5P_5^5 \equiv P_2$$

$$i = 5,6,7, - - -,19$$

Rearranging by powers of r

$$P_1 = g_o + g_1r + g_2r^2 + g_3r^3 + g_4r^4 + g_5r^5 \quad i = 0,1, - - -,5$$

$$P_2 = h_o + h_1r + h_2r^2 + h_3r^3 + h_4r^4 + h_5r^5 \quad i = 5,6, - - -,19$$

The integral becomes

$$k(\lambda) \approx \int_o^{r_5} P_1(r)J_o(\lambda r)dr + \lambda\int_{r_5}^{r_{19}} P_2(r)J_o(\lambda r)dr + \lambda r_{19}\phi(r_{19})\int_{r_{19}}^{\infty} J_o(\lambda r)dr$$

where

$$r_{19} \equiv r_c$$

Then

$$k(\lambda) = \lambda\sum_{\ell=o}^{5} g_\ell \int_o^{r_5} r\, J_o(\lambda r)dr + \lambda\sum_{\ell=o}^{5} h_\ell \int_{r_5}^{r_{19}} r J_o(\lambda r)dr + \lambda\, r_{19}\phi(r_{19})\, R$$

$$R = \int_{r_{19}}^{\infty} J_o(\lambda r)dr$$

But the indefinite integrals

$$\int r^\ell J_o(\lambda r)dr$$

can be evaluated analytically

$$\int_a^b J_o(\lambda r)dr = \frac{2}{\lambda}\left[J_1(\lambda r) + J_3(\lambda r) + J_5(\lambda r) + \ldots \right]_a^b$$

$$\int_a^b rJ_o(\lambda r)\,dr = \frac{1}{\lambda^2} J_1(\lambda r) \Big]_a^b$$

$$\int_a^b r^2 J_o(\lambda r)dr = \frac{1}{\lambda^3}\left[r^2\lambda^2 J_1(\lambda r) + r\,J_o(\lambda r) - 2(J_1(\lambda r) + J_3(\lambda r) + J_5(\lambda r) + \ldots) \right]_a^b$$

$$\int_a^b r^3 J_o(\lambda r)dr = \frac{1}{\lambda^4}\left[\lambda^3 r^3 J_1(\lambda r) - 2\lambda^2 r^2 J_2(\lambda r) \right]_a^b$$

$$\int_a^b r^4 J_o(\lambda r)dr = \frac{1}{\lambda^5}\left[(\lambda r)^4 J_1(\lambda r) - 3(\lambda r)^3 J_2(\lambda r) + 3(\lambda r)^2 J_3(\lambda r) + 3\lambda r J_4(\lambda r) + 18(J_5(\lambda r) + J_7(\lambda r) + J_9(\lambda r) + \ldots) \right]_a^b$$

$$\int_a^b r^5 J_o(\lambda r)dr = \frac{1}{\lambda^6}\left[(\lambda r)^5 J_1(\lambda r) - 4(\lambda r)^4 J_2(\lambda r) + 8(\lambda r)^3 J_3(\lambda r) \right]_a^b$$

The J_n can be evaluated by machine during the integration process. It is preferable, however, to decide on a fixed set of λ and r, and to obtain the values of the functions from tables (Harvard University Press series) which are then retabulated in the computer storage. Because the coefficients g and h often take on very large values, it is important that the values of the Bessel functions be quite accurate in absolute value. The above mentioned tables are of more than sufficient accuracy. In the evaluation of the infinite series, it was found necessary to use Bessel functions of order 29, with the maximum product $\lambda r = 38$ (at $\lambda = 2$). The final algebraic form of the integration was thus

$$= J_1(\lambda r_5)\left[\, 2(g_o-h_o) + \frac{g_1-h_1}{\lambda} + (g_2-h_2)(r_5^2-\frac{2}{\lambda^2}) + (g_3-h_3)r_5^3 + (g_4-h_4)r_5^4 + (g_5-h_5)r_5^5 \,\right]$$

$$+ J_2(\lambda r_5)\left[\, -2(g_3-h_3)\frac{r_5^2}{\lambda} - 3(g_4-h_4)\frac{r_5^3}{\lambda} - 4(g_5-h_5)\frac{r_5^4}{\lambda} \,\right]$$

$$+ J_3(\lambda r_5)\left[\, 2(g_o-h_o) - 2\frac{g_2-h_2}{\lambda^2} + 3\frac{(g_4-h_4)}{\lambda^2}r_5^2 + 8\frac{(g_5-h_5)r_5^3}{\lambda^2} \,\right]$$

$$+ J_4(\lambda r_5)\left[\, 3\frac{(g_4-h_4)r_5}{\lambda^3} \,\right]$$

$$+ 2\left[(g_o-h_o) - \frac{(g_2-h_2}{\lambda^2} + \frac{9(g_4-h_4)}{\lambda^4}\right]\left[\, J_5(\lambda r_5) + J_7(\lambda r_5) + J_9(\lambda r_5) + \ldots \,\right]$$

$$+ J_1(\lambda r_{19})\left[2h_o + \frac{h_1}{\lambda} + h_2(r_{19}^2-\frac{2}{\lambda^2}) + h_3 r_{19}^3 + h_4 r_{19}^4 + h_5 r_{19}^5 - 2r_{19}\phi(r_{19}) \,\right]$$

$$+ J_2(\lambda r_{19})\left[\, -\frac{2h_3}{\lambda}r_{19}^2 - \frac{3h_4}{\lambda}r_{19}^3 - \frac{4h_5}{\lambda}r_{19}^4 \right.$$

$$\left. + J_3(\lambda r_{19})\left[2\,h_o - \frac{2h_2}{\lambda^2} + \frac{3h_4}{\lambda^2}r_{19} + \frac{8h_5}{\lambda^2}r_{19}^3 - 2r_{19}\phi(r_{19}) \,\right]\right.$$

$$\left. + J_4(\lambda r_{19})\left[\, \frac{3h_4}{\lambda^3}r_{19} \,\right]\right.$$

$$\left. + \left[\, 2h_o - \frac{2h_2}{\lambda^2} + \frac{18h_4}{\lambda^4} - 2r_{19}\phi(r_{19}) \,\right]\left[\, J_5(\lambda r_{19}) + J_7(\lambda r_{19}) + J_9(r_{19}) + \ldots \,\right] = K(\lambda)\right.$$

The error introduced by using the polynomial rather than the data points was computed in each case,and was found to be well within the limits of accuracy.

An alternate scheme, proposed by Mooney (1955) is to fit second order polynomials to the points taken three at a time. The algebra is simplified considerably, but the question arises of fit between points, in complex segments of the curves. As a third, and certainly simplest, alternative, one might draw the $r\phi(r)$ curve very accurately and perform the entire integration using, say, Simpson's rule. This is essentially the same as Mooney's method.

BIOGRAPHICAL NOTE

The author was born in Minneapolis, Minnesota on January 26, 1928. He attended the University of Minnesota in 1944-1945, and 1948-1949, and received a Bachelor of Physics degree in July, 1949. From 1949-1951 he attended the Pennsylvania State College, and received the M.S. degree in June, 1951. The author attended the Massachusetts Institute of Technology from September, 1953 until June, 1955.